

Affinity purification and identification of unique, shared,
anti-IA-2 B cell clonotypes: A proteomic approach to
understanding the pathophysiological mechanisms
underpinning autoimmunity in Type 1 diabetes

By

Thilini Mendis

Thesis

Submitted to Flinders University

for the degree of

Doctor of Philosophy

College of Medicine and Public Health

16th of June 2023

Summary

Autoantibodies against Insulinoma associated autoantigen 2 (anti-IA-2) are a readily used prognostic and diagnostic biomarker for type 1 diabetes (T1D) utilised in clinical settings. While the role of anti-IA-2 antibodies in the T1D disease process is yet unknown, the elevated autoantibody titres is associated with the beta cell destruction and disease progression. Previous studies in systemic autoimmune disease, autoantibodies have been shown to play a pathogenic role in driving the disease. Subsequent proteomic studies have revealed that these autoantibodies are governed by unique B cell clonotypes specified by distinct heavy and light chain gene pairing. These findings suggested that the pathophysiological mechanisms driving autoimmune responses are clonally restricted. In this study we attempted to investigate whether the humoral responses in an organ confined autoimmune disease such as T1D is analogous to the autoimmune responses in systemic autoimmune diseases. The aim of this thesis was to examine the humoral response that targets the intracellular domain of a well-defined islet antigen, IA-2 (IA-2ic).

In order to investigate the antibody proteome, we first developed a method to detect the anti-IA-2 antibody responses in T1D patients with the use of IA-2 antigen expressed as a recombinant maltose binding protein (MBP) fusion protein. After the successful establishment of the IA-2 MBP fusion protein coated enzyme linked immunoassay (ELISA), this ELISA was incorporated in a four-plate affinity purification method described by Al Kindi et al (Al kindi et al. 2015). Affinity purified antibody samples were generated from two anti-IA-2 antibody positive sera, two anti-IA-2 antibody negative sera and two healthy controls. Subsequent Sodium dodecyl sulphate polyacrylamide gel electrophoresis (SDS-PAGE) of the affinity purified antibody samples with several control caprylic immunoglobulin G (IgG) samples of a range of concentrations demonstrated that the ELISA plate affinity purification method generates high yield pure IgG antibody samples with low impurity.

The affinity purified antibody samples were then subjected to mass spectrometry analysis. The peptide data obtained from the high-end performance liquid chromatography quadrupole time of flight (HPLC Q-TOF) mass spectrometer were

analysed using Peaks software. Peaks data were then analysed to select high quality peptides which were then assigned to gene families as per the selection criteria. The variable region (V) and joining region (J) gene family analysis of the heavy (H) and light chains (L) revealed that the anti-IA-2ic antibody responses in T1D patients is governed by a unique public class switched B cell clonotype specified by IGHV 3-23.IGHJ6 and IGKV 1-9.IGKJ2/IGKJ4. This suggested that the entire pathophysiological pathway from generation of the autoreactive B cell clone, bypassing of the tolerance check points to the targeting of the islet antigen is identical in all patients with T1D. Further analysis of gene family heat maps revealed the presence of common amino acid (aa) replacements. The presence of the shared aa mutations implicated that this unique B cell clonotype have escaped the central tolerance checkpoints and undergone antigen driven affinity maturation.

The identification of this unique class switched B cell clonotype that is potentially driving subset of the humoral response against the intracellular domain of the IA-2 antigen in T1D facilitate the development of novel therapeutic interventions to treat patients with T1D. In addition, this also allows the investigation of the autoimmune pathophysiological pathways that underpins the disease process.

Declaration

I certify that this thesis does not incorporate without acknowledgment any material previously submitted for a degree or diploma in any university and the research within will not be submitted for any other future degree or diploma without the permission of flinders university; and to the best of my knowledge and belief, does not contain any material previously published or written by another person except where due reference is made in the text.

Thilini Mendis

Acknowledgements

I wish to express my sincerest gratitude to my supervisor Dr. Michael Jackson for the continuous guidance, patience, enthusiasm, and paramount knowledge throughout my PhD candidature. I would like to thank Dr. Tom Gordon, Dr. Jing Jing Wang, Dr. Penny Adamson and Dr. Tim Chataway for their expert guidance and support. I would also like to thank all the members of the Department of Immunology, Allergy and Arthritis and Flinders proteomic facility including, Nusha Chegeni, Kamelya Aliakbari, Leo Ng, Barbora Filipova, Bridie Armour and Isabell Bastian for their valuable assistance throughout the years. Lastly, I would like to acknowledge the love and support of my dearest parents, brothers, sisters, and friends.

List of Publications

Mendis, T., Filipova, B., Wang, J., Pietropaolo, M., and Jackson, M. W. 2023, 'Affinity purification of serum-derived anti-IA-2 autoantibodies in type 1 diabetes using a novel MBP-IA-2 fusion protein', *Biochemistry and Biophysics Reports*, 33 (2023), 101413.

Alsheri, A. M., Mendis, T., and Jackson, M. W. 2018, 'A cell-based assay for the detection of pathogenic anti-voltage-gated calcium channel autoantibodies in immunoglobulin G from patients with type 1 diabetes', *Journal of Immunological Methods*, 460 (2018), 79-86.

List of abstracts and posters

Mendis, T., Wang J., Pietropaolo, M., Jackson, M., Affinity purification and identification of unique, shared, anti-IA-2 B cell clonotypes: A proteomic approach to understanding the pathophysiological mechanisms underpinning autoimmunity in T1D. 79th Scientific sessions held by the American Diabetes Association 2019, LA, US.

Mendis, T., Wang, J., Pietropaolo, M., Jackson, M., Affinity purification and identification of unique, shared, anti-IA-2 B cell clonotypes: A proteomic approach to understanding the pathophysiological mechanisms underpinning autoimmunity in T1D. 48th Annual scientific meeting of The Australian and New Zealand Society for Immunology, 2019, SA.

Mendis, T., Torpy, D., Wanzlau, J., Saremi, N., Mohansundaram, D., Jackson, M., Australian Society for Medical Research, 54th National Scientific conference 2015, SA.

Mendis, T., Skarstrand, H., Adamson, P., Al KIndi, M., Jackson, M., The use of MBP fusion protein of ZnT8 to characterise the autoantibody expression in T1D patients. Australian Society for Medical Research, 53rd National Scientific conference 2014, SA.

Table of Contents

Summary.....	I
Declaration.....	III
Acknowledgements	IV
List of abstracts and posters.....	VI
List of figures.....	XII
List of tables	XVI
List of abbreviations	XVIII

Chapter 1: Literature review

1.1. Introduction	1
1.2. Type 1 Diabetes	1
1.3. Epidemiology	2
1.4. Human Leukocyte Antigens (HLA) Genetic susceptibility	3
1.5. The immune system.....	3
1.6. Antigen presentation.....	5
1.7. T cells	6
1.8. B Cells	8
1.8.1. B cell immunoglobulin receptor	8
1.8.2. Plasma Cells	11
1.8.3. Memory B cells	12
1.9. Tolerance induction	12
1.10. Autoimmune T1D.....	14
1.11. Autoantigens.....	18
1.11.1. Insulin	18
1.11.2. Glutamic Acid Decarboxylase.....	18

1.11.3.	IA-2.....	19
1.11.4.	Zinc transporter (ZnT8).....	20
1.11.5.	Other autoantigens.....	23
1.12.	Islet autoantibodies.....	25
1.12.1.	Multiple islet autoantibodies.....	25
1.12.2.	Autoantibody patterns.....	25
1.12.3.	Autoantibody isotopes.....	26
1.12.4.	IAA.....	26
1.12.5.	GADA.....	27
1.12.6.	ZnT8A.....	27
1.12.7.	IA-2 Antibodies.....	28
1.13.	Autoantibody epitopes.....	29
1.14.	Autoantibody affinity.....	30
1.15.	Use of MBP affinity tags in the expression of recombinant fusion proteins... 30	
1.16.	Analysis of clonality and variable region gene usage of anti-IA-2 antibodies using mass spectrometry sequencing.....	32
1.17.	Specific aims and hypothesis.....	32

Chapter 2: Materials and Methods

2.1.	Patients and controls.....	34
2.2.	Statistical analysis.....	37
2.3.	RSR ELISA for the detection of IA-2, ZnT8 and GAD antibodies in T1D patients.....	37
2.4.	Development of IA-2, ZnT8R and ZnT8W MBP fusion protein ELISA assays .	38
2.4.1.	Generation of recombinant maltose binding fusion proteins.....	38
2.4.2.	Miniprep of transformed cells.....	41
2.4.3.	Verification of Plasmid DNA.....	41
2.4.3.1	Plasmid DNA extraction from transformed E. Coli cells for agarose gel electrophoresis and Sanger sequencing.....	41
2.4.3.2	Plasmid DNA digestion for agarose gel Electrophoresis.....	42

2.4.4. Purification of fusion proteins using column chromatography	44
2.4.5. Protein concentration determination of the recovered fusion protein samples by Bradford or EZQ Protein quantification assay.	45
2.4.6. EZQ protein quantification assay	45
2.4.7. Verification of expressed fusion proteins via 1D SDS gel electrophoresis	46
2.4.8. The assessment of fusion proteins by western blotting	48
2.4.9. Maxiprep of transformed cells.....	49
2.4.10. ELISA plate coating and serum concentration Optimization.....	50
2.5. Proteomic analysis of T1D specific autoantibodies	56
2.5.1 Elution of bound antibodies from fusion protein coated ELISA plates	56
2.5.2 Preparing the antibody sample for mass spectrometry	57
2.5.3 Mass spectrometry	58
2.5.4 Proteomics data analysis.....	58

Chapter 3: Development of a MBP fusion protein ELISA method for the detection of IA-2, ZnT8R and ZnT8W autoantibodies in sera from patients with Type 1 diabetes

3.1 Introduction	60
3.2 Methods	62
3.2.1 Patient and control Sera.....	62
3.2.2 RSR ELISA assay.....	62
3.2.3 Fusion protein ELISA.....	62
3.2.4 Statistical analysis	63
3.3 Results	64
3.3.1 Optimization of serum concentrations for IA-2 fusion protein ELISA.....	64
3.3.2. Optimization of serum concentrations for ZnT8R fusion protein ELISA..	65
3.3.3. Confirmation of fusion protein ELISA specificity.....	67
3.3.4. Prevalence of antibodies against islet antigen IA-2, GAD65 and ZnT8 in a cohort 1 of T1D patients.....	70
3.3.5. Selection of patients for the development of fusion protein ELISA	74
3.3.6. Optimization of IA-2ic and ZnT8 MBP fusion protein ELISAs.....	75
3.3.7. Detection of anti-IA-2 antibodies in cohort 2 of T1D patients	78

3.3.8. Comparison of RSR ELISA with MBP fusion protein ELISA	78
3.3.9. Screening of an additional cohort of T1D patient sera using RSR ELISA	80
3.3.10. Detection of high titer anti-IA-2 autoantibody sera using IA-2ic MBP fusion protein ELISA	82
3.3.11. Detection of high titer anti-ZnT8R autoantibodies in T1D sera using ZnT8R MBP fusion protein ELISA	84
3.3.12. Detection of anti-IA-2 antibodies and anti-ZnT8R antibodies by IA-2ic MBP fusion protein and ZnT8R fusion protein in Cohort 1 and Cohort 2.....	86
3.3.13. Confirmation of fusion protein ELISA specificity	88
3.4. Discussion.....	92

Chapter 4: Affinity purification of antibodies that target epitopes within IA-2ic antigens with the use of a novel ELISA plate purification method

4.1. Prologue to chapter 4.....	96
4.1.1. Prologue to affinity purification of anti-IA-2 antibodies	96
4.1.2. Methods	96
4.1.3. Results	97
4.2. Introduction	99
4.3. Materials and Methods	100
4.3.1. Selection of patient and control sera for affinity purification experiments	100
4.3.2. Affinity purification of IA-2 antibodies	100
4.3.3 Quantification of purified IgG by western blot densitometry analysis	101
4.3.4. Reactivity ELISA	104
4.3.5. SDS-PAGE gel electrophoresis of eluted IgG for isolation of heavy and light chains for mass spectrometry	104
4.4. Results	105
4.4.1. Affinity purification of anti-IA-2 antibodies targeting the epitopes within the fusion protein IA-2	105
4.4.2. Specificity ELISA	109
4.5. Discussion.....	115

Chapter 5: Proteomic analysis of clonally restricted IA-2 autoantibody response in T1D

5.1 introduction..... 118

5.2. Methods 120

 5.2.1. Patients and samples..... 120

 5.2.2. Samples analyzed 120

 5.2.3. Sample preparation..... 120

 5.2.4. Proteomic analysis..... 122

5.3. Results 122

 5.3.1. Quantification of affinity purified antibody 122

 5.3.2. Confirmation of peptide digestion and sample integrity 123

 5.3.3. Protein sequence data analysis 125

 5.3.4. Gene family assignment using proteomics analysis of variable region gene family usage in anti-IA-2 antibody repertoires 126

 5.3.5. Analysis of peptide maps derived from IA-2 specific V regions reveals idiotypic and shared amino acid (aa) substitutions..... 140

5.4. Discussion..... 162

Chapter 6: Concluding remarks

6.1. Summary and Conclusions 172

6.2 Future directions 183

Appendices 185

Reference List 186

List of figures

Figure 1.1.	The immune system is comprised of two main divisions, Innate and adaptive immune responses	5
Figure 1.2.	Schematic diagram of immune response to a primary antigen over the first 30 days.	7
Figure 1.3.	Schematic diagram of IgG antibody structure. The germline V, D, J and C segments are labelled in the top chains.	10
Figure 1.4.	Major intracellular pancreatic beta cell autoantigens that are targeted in T1D.....	16
Figure 1.5.	Amino acid sequence of preproinsulin (PPI) displaying A chain, B chain and C peptide	17
Figure 1.6.	Schematic diagram of islet antigen Glutamic Acid Decarboxylase enzyme.....	18
Figure 1.7.	Schematic diagram of full-length IA-2.....	19
Figure 1.8.	A model of the ZnT8 transmembrane protein.	21
Figure 1.9.	Zn transporters in different types of islet cells.	22
Figure 2.1.	pMAL-c5X plasmid with the encoding for IA-2ic MBP fusion protein	39
Figure 2.2.	pETMBP_1a 7181 bp plasmid map with the encoding for ZnT8R/W/Q MBP fusion protein	42
Figure 2.3.	Agarose gel electrophoresis of digested pETMBP_1a 7181 bp ZnT8R/W/Q plasmid DNA.	43
Figure 2.4.	Confirmation of purity and integrity of the purified recombinant MBP fusion proteins by 1D SDS gel electrophoresis	46
Figure 2.5.	Confirmation of the integrity of the recombinant MBP fusion proteins by western blotting	48
Figure 2.6.	Assessment of IA-2ic MBP fusion protein coating concentration sensitivity.....	50
Figure 2.7.	Assessment of ZnT8R/ZnT8W MBP fusion protein coating concentration sensitivity	51

Figure 2.8.	Evaluation of optimal serum concentration for the detection of true anti-IA-2 antibody binding by IA-2ic MBP fusion protein ELISA...	52
Figure 2.9.	Evaluation of optimal serum concentration for the detection of true anti-ZnT8R antibody binding by ZnT8R MBP fusion protein ELISA	53
Figure 2.10.	Estimation of optimal serum concentration for the detection of anti-ZnT8W antibodies by using ZnT8W MBP fusion in ELISA.....	54
Figure 3.1.	Additional assessment of optimal serum concentration required to detect anti-IA-2A antibodies by IA-2ic MBP fusion protein ELISA	64
Figure 3.2.	Further assessment of optimal serum concentration required for the detection of anti-ZnT8R antibodies by ZnT8R MBP fusion protein ELISA.....	66
Figure 3.3.	The specificity of the IA-2ic MBP fusion protein ELISA was further verified by testing the prototype positive, negative, and healthy control sera on MBP and GST calreticulin proteins.....	68
Figure 3.4.	Incidence of IA-2A, GADA and ZnT8A in cohort 1 (local cohort of T1D patients n=36) detected using RSR ELISA.	71
Figure 3.5.	The validity of the MBP fusion protein ELISAs was tested by using prototype RSR positive and negative patient sera.	75
Figure 3.6.	Anti-IA-2 antibody binding and background binding tested by IA-2ic MBP fusion protein ELISA.	76
Figure 3.7.	The Presence of anti-IA-2 antibodies in cohort 2 (T1D patients n=30) detected using RSR version 2 ELISA assay	79
Figure 3.8.	The presence of anti-ZnT8 antibodies in T1D cohort 2 detected by ZnT8R RSR ELISA.....	80
Figure 3.9.	Establishment of assay cut off for the determination of high titre anti-IA-2 antibody positive serum	82
Figure 3.10.	Establishment of assay cut off for the determination of high titre anti-ZnT8R antibody positive serum	84
Figure 3.11.	The presence of anti-IA-2 autoantibodies in T1D patient sera (Cohort 1 and 2) and healthy controls sera detected using IA-2ic MBP fusion protein ELISA.....	85

Figure 3.12.	The presence of anti-ZnT8R autoantibodies in T1D patient and healthy control sera detected using ZnT8R MBP fusion protein ELISA.....	86
Figure 4.1.	Kappa and lambda light chain distribution in the anti-IA-2 IgG affinity purified antibody sample generated from T1D069 sera	97
Figure 4.2.	Representative western blot used for densitometry analysis.....	101
Figure 4.3.	Representative linear regression standard curve	101
Figure 4.4.	ELISA carried out in parallel to affinity purification process to confirm the integrity of the reaction.....	107
Figure 4.5.	Reactivity ELISA of the affinity purified antibody samples generated using the IA-2ic MBP fusion protein ELISA plate affinity purification method	112
Figure 4.6.	Representative gel image of 1D SDS gel electrophoresis of an affinity purified antibody generated by IA-2ic MBP fusion protein ELISA plate affinity purification method.....	113
Figure 5.1.	Proteomics workflow for the investigation of clonality of secreted anti-IA-2 antibodies affinity purified from T1D sera.....	120
Figure 5.2.	Representative figure of total iron current spectra obtained from the mass spectrometer for each heavy and light chain sample.....	123
Figure 5.3.	IGHV 3-23 heavy chain variable region heat map constructed from de novo sequencing data from affinity purified anti-IA-2 antibody samples generated from anti-IA-2 antibody positive sera displaying aa replacements compared to the germline sequence.....	146
Figure 5.4.	IGHV 3-23 heavy chain variable region heat map constructed from de novo sequencing data from affinity purified anti-IA-2 antibody samples generated from anti-IA-2A negative sera and healthy control sera.....	148
Figure 5.5.	IGKV 3-20 light chain variable region heat map constructed from de novo sequencing data from affinity purified anti-IA-2 antibody samples	150
Figure 5.6.	IGKV 3-20 light chain variable region heat map constructed from de novo sequencing data from affinity purified anti-IA-2 antibody	

	samples generated from anti-IA-2A negative sera and healthy controls	152
Figure 5.7.	IGKV 1-9 light chain variable region heat map constructed from de novo sequencing data from affinity purified anti-IA-2 antibody samples generated from anti-IA-2A positive sera	154
Figure 5.8.	IGKJ2 light chain joining region heat map generated from de novo sequencing data from affinity purified anti-IA-2 antibody samples generated from anti-IA-2A positive patients, negative patients and healthy controls compared to the germline sequence	156
Figure 5.9.	IGKJ4 light chain joining region map constructed from de novo sequencing data from affinity purified anti-IA-2 antibody samples generated from anti-IA-2A positive and negative patients and healthy controls aligned with the germline sequence.....	157
Figure 5.10.	IGHJ6 heavy chain joining region map generated from de novo sequencing data from affinity purified anti-IA-2 antibody samples generated from anti-IA-2A positive patients, negative patients and healthy controls aligned with the germline sequence	158
Figure 5.11.	Schematic diagram of the putative anti-IA-2ic antibody identified in the affinity purified anti-IA-2ic antibody samples	160

List of tables

Table 2.1.	Patient demographics of the T1D cohort 1	34
Table 2.2.	Patient demographics of the T1D cohort 2	35
Table 3.1.	Patient demographics matched to the positivity and negativity for islet autoantibodies IA-2A, GADA and ZnT8A by RSR ELISA	72
Table 3.2.	Patients selected for the development of IA-2, ZnT8R and ZnT8W MBP fusion protein ELISA.	73
Table 3.3.	Patients selected for the development of ZnT8R and ZnT8W MBP fusion protein ELISA.....	74
Table 3.4.	Comparison of Anti-IA-2 antibody positivity and mean OD values as detected by RSR and IA-2ic MBP fusion protein ELISA in cohort 1 and 2 of T1D patients	88
Table 3.5.	Comparison of anti-ZnT8R antibody positivity and mean absorbance values as detected by RSR ELISA and ZnT8R MBP Fusion protein ELISA for T1D patient cohort 1 and 2	90
Table 4.1.	Representative table of the protein intensity data.....	102
Table 4.2.	Representative yields of affinity purified antibodies produced from approximately 1 mL sera	102
Table 5.1.	Relative quantities of the affinity purified antibodies run on 1D gel prior to introduction to the mass spectrometer	122
Table 5.2.	Representative table of peptide comparison across the antibody samples for high quality	127
Table 5.3.	Heavy chain variable region gene expression in the anti-IA-2 affinity purified antibody samples from T1D019 and T1D069 patient sera	134
Table 5.4.	Heavy chain variable region gene family expression in the affinity purified antibody samples generated from negative control and healthy control serum samples.	135
Table 5.5.	Light chain variable region gene family expression across the affinity purified anti-IA-2 antibody samples from T1D019 and T1D069 patient sera.....	136

Table 5.6.	Light chain variable region gene family expression across the affinity purified antibody samples generated from negative control and healthy control serum samples.	137
Table 5.7.	Assignable heavy chain gene family shared across the affinity purified anti-IA-2 antibody samples generated from anti-IA-2 antibody positive sera	138
Table 5.8.	Assignable light chain gene families shared across the affinity purified anti-IA-2 antibody samples generated from anti-IA-2 antibody positive sera	138

List of abbreviations

T1D.....	Type 1 diabetes
IA-2.....	Insulinoma antigen 2
Anti-IA-2A	Anti-IA-2 autoantibodies
IA-2ic.....	Intracellular domain of IA-2
MBP.....	Maltose binding protein
ELISA.....	Enzyme linked immunoassay
SDS-PAGE.....	Sodium dodecyl sulphate polyacrylamide gel electrophoresis
IgG.....	Immunoglobulin G
HPLC Q-TOF.....	high-end performance liquid chromatography quadrupole time of flight
H.....	Heavy chain
L.....	Light chain
V.....	Variable region
aa.....	Amino Acid
D.....	Diversity
J.....	Joining region
IAA.....	Insulin autoantibodies
GAD.....	Glutamic acid decarboxylase
GADA.....	Glutamic acid decarboxylase antibodies
ZnT8.....	Zinc transporter 8
ZnT8A.....	Zinc transporter 8 antibodies
LADA.....	Latent autoimmune diabetes in adults
TLR.....	Toll like receptors
PAMPs.....	Pathogen associated molecular patterns
HLA.....	Human leukocyte antigens
MHC.....	major histocompatibility complex
IL-2.....	interleukin-2
Th-1.....	T helper 1
Th-2.....	T helper 2
IFN- γ	interferon-gamma
BCR.....	B cell antigen receptor
CDR.....	complementary determining regions

FR	framework
APC	antigen presenting cells
Fab	fragment antigen binding region
DCs	dendritic cells
PLN	pancreatic lymph nodes
HMBG1	high mobility group B1
PPI	Amino acid sequence of preproinsulin
GABA	gamma aminobutyric acid
PTP	protein tyrosine phosphatase
EC	extracellular domain
TM	Transmembrane region
SNP	single nucleotide polymorphisms
Sox	Sry related HMG box
R	Arginine
W	Tryptophan
Q	Glutamine
E. Coli	Escherichia coli
OD	optical density
PBS	phosphate saline buffer
T	Threonine
K	Lysine
A	Alanine
Y	Tyrosine
F	Phenylalanine
I	Isoleucine
V	Valine
E	Glutamic acid
P	Proline
D	Aspartic acid
S	Serine
G	Glycine
L	Leucine
N	Asparagine

CVB	Coxsackievirus B
CTLA-4	Cytotoxic T-lymphocyte associated protein 4
AB.....	Antibody
AP.....	Affinity purified
E1	ELISA 1
E2.....	ELISA 2
E3.....	ELISA 3
E4.....	ELISA 4

Chapter 1. Literature review

1.1. Introduction

Type 1 diabetes (T1D) is a chronic organ specific autoimmune disease characterized by hyperglycaemia due to the destruction of pancreatic beta cells (Mobasseri et al., 2020). T1D is known to arise due to a combination of genetic susceptibility and environmental factors. To date, four major islet autoantibodies, IAA, IA-2A, GADA and ZnT8A, have been revealed to be associated with T1D disease process (figure 1.4). These autoantibodies are readily used prognostic and diagnostic markers of T1D and are generally detected in immunofluorescence, radiobinding or solid phase immunoassays. While the structure, epitopes and function of the islet antigens targeted by these autoantibodies have been studied extensively, little is known of the molecular characteristics or the function of the antibodies themselves. Examining the molecular signatures of the autoantibodies may provide a better understanding of the pathophysiological mechanisms that may be driving the disease process (DiMeglio et al., 2018).

This thesis attempts to investigate the molecular characteristics of the antibody response against a clinically relevant islet antigen IA-2, by high resolution mass spectrometry sequencing. Firstly, a MBP fusion protein ELISA was developed to detect antibody against the intracellular domain of IA-2. Secondly, the MBP fusion protein ELISA was incorporated in an ELISA plate affinity purification method to isolate autoantibodies from T1D sera. Thirdly the affinity purified antibody samples were analysed by mass spectrometry.

1.2. Type 1 Diabetes

Type 1 diabetes (T1D) also known as Insulin dependent diabetes is a chronic autoimmune disease associated with destruction of 80-90% of the islet beta cells and insulin deficiency that leads to hyperglycaemia (DiMeglio et al., 2018, Kong et al., 2013). T1D disease development is characterized by the presence of high titres of autoantibodies against islet antigens such as Insulin (IAA), Insulinoma associated

autoantigen 2 (IA-2A), glutamic acid decarboxylase (GADA) and Zinc transporter 8 (ZnT8A) (Figure 1.4). These autoantibodies were first described over 50 years ago and are readily used serological markers of autoimmunity utilized in clinical settings for T1D (Pihoker et al. 2005). However, Type 1 diabetes is generally diagnosed first based on the presentation of symptoms such as weight loss, ketoacidosis, polyuria, polydipsia and hyperglycaemia with a fasting blood glucose level above 7.0 mmol/L, or a random blood glucose level above 11.1 mmol/L (DiMeglio et al., 2018). Patients with T1D have been reported to later develop other severe health conditions such as kidney failure, heart disease, blindness, stroke, and ketoacidosis (tom et al. 2011). Autoimmune diabetes is predominantly found in individuals younger than 30 years of age leaving them dependent on insulin therapy for the remainder of their life (tom et al. 2011). To date, T1D is known to arise due to a combination of environmental factors and genetic susceptibility (von Scholten et al., 2021).

1.3. Epidemiology

The incidence of Type 1 diabetes predominantly occurs at ages of 5-7 years old or proximate puberty while Latent autoimmune diabetes in adults (LADA) occur in the later years (age onset of >30 years) (Pozzilli and Pieralice, 2018). Although most autoimmune diseases are more commonly found in women, Type 1 diabetes does not appear to show a gender bias (Atkinson et al., 2014, Warshauer et al., 2020). T1D is most prevalent in Sardinia and Finland >40 and 60 cases per 100 000 people each year, respectively. In contrast the prevalence of T1D in Venezuela, China and India is approximately 0.1 cases per 100 000 per year (Atkinson et al., 2014). Incidence of T1D in Australia has been reported to be approximately 12 cases per 100 000 per year (Health and Welfare, 2020). However, incidence of T1D has been reported to be increasing annually worldwide, for instance an annual increase in incidence of 2.4%, 2.6% and 3.3% have been reported in Finland, Germany and Norway (Patterson et al., 2019, Atkinson et al., 2014).

1.4. Human Leukocyte Antigens (HLA) Genetic susceptibility

Typing of HLA DR and DQ gene usage and family history of T1D has been used to predict the risk of T1D onset. HLA genes are classified into three classes, class I, Class II, and class III. Class II has three regions, DR, DQ and DP. The alleles within these regions are polymorphic and inherited together as haplotypes. Type 1 diabetes is known to be a polygenic disease with the HLA region on chromosome 6 (chromosome 6p21.3) conferring the highest risk of disease onset (Sticht et al., 2021). The alleles in the DR and DQ region of class II, more specifically haplotypes involved in the antigen presentation HLA DRB1*0301-DQA1*0501-DQ*B10201 (DR3) and HLA DRB1*0401-DQA1*0301-DQB1*0301 (DR4-DQ8) and have been reported to be associated with 50% of the genetic susceptibility to disease onset (DiMeglio et al., 2018, Atkinson et al., 2014, Kockum et al., 1999). Studies have shown that the risk of type 1 diabetes onset and islet autoimmunity is approximately 50% in infants with multiple first-degree family history of T1D and HLA DRB1* 0301/DRB1*04-DQB1*0302 genotype (Bonifacio, 2015). In contrast, the inheritance of DRB1*1501 and DQA1*0102-DQB1*0602 are reported to provide resistance to disease (DiMeglio et al., 2018).

1.5. The immune system

The immune system is composed of two main divisions, innate and adaptive immune responses that contributes to the protection from pathogens, clearance of apoptotic cells and wound repairing (Nguyen and Soulika, 2019) (Figure 1.1). The innate immune system contains cells such as macrophages, monocytes, neutrophils, natural killer cells, basophils, mast cells, and eosinophils that are involved in phagocytosis and releasing inflammatory mediators including cytokines and interferons (Delves and Roitt, 2000). These innate immune cells use their membrane bound toll like receptors (TLR) for recognition of foreign bodies through their pathogen associated molecular patterns (PAMPs) on their surface. The presence of these receptors helps the innate immune system to broadly distinguish pathogens from self-proteins (Bean et al., 2013). In addition to the cellular components and their secretions there are also other contributors such as liver generated complement proteins and C reactive proteins. Generally, the

innate immune system initiates proinflammatory responses including changes to local vasculature, recruitment of other immune cells to the site of infection and systemic changes such as fever responses in the presence of a challenge such as infection (Sadighi Akha, 2018).

In contrast to innate immunity, the adaptive immune system incorporates features of diversity, specificity, and memory. This is achieved through the generation of antigen specific responses such as generation of modifiable unique antigen specific immunoglobulins and clonal expansion of those specific responses that allows long term survival and memory in addition to the use of TLR receptors upon communication with the innate immune system. Adaptive immune response includes more specialized cells such as T and B cells that are generated in the thymus and bone marrow, respectively. Upon communication with the innate immune system, B and T cell compartments are modified to generate antigen specific effector responses including clonal expansion of T helper, CD8⁺ cytotoxic T cells and B lymphocytes that generate antigen specific antibody responses (Steinman, 2012).

Figure 1.1. The immune system is comprised of two main divisions, innate and adaptive immune responses. The innate immune system consists of immune cells such as phagocytes, mast cells, dendritic cells, neutrophils, basophils, and natural killer cells. Upon communication with the innate immune system, adaptive immune system that consist of T and B cells generate antigen specific diverse immune responses (Abbas et al., 2014). This image has been removed due to copyright restriction. Available online from

https://books.google.com.au/books?hl=en&lr=&id=RWYWBAQAQBAJ&oi=fnd&pg=PP1&dq=Cellular+and+molecular+immunology+e-book,+Elsevier+Health+Sciences&ots=fv2eg2xGQ3&sig=_BGhuWv9_N_Twx6v0E0_640ydPw#v=onepage&q=Cellular%20and%20molecular%20immunology%20e-book%2C%20Elsevier%20Health%20Sciences&f=false

1.6. Antigen presentation

Antigen presentation is the presentation of antigenic peptides on the surface of antigen presenting cells such as macrophages, B cells or dendritic cells (DCs) to the T cell receptors on T cells (Pober et al., 2017). T cells are a major regulator of adaptive immune responses upon communication with the antigen presenting cells of innate immunity (Steinman, 2012). During antigen presentation, the antigens presented on major histocompatibility complex (MHC) class I molecules interact with T cell receptors on CD8⁺ cytotoxic T cells and antigens presented on MHC class II molecules interact with T cell receptors on CD4⁺ helper T cells (Crespo, H. J., et al. 2013, Ganguly et al., 2013). Following interaction with the antigen, CD4⁺ T helper cells undergo activation and release autologous cytokines such as interleukin-2 (IL-2) that induce their own IL-2 receptors. The secreted IL-2 also stimulates the IL-2 receptors expressed on other CD4⁺ T lymphocytes and antigen presenting cells such as mononuclear phagocytes resulting in enhanced microbicidal activity and class switched antibody

generation by B lymphocytes. The regulatory mechanism that allows the activation of T cells involves multiple signals that facilitate co-stimulation. For instance, in an inflammatory setting, antigen presenting cells express co-stimulatory signals such as C28 and CD40 that helps T cells undergo activation and proliferation (Cruse et al. 2004).

1.7. T cells

Productive T cells are generated and educated in the thymus and include processes such as the generation of unique immunoglobulin surface receptors. Following interaction with either MHC I or MHC II on thymic endothelial cells in the thymus, thymocytes become either CD4⁺ T cells or CD8⁺ cytotoxic T cells (Figure 1.2). They are then further educated against self-antigens during a process called tolerance. The single positive naïve T cells (CD4⁺ or CD8⁺) then leave the thymus and migrate to the lymphoid tissue where they encounter antigen presenting cells and undergo activation (Kumar et al., 2018). Once induced, the CD4⁺ T cells further differentiate into T helper cells including, T helper 1 cells (Th-1) or T helper 2 cells (Th-2) depending on the specific cytokine interaction. Th-1 cells are induced by cytokines such as IL-2 and interferon-gamma (IFN- γ). T helper-2 (Th-2) cells are stimulated by IL-2, IL-4, and IL-12. In the case of an infection, CD8⁺ cytotoxic T cells can recognize the pathogen derived antigens expressed on the surface of the cell and kill the infected cells (Sallusto and Lanzavecchia, 1994). During differentiation following primary antigen stimulation, a subset of the T cells becomes memory cells. Both CD4⁺ and CD8⁺ cells are able to establish memory, hence upon re-activation respond faster than the initial encounter with the antigen. (Wing et al., 2005a).

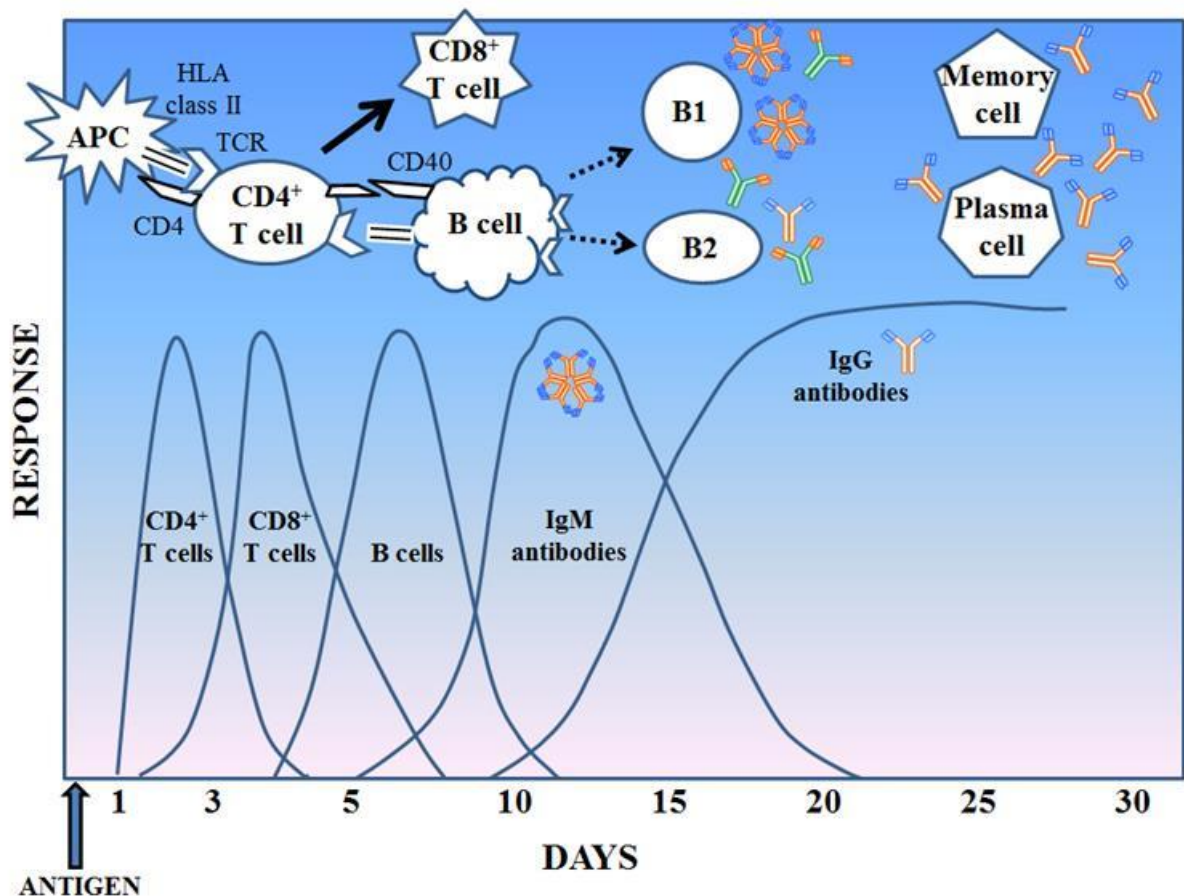


Figure 1.2. Schematic diagram of immune response to a primary antigen over the first 30 days. The innate immunity occurs within the first 0-4 hours of infection that remove the infectious agent. Adaptive autoimmunity occurs approximately >96 hours later as the antigen specific cells first undergo clonal expansion before becoming effector cells. Pre-formed protective immunity including recognition by memory B cell and T cells then takes place in response to a re-infection event (Skarstrand, H. 2014).

Treg cells are another sub-type of T cells that arise in the thymus. Like other T cells, Treg cells are induced by TCR stimulation and antigen presenting cells (Wing et al., 2005a). Once activated, they suppress immune responses with the help of CTLA-4 ligand expressed on the surface in a specific manner during antigen presentation (Clark et al., 2017). This down regulation allows the presentation of self-antigens in a non-inflammatory manner by the APCs. It is suggested that deficiencies in the Treg cell

compartment is correlated to the dysregulation tolerance and autoimmunity (Wing et al., 2005b).

1.8. B Cells

B cells are generated through a sequence of developmental stages where a B cell receptor (BCR) is assembled, expressed, and eventually secreted. B lymphocytes are derived from hematopoietic stem cells in the bone marrow. Progenitor B cells in the bone marrow undergo somatic recombination of the variable (V), diversity (D), Joining (J) and VJ region gene segments of the heavy and light chains respectively to express a complete IgM immunoglobulin heterodimer on the surface of the immature B cell (Cyster and Allen, 2019). The immature B cells are then exposed to self-antigens during tolerance check points. Mature B cells that bypass the tolerance check points leave the bone marrow and migrate to lymphoid organs where they are available for activation against a specific antigen. Once induced, B cells undergo activation and clonal division. B cells can receive further help from T cells to undergo T cell dependent affinity maturation and class switching to further refine the immunoglobulin response (Shahaf et al., 2016, Brady et al., 2010).

1.8.1. B cell immunoglobulin receptor

A diverse repertoire of immunoglobulin B cell receptors (BCRs) are necessary for a vigorous, effective adaptive immune system. Diversity of the BCR is determined by the assembling of the receptor by somatic recombination of immunoglobulin gene segments. This process generates the potential to express approximately 1×10^{15} BCRs with different antibody binding site sequences which is greater than the number of B-lymphocytes in the human body ($\sim 1-2 \times 10^{11}$) (Schroeder, 2006).

B cell immunoglobulins consist of constant and variable regions. They are comprised of heavy and light chains (Kappa or Lambda) which are linked by disulfide bonds. The variable domain includes the Fragment antigen binding region (Fab) that binds to specific epitopes of an antigen, and an Fc domain that is involved in engagement with

Fc receptors, complement fixing and determines the immunoglobulin class (Figure 1.3) (Neuberger et al., 2000). During B cell development, the variable region of the heavy chain of the immunoglobulin (IgH) undergoes gene recombination followed by the recombination of the variable region of the immunoglobulin light chain (IgL) in the bone marrow (Cyster and Allen, 2019).

VDJ recombination involves the gene rearrangement of the variable (V), diversity (D) and joining (J) germline gene segments (Batista and Harwood, 2009). This process involves the random selection of genes from multiple available gene opportunities and allelic exclusion in the V, D and J regions. Genetic recombination also generates more diversity through deletion and addition of nucleotides between ligated gene fragments. DNA polymerases randomly insert templated palindromic or non-templated nucleotides and DNA exonucleases can trim the ends of the gene segments (Georgiou et al., 2014). Once the heavy and light chain genes are fully rearranged, the gene encoding results in the expression of the heterodimer immunoglobulin on the B cell surface. The sequence of rearrangements ensures that a B cell only produces one immunoglobulin receptor specific to a target epitope (Brady et al., 2010).

Mature B cells with IgM receptors migrate from the bone marrow to the periphery where they can take residence in circulation, lymph node or lymphoid tissue and can undergo activation when exposed to exogenous and/or endogenous antigens. Once induced, these B cells undergo clonal expansion and differentiation. A subset of these B cells subsequently proliferates and differentiate into short lived IgM producing plasma cells.

Clonally expanded B cells expressing IgM receptors can also receive T cell help in T cell rich regions such as secondary lymphoid organs (for example, Spleen, lymph nodes), move into a follicle and form germinal centre reaction. Herein, B cells are able to act like antigen presenting cells where they bind to the antigen with the help of BCR, internalize the antigen bound BCR, enzymatically process the antigen BCR complex and present smaller antigenic peptides on the MHC class II molecules on the surface of the cell B cell (McHeyzer-Williams et al., 2012). Antigen specific CD4⁺ T cells recognize the antigenic peptides presented on the surface of the B cell, which in turn

receive assistance by co-stimulatory signals and proliferative cytokines such as, IL-4 and IL-5 (Lanzavecchia and Sallusto, 2000). Subsequently, B cells undergo activation, clonal expansion, affinity maturation and class switching (Lanzavecchia, 1985).

During this process, the subsequent rounds of divisions allow for the accumulation of somatic hypermutation of the variable regions of the B cell immunoglobulins somatic hypermutation with the help of activation induced cytidine deaminase. Somatic hypermutation of the BCRs improves the affinity of the B cells for specific antigens (Fagarasan and Honjo, 2000). In turn B cells with the highest affinity undertake preferential expansion and survival, this is known as affinity maturation (Capra and Kehoe, 1974). Activation induced cytidine also instigate class switching where antibodies with different constant regions (α , δ , γ , ϵ , μ) are generated. A subset of these B cells then differentiates into plasma cells that generate high affinity antigen specific antibodies. Another subset of these B cells with somatically mutated, high affinity antigen specific BCRs differentiate into long-lived, class switched memory cells (Hibi and Dosch, 1986).

Figure 1.3. Schematic diagram of IgG antibody structure. The germline V, D, J and C segments are labelled in the top chains. The framework (FR) and complementary determining regions (CDR) are shown in the bottom chains. The dashed lines represent the disulphide bonds (Georgiou et al., 2014). This image has been removed due to copyright restriction. Available online from <https://www.nature.com/articles/nbt.2782.pdf>

1.8.2. Plasma Cells

Plasma cells are antibody producing B cells that arise when B cells undergo activation. The antibodies expressed by plasma cells are identical to the immunoglobulin receptor expressed on the surface of the B cell they arise from. B cells that undergo activation in the periphery generally become IgM producing short lived plasma cells while B cells that undergo activation with T cell help in the germinal centres can become either short lived or long lived, affinity matured, class switched antibody producing plasma cells. These antibodies are secreted into the blood, and they are able to bind to antigens circulating in the body, neutralizing them, functionally modifying, aid in clearing through immune complex formation or promoting inflammation. As discussed previously, B cells that have received T cell help and differentiate into plasma cells

undergo somatic hypermutation, affinity maturation and class switching that increase the specificity and affinity of the antibody repertoire through incorporation of variable number of substitutions of nucleotides on the V region of the Ig molecule (Neuberger et al., 2000). Secreted antibodies can carry around 20 amino acid (aa) substitutions within the V-region. The number of mutations increases as the immune response mature. Ultimately, B cells with the highest affinity will survive (Neuberger et al., 2000).

1.8.3. Memory B cells

Memory B cells arise in the lymphoid organs after B cells undergo T cell dependent activation in the germinal centres (Cyster and Allen, 2019). Memory B cells preserve specificity for the same antigen as the B cell clone it arises from. Henceforth, they are able to become activated and respond to the antigen rapidly with high affinity class switched antibody responses. These cells are able to swiftly divide and differentiate into plasma cells and secrete high affinity antibodies. Memory B cells generally have variable lifespans that ranges from short life spans such as six months to 10 years or more (Batista and Harwood, 2009).

1.9. Tolerance induction

Immune tolerance is the mechanism through which activation of innate and adaptive immune responses against self-antigens is prevented. There are two main processes, central and peripheral tolerance through which the immune system regulate tolerance. Central tolerance involves the education of T and B cells in the thymus and bone marrow respectively to distinguish between self and foreign antigens (Clement and Santambrogio, 2013). This process involves the negative selection of autoreactive lymphocyte clones (Lu and Zhang 2018).

Thymic medullary epithelial cells, conventional DCs (cDCs) and plasmacytoid DCs (pDCs), remove T cells that bind with high affinity to the self-antigens presented on the MHC class II molecules (Ganguly et al., 2013). This eliminates any self-reactive T cells

at the completion of the maturation process. Similarly, B cells also undergo self-tolerance induction. Receptor editing is the crucial mechanism of central tolerance by B cells (Halverson et al., 2004). B cell receptors with mild or high affinity to self-antigens are regulated by deletion or receptor editing (Basten and Silveira, 2010).

Moreover, each pro B cell undergoes VDJ rearrangement of the Immunoglobulin heavy chain locus. This rearrangement gives rise to a unique heavy chain VDJ sequence that drives the expression of a heavy chain protein. H chain rearrangement initiates the proliferation of the pre-B cells, cell cycle exit and recombination of the immunoglobulin light L chain. Recombination of the light chain involves the rearrangement of V and J elements of either Kappa or lambda light chain Loci. The light chain protein is then expressed on the surface of the B cell paired with the heavy chain. The immature B cell receptor with the unique combinations of heavy and light chains then engage with antigens during central tolerance checkpoints in the bone marrow. BCRs that recognise autoantigens with high affinity induce regulatory mechanisms that assist in evading autoreactivity towards self-antigens by deletion of the autoreactive B cell clones. During central tolerance checkpoints, receptor editing reduces autoreactivity by modifying the specificity and affinity of the receptors resulting in replacement of the light chains bypassing deletion of the B cell clone.

Peripheral tolerance occurs in tissues and lymph nodes that hinders overactive immune responses to self-antigens. This process includes anergy, deletion and suppression by regulatory T cells. In the periphery, in addition to Treg cells, DCs and macrophages inhibit T cells from further maturation (Gallegos and Bevan, 2004). B cells that retain self-reactivity undergo clonal deletion and subsequent cell death by apoptosis (Basten and Silveira, 2010). Breakdown of tolerance leads to autoimmune diseases such as type 1 diabetes, systemic lupus erythematosus, rheumatoid arthritis and Sjogren's syndrome (Lu and Zhang 2018).

Autoimmune diseases and loss of tolerance to self-antigens has also been reported to be associated with the transcription factor autoimmune regulator (AIRE). An AIRE knock out mice study has shown that the expression of self-antigens is reduced in these mice resulting in the escape of self-reactive T cells from negative selection, migration

to periphery and initiation of autoimmune responses to self-antigens. As discussed previously, Treg cells (CD4⁺CD25⁺) are involved in the suppression of immune responses and the absence of Treg cells have been known to result in inflammation and autoimmune diseases. Furthermore, Forkhead box P3 (Foxp3) is a transcription factor expressed by the Treg cells that mediate their own development and function. Interestingly, a mice study has shown that Knockout or mutated Foxp3 gene result in the development of systemic autoimmune disease. In humans, mutation in Foxp3 gene leads to a genetic disease called immunodysregulation polyendocrinopathy enteropathy X linked syndrome (Lu and Zhang 2018). The deletion of self-recognising mature T and B cells is also regulated by Fas (CD95) receptor of the tumour necrosis factor (TNF) receptor family ligand binding. This process prevents over active immune responses (Kappler et al., 1987). In addition to genetic susceptibility, environmental factors have been reported to contribute to the development of autoimmune diseases. This is supported by the lack of concordant rates of autoimmune diseases in Monozygotic twins. Epigenetic studies have shown that breakdown of immune tolerance leading to autoimmune disorders may also potentially result from DNA methylation and post translational modification of histones (Lu and Zhang 2018).

1.10. Autoimmune T1D

As discussed previously, T1D is a chronic autoimmune condition that is known to arise due to the infiltration of pancreas by adaptive and innate immune cells. Subsequent chronic inflammation and destruction of the beta cell mass is known to result in hyperglycaemia and T1D clinical onset. T1D has been reported to be predominantly a T cell driven autoimmune disease that occur in children and adolescents while another subtype of T1D occur due to self-reactive innate immune effectors. Both CD4⁺ and CD8⁺ T cells are involved in beta cell destruction. CD8⁺ T cells are known to drive beta cell destruction via perforin and granzyme B- and Fas-Fas ligand interactions. In contrast, CD4⁺ cells mediate beta cell destruction by secretion of proinflammatory cytokines. Development of autoimmune T1D may be a result of the breakdown of central and peripheral tolerance resulting in events such as the expansion of beta cell specific effector T cells and suppression of T regulatory cells, faulty processing of self-antigens and altered beta cell responses. These maybe attributed to both genetic and environmental factors (Clark et al., 2017).

One mechanism through which beta cell specific autoreactive TCRs are generated is ineffective negative selection of self-reactive single positive thymocytes in the thymus. In healthy individuals, recognition of self-peptides bound to MHC complexes with high affinity/avidity leads to enhanced TCR signalling and thymocyte apoptosis. Breakdown of this regulatory process may result in the accumulation of high affinity self-reactive T cells. NOD mice study has reported that elevated protein tyrosine phosphatase non-receptor 22 (PTPN22) activity reduces TCR signalling which in turn hinder the apoptosis of self-reactive thymocytes indicating that the development of T1D may be attributed to elevated PTPN22 activity. Enhanced PTPN22 activity is also known to reduce the generation of Foxp3 expressing Treg cells which in healthy conditions facilitate the suppression of high affinity/avidity autoreactivity against self-peptides. In addition, a NOD mice study has reported that the reduced AIRE expression may potentially result in the development of autoimmune T1D. As discussed previously, insulin is one of the major autoantigens targeted in T1D. It has been reported that individuals with 26-63 variable number of tandem repeats (VNTRs) prior to the insulin coding gene INS, have reduced thymic INS2 expression and elevated risk of developing T1D. Furthermore, reduced thymic expression of INS has been reported to down regulate negative selection and subsequent development of insulin specific thymocytes (Clark et al., 2017).

DCs have been speculated to be associated with pathogenesis in autoimmune diseases such as T1D (Ganguly et al., 2013). It is well established that beta cell derived antigens are constantly being presented on DCs to T cells in the pancreatic lymph nodes (PLN). However, it is not understood why these cells provoke an immune reaction instead of tolerance in response to antigens. It is hypothesized that the apoptotic pancreatic beta cells release DNA binding protein high mobility group B1 (HMBG1) which activate DCs via TLR-2 and TLR-4 interaction. (Ganguly et al., 2013). In addition to DCs, studies have shown an association between the lack of T cell tolerance and autoimmune diabetes. It is suggested that autoreactive T cells that escape central tolerance checkpoints in the thymus and come into contact with beta cell antigen in the pancreatic lymph nodes. T cells maybe recognizing these beta cell antigens because they were presented on DCs following beta cell death. When auto reactive T cells in the PLN

identify beta cell antigens as foreign, they undertake activation and clonal expansion. They then migrate to the islets to cause beta cell destruction (Mathis et al., 2001).

It is considered that along with T cells and DCs, impaired B cell tolerance may also contribute to T1D progression. Disruption of the central tolerance check points may lead to the T1D disease process. It is possible that within the bone marrow in T1D patients, there is a deficiency in the presentation of pancreatic islet antigens to the immature B cells in comparison to healthy individuals. Another possibility is that the mechanism that drives apoptosis of B cells that bind to self antigens with high affinity is disrupted. On the other hand, it is also likely that the mechanism that initiate receptor editing of the BCR during central tolerance that modifies the affinity and specificity of the receptor is dysregulated.

In the case of disrupted central tolerance due to the putative mechanisms discussed above unique VDJ recombination may give rise to distinct B cell clones that may be autoreactive. These autoreactive B cell clones that bind to self-antigens with high affinity will move on to the lymphoid organs where they undergo positive selection and affinity maturation. Therefore, the B cells with variable region heavy and light chain rearrangements that are autoreactive will undergo proliferation of autoreactive B cell clones. This will result in pathophysiological pathways that drive inflammation in the pancreas and in turn give rise to autoimmune reactions towards self-antigens within the pancreas (Wong and Wen, 2005). Therefore, it is likely that genetic predisposition coupled with absence of tolerance causes autoimmune T1D.

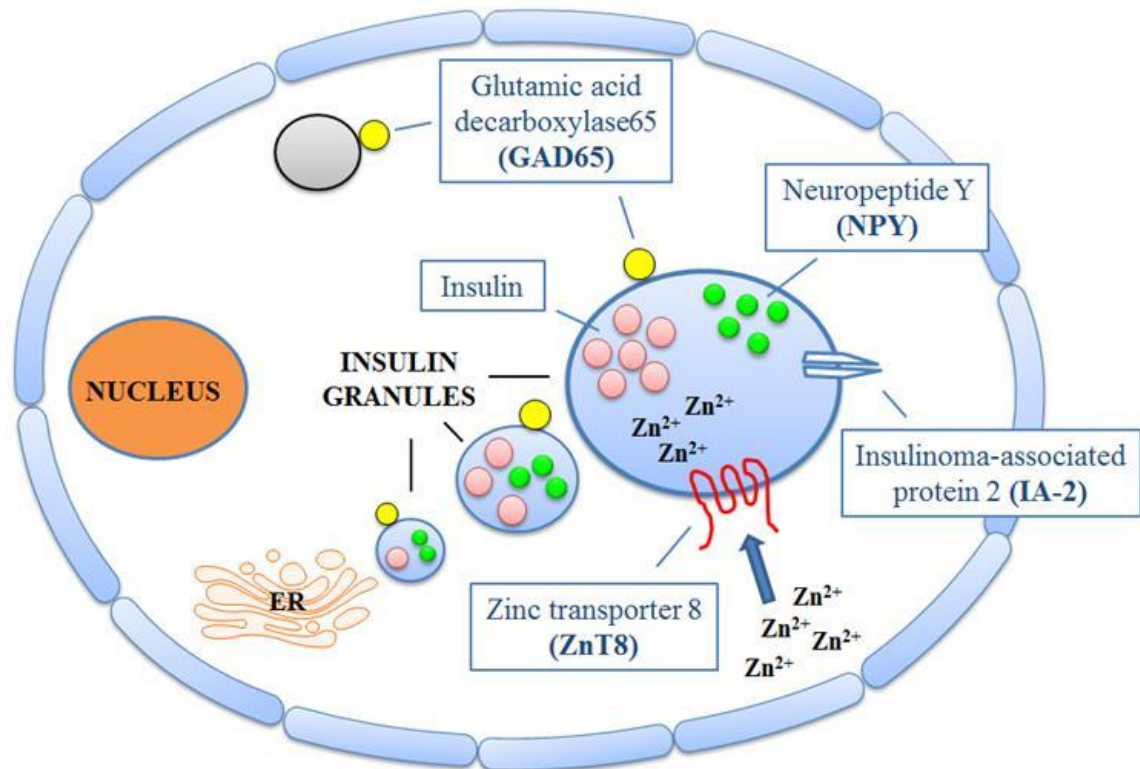


Figure 1.4. Major intracellular pancreatic beta cell autoantigens that are targeted in T1D. Insulin is found within the insulin secretory granule while GAD65, IA-2 and ZnT8 are found within the transmembrane of the secretory granule (Skarstrand, H. 2014).

1.11. Autoantigens

1.11.1. Insulin

Insulin is the major islet antigen in T1D, and it is secreted by the pancreatic beta cells. Insulin is initially formed as a prepro-hormone composed of B-chain, C-peptide, A-chain, and a signal peptide (Figure 1.3.). There are epitopes for autoantibody binding on the A chain between aa 8-13 and aa 28-30 on the B chain (Shen et al., 2019). In the endoplasmic reticulum (ER), the signal peptide cleaves off producing proinsulin. Endopeptidases in the ER then cleave off the C-peptide forming the mature form of insulin. In the Golgi, C peptides and mature insulin is bundled into secretory granules and excreted into the cytoplasm. When induced, insulin is secreted into the blood stream (Culina et al., 2013a).

Figure 1.5. Amino acid sequence of preproinsulin (PPI) displaying A chain, B chain and C peptide. Disulphide bonds are represented by S-S (Culina et al., 2013b).

This image has been removed due to copyright restriction. Available online from <https://academic.oup.com/ejendo/article-abstract/168/2/R19/6659660?redirectedFrom=fulltext&login=false>

1.11.2. Glutamic Acid Decarboxylase

Glutamic acid decarboxylase (GAD) is an enzyme that takes part in the synthesis of neurotransmitter gamma aminobutyric acid (GABA) (McKeon and Tracy, 2017). Two

isoforms are found in mammals GAD65 and GAD67. Their molecular weights are 65 and 67 kDa respectively and share 65% of the sequence. GAD65 is found in neuroendocrine cells including pancreatic islet cells and pancreatic neurons. GAD65 takes 3 forms in the beta cells fixed membrane bound form, soluble hydrophobic form with low membrane avidity and a hydrophilic form (Christgau et al., 1992).

Figure 1.6. Schematic diagram of islet antigen Glutamic Acid Decarboxylase enzyme. The antigenic epitopes within the C and N terminal are recognized in various diseases including T1D (Baizabal-Carvallo and Jankovic, 2015). This image has been removed due to copyright restriction. Available online from https://jnnp.bmj.com/content/jnnp/86/8/840.full.pdf?casa_token=Exw4IIvqCO4AAA:AA:eTUncvF8sjJ1yiyJ8hDvHVso_16xMS_bRF0b8kjvNRREpMTKRk2bv-5zkREEXahFV2Bwf3weYow

1.11.3. IA-2

Islet antigen-2, previously identified as ICA-512, neuroendocrine antigen IA-2, *Insulinoma-associated protein 2* was isolated by several groups simultaneously. Another isoform found in T1D patients is IA-2 β phogrin islet cell antigen (Acevedo-Calado et al., 2019). The two proteins share 88% of the PTP like domain aa sequence, less than 50% of the juxtamembrane domain sequence and approximately 10% of the extracellular domains (Bonifacio et al., 1998).

IA-2 is a protein tyrosine phosphatase (PTP) like transmembrane protein of 979 aa. The molecular mass of IA-2 has been reported to be 106 kDa. It has been shown that IA-2 antigen is expressed in the reticulocyte transcription/translation system (Lu et al., 1996). IA-2 has been reported to have no enzymatic activity owing to a few substitutions in the conserved sites (877 and 911) however; IA-2 β has been reported to have weak enzymatic activity. As well as that, there is some evidence that IA-2 may

have an effect on exocytosis (Buzzetti et al., 2015). IA-2 is composed of intracellular transmembrane portion and an extracellular portion. This protein is generally found in secretory vesicles and neuroendocrine cells in beta cells. It was known that autoantibodies primarily target the intracellular portion (PTP domain of ~300 aa along with juxtamembrane domain of <100 aa), which extends into the cytoplasm, which is only available for antibody binding during cell damage. Recently, IA-2Abs have been directed against the extracellular region. Luminal ectodomains are 600 aa and are cleaved to produce ~64 kDa mature proteins (Solimena et al., 1996).

Currently, sensitive radioimmunoassay are used to detect IA-2 antibodies (Notkins and Lernmark, 2001). Radiolabelled constructs used for screening are full length IA-2_{FL} (1-979), the truncated NH₂-terminally spliced IA-2 lacking exon 13 IA-2_{BDC} (256-556: 630-979) and the IA-2_{IC} (605-979) construct. A study has shown that IA-2_{IC} is most effective at detecting IA-2 antibodies with the highest sensitivity in pre-diabetic and newly diagnosed type 1 diabetic patients. However, the same study revealed that intracytoplasmic construct did not represent the complete humoral immune response in type 1 diabetes. They reported that other constructs such as the extracellular construct showed additional immunoreactivity which were not detected by IA-2_{IC} (Bearzatto et al., 2002).

Figure 1.7. Schematic diagram of full-length IA-2. IA-2 consist of an extracellular domain (EC), Transmembrane region (TM), and intracellular cytoplasmic domain of IA-2 containing Juxtamembrane region (JM) and PTP like domain. The IA-2_{ic} construct utilized in this study contains the intracellular domain including the JM and PTP regions (Bearzatto et al., 2002). This image has been removed due to copyright restriction. Available online from <https://journals.aai.org/jimmunol/article/168/8/4202/34374/Two-Distinctly-HLA-Associated-Contiguous-Linear>

1.11.4. Zinc transporter (ZnT8)

ZnT8 protein is a transmembrane protein with 6 domains. Both C and the N-terminal

ends of the ZnT8 protein are found in the cytosol of the cell (Figure 4) (Huang et al., 2019). The histidine rich loop between 4th and the 5th domain is a putative binding site for Zinc in the cytosol. ZnT8 transporter belongs to the ZnT family of zinc transporters, which are involved in transporting cytosol zinc into the secretory vesicles (Palmiter and Huang, 2004). ZnT8 protein is mainly expressed in the beta cells of the islets of the Langerhans but also found in alpha cells together with testes and kidneys. In addition, transporters belonging to ZnT family such as, ZnT3, ZnT5 and ZnT7 are found in beta cells in rodents (Chimienti et al., 2004).

SLC30A8 gene on chromosome 8 encodes ZnT8 protein. The 325 aa on the C-terminal of ZnT8 protein is encoded by two single nucleotide polymorphisms (SNP) rs13266634 and rs16889462 in SLC30A8 (Sladek et al., 2007). The SNP rs13266634 causes a substitution from Arginine (R) encoded by CGG (C-allele) to tryptophan (W) encoded by TGG (T-allele). In the common Caucasian population, the C/C genotype (R/R) is present in 46-48%, T/T genotype (W/W) is found in 10-13% and C/T heterozygous genotype is found in 40-42% (Gohlke et al., 2008).

The SNP 16889462 instigates a substitution from R (CGG) to Glutamine (Q) encoded by CAG (A-allele). This SNP and its incidence are not well understood. However, in China, A/A genotype (Q/Q) is found in less than 1% of the general population. Moreover, 91% of the population was G/G genotype (R/R) and 9% were A/G genotype (Huang et al., 2010).

Zinc (Zn) plays an imperative role in cellular homeostasis and regular physiological processes. These processes include enzyme activity, intracellular signalling and protein and DNA synthesis. It is the highest abundant element in the human body (2-4g in the body) (Jansen et al., 2012). In the pancreas, Zn is involved in digestive enzyme activity, glucagon secretion, insulin packaging, secretion, and signalling. As Zn is an essential component any irregularity in Zn, impairs significant mechanisms (Kelleher et al., 2011). Two families of zinc transporters, SLC30A (ZnT) family and SLC39 (ZIP) family regulate zinc homeostasis. The ZnT transporters are involved in transporting zinc out of the cytosol into organelles or extracellular spaces (Figure 5). The Zip family transports Zn into the cytosol from extracellular regions and intracellular organelles (Eide, 2006). Demand of Zn mediates the expression and activity of these transporters (Huang, 2014).

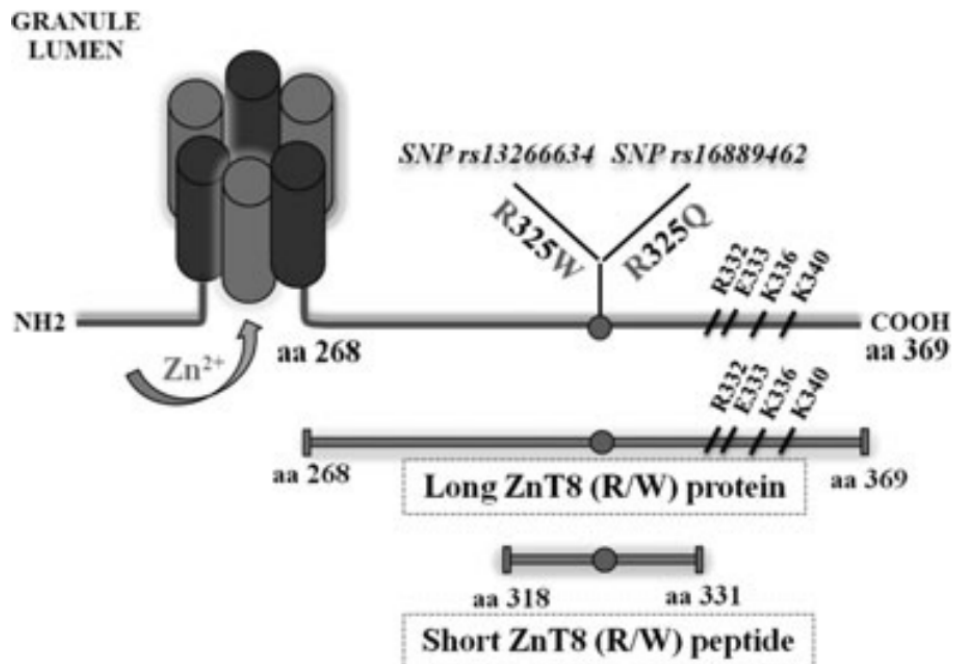


Figure 1.8. A model of the ZnT8 transmembrane protein. ZnT8 protein is comprised of 6 domains, N-terminal, cytoplasmic C-terminal and the Histidine rich region (Chimienti et al., 2006).

Figure 1.9. Zn transporters in different types of islet cells. Zip1, Zip10 and Zip14 transporters found in alpha cells are reported to be involved in Zn movement into the cells. Zn then binds and open ATP dependent K⁺ channels and inactivate voltage dependent calcium channels that results in decline in glucagon secretion. Zip4 allows the Zn movement into the beta cells. ZnT8 allows the movements of Zn into the insulin granules. Zip 5 allows the movement of Zn into Acinar cells. Zn moves into the Zymogen granules via ZnT2 (Kelleher et al., 2011). This image has been removed due to copyright restriction. Available online from <https://www.sciencedirect.com/science/article/pii/S2161831322005701?via%3Dihub>

Type 1 and 2 diabetes is associated with incoherent Zn homeostasis. It has been shown that Zn insufficiency influences glucose metabolism and insulin secretion. In addition, Zn is critical for the crystallization of the insulin hexamer, which has two Zn ions in its the centre (Dunn, 2005). Although the main function of the ZnT8 transporter is to facilitate Zn movement into the cytosol, its role in glycaemic control is not well described (Rungby, 2010).

SNP rs13266634 in SLC30A8 is associated with T2D as well as reduced insulin secretion in healthy individuals who carry the C-allele (R325W) (Staiger et al., 2007). It has been shown that T2D patients have decreased plasma Zn levels in comparison to healthy controls. Recent studies have revealed that beta cell specific ZnT8 knock out mice as well as humans carrying SNP with the risk C-allele have lowered blood insulin levels (Boesgaard et al., 2008). In coherent, individuals with the C-allele (R325W) were speculated to have impaired proinsulin conversion in the beta cells causing a reduction in peripheral insulin level (Kirchhoff et al., 2008).

1.11.5. Other autoantigens

There are other minor autoantigens, which are present in approximately 35% of the newly diagnosed T1D patients (Hirai et al., 2008). For instance, the islet cell protein 12 (ICA12) also known as a partial clone of SOX13 which is a member of Sox (Sry related

HMG box) transcription factor family. A study reported that about 18% of T1D patients are positive for antibodies against SOX13 (Kasimiotis et al., 2001). Vesicle associated membrane protein 2 (VAMP-2) and Neuropeptide Y (NPY) are other autoantigens associated with T1D (Regazzi et al., 1995) (Hirai et al., 2008).

1.12. Islet autoantibodies

Islet autoantibodies are biomarkers of T1D. An islet antibody can arise at any age and have been reported to appear as early as 6 months and peak around 2 years of age in genetically susceptible individuals prior to symptomatic clinical onset (Atkinson and Eisenbarth, 2001). The presence of the first autoantibody is generally followed by the appearance of multiple autoantibodies within one year period (Yu et al., 1996).

To date, there are four primary islet autoantibodies associated with the development of T1D, IAA, IA-2A, GADA and ZnT8A (Lampasona and Liberati, 2016). Approximately 90% of the newly diagnosed T1D patients have one or more islet autoantibodies (Atkinson et al., 2014). It has been reported that 98% of the first-degree relatives who later developed the disease had one or more islet autoantibodies. In addition, individuals who were positive for two or more autoantibodies have been shown to have a 68% risk of developing the disease within the next five years. It was also reported that the risk of disease onset increased rapidly with positivity to each additional autoantibody in first degree relatives (Pihoker et al., 2005).

1.12.1. Multiple islet autoantibodies

It has been shown that 70-90% of the healthy children with HLA risk gene along with positivity for two or more islet autoantibodies developed T1D within 10 years, in comparison only 15% of children with single autoantibody developed the disease. The risk of clinical onset was 0.4% if the children had no autoantibodies (Steck et al., 2011). Children who underwent multiple seroconversions before the age of 3 years (75%) progressed to clinical onset earlier than the children older than 3 years of age (61%) (Ziegler et al., 2013).

1.12.2. Autoantibody patterns

It has been shown that the time of first antibody arrival is correlated to the rate of progression to disease onset. Therefore, the first antibody appearance at younger age leads to earlier age disease onset (Knip et al., 2010). The first antibody that appears in

healthy children at risk is known to be IAA. This antibody level peaks around the age of two years. Subsequently, GADA appears at 3-5 years of age (Ilonen et al., 2013). IA-2A is the least likely to be the first antibody to appear. Offspring to parents with T1D produce these multiple antibodies. Children who were diagnosed at the age of 2 years or earlier had higher titres of IAA, but not GADA and IA-2A, in comparison to children who were diagnosed at a later stage. Unfortunately, the end-point titres of the islet autoantibodies are not well reported. It has been discussed that sera with high levels of antibodies, may give false negatives due to prozone phenomenon (Hansson et al., 2011). This is where non-specific blocking antibody level is high, which in turn prevents the specific antibody from binding to the antigen. Nevertheless, if the serum were diluted, the concentration drops enough to allow accurate precipitation reaction to take place. Antibodies are known to be valuable tools for disease prediction, diagnosis, disease therapy and prenatal therapy. However, there is only limited understanding of antibody function at cellular level, which may be contributing to the disease progression (Lampasona and Liberati, 2016).

1.12.3. Autoantibody isotopes

Each antibody type plays a different role when an immune response is induced. The first antibody produced in an immune response is IgM followed by IgG depending on the cytokines produced by the T cells (Figure 2). It was speculated that in healthy children at risk of developing diabetes, the initial antibody response was IgM followed by class switched IgG response. In healthy children without risk IgM declines and eventually disappear. Studies also propose that IgG response is predominantly IgG1 type and IgG3 type were also found in the immune response (Hawa et al., 2000).

1.12.4. IAA

Insulin antibody was first detected in serum from newly diagnosed T1D patients in a competitive radiobinding assay and was hypothesized to be a marker of beta cell damage (Palmer et al., 1983). These autoantibodies may be found in individuals as early as 9 months of age (Pociot and Lernmark, 2016). IAA may be present at the age of 6

months; however, these are likely to be originating from the mother. Children who are IAA positive at 9 months of age had 27% risk of developing the disease. The risk increases to 100% if multiple autoantibodies are present at 9 months (Palmer et al., 1983). Studies have reported that, IAA is predominantly detectable in patients with an onset age of less than five years. Furthermore, the levels of IAA have been reported to decline with increasing age (Ziegler et al., 1999).

As mentioned earlier there are several autoantigenic epitopes on the A and B chain of the insulin molecule. In addition, T cells were shown to identify aa 10-18, 9-23, and 15-24 regions on the signal peptide (Bulek et al., 2012). It has been revealed that B chains from the pro-insulin peptides are presented on the HLA DR4 and HLA DQ8 molecules of the CD4⁺ T cells. It is speculated that the type of DCs determines which epitopes are presented for processing. Furthermore, numerous studies have shown a close association between IAA and HLA DQ8 (Kanatsuna et al., 2012).

1.12.5. GADA

Autoantibodies against GAD65 were first identified in newly diagnosed T1D patients in 1982. These antibodies are present in approximately 70-80% of the newly diagnosed T1D patients (Bonifacio et al., 1995) while only 2-4% in the general population (Hagopian et al., 1995). The incidence of GADA was reported to be 55% in the acute onset patients in the Chinese population (Chao et al., 2013). Relatively, 70% of the GADA positive individuals developed T1D within 8 years (Kulmala et al., 1998). Anti-GAD antibodies have been reported to be associated with the slow progression of T1D onset (Christie et al., 1994). The GADA titres are shown to remain stable after the clinical onset for several years (Vaziri-Sani et al., 2010). GADA has been reported to be associated with DQ2 and DQ8 haplotypes (Sabbah et al., 1999).

1.12.6. ZnT8A

This is the most recently identified T1D autoantibody. They are three known variants ZnT8R autoantibodies (ZnT8RA), ZnT8W autoantibodies (ZnT8WA), and ZnT8Q

autoantibodies (ZnT8QA) (Wenzlau et al., 2008b). These antibodies are directed against the polymorphic region aa 325 of the C-terminal part of the ZnT8 protein (Gu et al., 2021). In newly diagnosed T1D patients the prevalence of ZnT8A is 58-83% (Kawasaki et al., 2011). In the Caucasian population ZnT8RA (50-54%) are more prevalent compared to ZnT8WA (41-50%) and ZnT8QA (32-36%). ZnT8QA are generally only found in combination with either ZnT8WA or ZnT8RA. Furthermore, it has been shown that T1D patients with C allele have ZnT8RA and patients with T-allele had ZnT8WA (Wenzlau et al., 2008a). Interestingly, 30-44% of ZnT8A positive patients have antibodies against all three variants. It is known that regardless of a patient being homozygous for R-variant, the individual will be positive for antibodies against the W variant (Delli et al., 2012).

The prevalence of ZnT8A declines with increasing age. ZnT8A are seldom detected in children before two years of age, however; they have also been associated with older onset age (>8 years) (Salonen et al., 2013). ZnT8A presence was closely related to HLA DQ6.4 (DQA1-B1*X-06:04) and DQ8 (DQA1-B1*03-0302) but was negatively correlated to DQ2 (DQA1-B1*05:02) and DR3/DR4 (Andersson et al., 2013).

When newly diagnosed T1D patients were investigated for six years, it was shown that the ZnT8A (ZnT8WA and ZnT8QA) levels declined over the span of the disease along with C-peptides. This implies that presence of ZnT8A diminishes beta cell function (Sorensen et al., 2012). In addition, ZnT8QA have been associated with lowered glucose metabolism measured by oral glucose tolerance test (OGTT) or intravenous glucose tolerance test (IvGTT). Furthermore, ketoacidosis is more prevalent in ZnT8A negative patients compared to ZnT8A positive patients (Salonen et al., 2013).

1.12.7. IA-2 Antibodies

Approximately 70% of T1D patients were found to be positive for antibodies against IA-2 (Acevedo-Calado et al., 2019). Presence of antibodies to IA-2 was identified as a good predictive marker for the disease development (Lu et al., 1996). It has been shown that in children with multiple autoantibodies, presence of IAA together with IA-2A

confers a higher risk (84%) of disease onset within 10 years when compared to combination of IAA and GADA (55%). The presence of IA-2A in individuals at risk was related to high possibility of disease development. Research has shown that IA-2A is found earlier in children with shorter prodromal stage (<3 years) in comparison to islet autoimmunity in children with longer prodromal stage (>10 years). Majority of the newly diagnosed T1D patients are positive for these antibodies as compared to <2% of the normal controls. Approximately, 60-80% of the newly diagnosed T1D patients in USA and Europe are positive for IA-2 Abs. The prevalence drops to approximately 45% in those diagnosed after 20 years of age (Decochez et al., 2000). T1D patients have been found to have antibodies against the intracellular portions of both IA-2 and IA-2 β which were shown to be cross reactive (Bonifacio et al., 1998). A recent study has shown that the IA-2 autoantibodies are closely related to the BMI of the T1D patients (Buzzetti et al., 2015). In a study where radiolabelled insulinoma cell lysates were incubated with diabetic sera then treated with trypsin presented a precipitation of 37 kDa and 40 kDa tryptic fragments. Antibodies to these fragments were found in high levels in diabetic patients.

1.13. Autoantibody epitopes

It is known that multiple epitope presentation is correlated with progression of T1D (Miao et al., 2002). In early stages of disease, IA-2 antibodies identify epitopes in the juxtamembrane domain and in later stages they also detect epitopes in the IA-2 β domain. This suggests epitope spreading related to disease progression (Naserke et al., 1998). Conversely, another study has shown that younger children have more epitope spreading than at clinical onset than older children who had stable epitopes. GADA were shown to mainly recognize the middle region of the conformational epitope (Hampe et al., 2000). GADA positive patients were also found to identify linear epitopes. ZnT8 antibodies react depending on the aa at the position 325. Although aa 325 on the C-terminal is considered to be the main epitope, the adjacent R332, E333, K336 and K340 were also considered to be antigenic and associated with aa325 epitope (Wenzlau et al., 2011).

1.14. Autoantibody affinity

Children who were only positive for IAA had reduced affinity compared to when multiple antibodies were present. High-affinity IAA identified epitopes on the insulin A chain and proinsulin; meanwhile, the low-affinity antibodies only detected epitopes on the C-terminal insulin B chain. The IAA affinity was not correlated to their titres. GADA affinity was found to be incoherent with IAA. Children with multiple antibodies showed high affinity to GADA (Mayr et al., 2007).

1.15. Use of MBP affinity tags in the expression of recombinant fusion proteins

Proteins are not soluble in aqueous solvents due to high hydrophobic amino acid content on the surface. Solubility of a protein increases as charged and polar surface residues interact with ionic groups in the solution (Baneyx, 1999). *Escherichia coli* (*E. Coli*) maltose-binding protein (MBP) is a useful affinity tag as it is known to improve solubility and promote proper folding of fusion proteins (Ki and Pack, 2020).

Affinity tags are known to enhance recombinant protein throughout, protect from intracellular proteolysis as well as improve their solubility (Routzahn and Waugh, 2002). *E. Coli* MBP used in the proteins of interest is well known to be effective in enhancing solubility. This maybe because MBP swiftly and effectively come to its innate conformation, as it exists the ribosome and this endorses correct folding by isomerization pathway. This makes MBP an appealing tag given that insolubility is found to be the major impediment in high throughput protein expression and purification (Edwards et al., 2000).

Unfortunately, MBP fusion proteins do not always bind competently to amylose resin. Furthermore, is difficult to yield a satisfactory pure sample from a single affinity purification step. To address this challenge additional tags could be incorporated into framework of the MBP fusion protein. These tags could be used in coherent with MBP in order to achieve a higher purity (Pryor and Leiting, 1997).

IA-2ic recombinant fusion protein was used in ELISA since, Lampasona and the colleagues exhibited that the intracytoplasmic region of IA-2 antigen is the main target of humoral autoimmunity, and the antigenic epitopes lie within the JM (aa 601-682) and PTP domain (687-979). Lampasona et al. also reported that IA-2ic region is the most effective in detecting IA-2 autoantibodies in T1D patients (Lampasona et al., 1996).

ZnT8 cytoplasmic fragment was used for detecting autoantibodies in sera. It has been shown that the single nucleotide polymorphism at aa 325 determines the antigenicity of the protein. Skarstrand et al reported that ZnT8 recombinant protein comprising aa 268-369 with the single nucleotide polymorphism at aa 325 is able to detect autoantibodies against the three variants of ZnT8 in T1D sera (Skärstrand et al., 2013). These antigenic recombinant proteins were fused with maltose binding protein which is an affinity tag that improves solubility and correct folding (Rondard et al., 1997).

1.16. Analysis of clonality and variable region gene usage of anti-IA-2 antibodies using mass spectrometry sequencing

Proteomic studies of autoantibodies in systemic autoimmune diseases have reported that the humoral response against a common antigen may be clonally restricted and shared among unrelated patients. However, little is known about the nature of the autoimmune responses in T1D. A single cell study that looked at the V region of monoclonal antibodies that targeted the PTP domain of IA-2 reported that the antibody response is governed by V_H germline gene (DP-71) (Kolm-Litty et al., 2000). However, this study was unable to accurately represent the B cell repertoire driving the disease humoral response in T1D patients and involves a selection bias. To our knowledge, this thesis attempts for the first time to understand the secreted circulating autoantibody repertoire that targets the IA-2 antigen in T1D patients. We discuss a novel bottom-up approach to affinity purify and analyse the molecular signature of serum derived anti-IA-2ic antibodies by high-throughput mass spectrometry.

1.17. Specific aims and hypothesis

As discussed previously, T1D is characterised by the presence of autoantibodies against pancreatic islet antigens and beta cell destruction. However, little is known about the molecular characteristics and the role of these autoantibodies in the disease process at the cellular level. While the presence of clonally restricted pathogenic antibodies has been demonstrated in systemic autoimmune diseases, investigation of autoantibodies in organ confined autoimmune diseases such as T1D has been hindered due to the complexity of the disease and low antibody titres. This study attempted to develop an ELISA based approach utilising recombinant MBP fusion protein of IA-2ic domain to firstly detect anti-IA-2 antibodies from T1D sera. Secondly the IA-2ic MBP fusion protein ELISA was utilized in an ELISA plate affinity purification method to isolate anti-IA-2 antibodies from T1D sera. The affinity purified antibodies were then assessed for clonality, variable region gene usage and aa mutation distribution by high resolution mass spectrometry sequencing to characterise the molecular signature of the anti-IA-2ic antibodies of T1D patients.

The specific aims and hypotheses of thesis are as follows:

Aim 1. To develop an ELISA assay to detect anti-IA-2 antibodies from T1D sera using a recombinant MBP fusion protein incorporating the intracellular domain of IA-2 protein.

Hypothesis. Anti-IA-2 antibodies from T1D patient sera will recognize epitopes within the intracellular domain of IA-2 expressed as a recombinant MBP fusion protein.

Aim 2. To develop an affinity purification method capable of isolating anti-IA-2 antibodies that recognize epitopes within the intracellular domain of IA-2.

Hypothesis. The anti-IA-2 antibodies that targets epitopes within the intracellular domain of IA-2 can be affinity purified using the IA-2ic MBP fusion protein ELISA plate affinity purification method.

Aim 3. To determine the clonality and variable and joining region gene usage of the affinity purified secreted anti-IA-2ic antibodies using de novo mass spectrometric sequencing.

Hypothesis. The secreted antibodies that target the intracellular domain of IA-2 in T1D patients are derived from a clonally restricted public B cell clonotype.

Chapter 2: Materials and Methods

2.1. Patients and controls

Blood samples were collected from patients with T1D (35 males and 31 females, mean age 37.78 ± 15.87 years, range of age 17-75) attending outpatient clinics at the Flinders Medical Centre, South Australia. Samples were also collected from healthy volunteers (6 females and 7 males, mean age $32.23, \pm 9.65$, range of age 22-55). Cohort 1 comprises of sera collected in 2003-2013 and screened using IA-2 RSR ELISA kit Version 1. Cohort 2 comprises sera collected in 2013-2015 and screened using IA-2 RSR ELISA kit Version 2. Sera were obtained by centrifuging blood samples at 2500 rpm for 10 minutes. Recruitment of patients for the study was approved by Southern Adelaide Clinical human research ethics committee.

Table 2.1. Patient demographics of the T1D cohort 1. Cohort 1 was screened using the RSR and MBP fusion protein ELISA for the presence of anti-IA-2 and anti-ZnT8R antibodies.

	Patient code	Gender	Age
1.	T1D019	F	-
1.	T1D008	M	33
2.	T1D046	M	26
3.	T1D035	M	19
4.	T1D011	M	38
5.	T1D016	F	60
6.	T1D051	F	34
7.	T1D045	M	25
8.	T1D030	M	57
9.	T1D040	M	23
10.	T1D047	M	35
11.	T1D034	M	40
12.	T1D039	F	22
13.	T1D041	M	28
14.	T1D002	F	-
15.	T1D042	F	28
16.	T1D010	F	40
17.	T1D044	M	24
18.	T1D013	F	20
19.	T1D043	M	27
20.	T1D005	M	60
21.	T1D049	M	28
22.	T1D021	M	27
23.	T1D050	M	20
24.	T1D015	-	-
25.	T1D037	F	40
26.	T1D028	F	60
27.	T1D003	F	55
28.	OTH121	-	-
29.	T1D038	M	22
30.	OTH126	-	-
31.	T1D004	M	63
32.	T1D022	F	18
33.	T1D007	M	31

Table 2.2. Patient demographics of the T1D cohort 2. This cohort was also screened using the RSR and MBP fusion protein ELISA for the presence of anti-IA-2 and anti-ZnT8R antibodies.

	Patient code	Gender	Age
1.	T1D057	F	50
1.	T1D069	F	17
2.	T1D001	M	38
3.	T1D014	F	75
4.	T1D065	F	50
5.	T1D019	F	-
6.	T1D009	F	-
7.	T1D012	M	34
8.	T1D017	F	64
9.	T1D023	M	58
10.	T1D024	F	-
11.	T1D025	M	-
12.	T1D026	M	55
13.	T1D027	F	-
14.	T1D029	F	35
15.	T1D036	F	39
16.	T1D048	M	31
17.	T1D051	M	46
18.	T1D052	M	27
19.	T1D054	F	26
20.	T1D056	F	26
21.	T1D058	M	17
22.	T1D059	F	27
23.	T1D061	F	26
24.	T1D062	M	40
25.	T1D063	M	23
26.	T1D064	F	55
27.	T1D066	M	32
28.	T1D067	M	42
29.	T1D068	M	72
30.	T1D010	F	-
31.	T1D074	-	-

2.2. Statistical analysis

ANOVA non-parametric testing was used to analyse correlations between serial dilution binding of patient sera to IA-2 fusion protein.

2.3. RSR ELISA for the detection of IA-2, ZnT8 and GAD antibodies in T1D patients

Patient sera were screened for the presence of autoantibodies against IA-2, ZnT8 and GAD antigens using RSR ELISA assay (Limited, Pentwyn Cardiff, United Kingdom). The kit incorporates recombinantly expressed IA-2 fragment (aa 604-979), full length GAD65 and ZnT8 fragment (aa275-369). Briefly, all reagents were reconstituted and allowed to stand at room temperature for 30 minutes before use. As per manufacturer's instructions, 50 μ L of patient sera (neat), negative controls and calibrators were transferred to the wells in duplicate and the ELISA plate was incubated overnight at 4°C to allow specific antibodies in the patient sera to interact with the antigens coated onto ELISA plate wells. Two wells were left as blanks for the determination of background. Following incubation, samples were discarded leaving the bound antibody in the wells. Reaction enhancer (25 μ L) was added to the wells and briefly agitated on an orbital shaker (5 seconds, 500 shakes per minute). The reaction plate was then incubated overnight at 4°C followed by washing (x3). Reconstituted IA-2 Biotin (100 μ L) was added to the wells where immobilized specific antibody binds divalently to the biotin. Reaction assay was incubated for 1 hour at 4°C and washed 3 times. Streptavidin peroxidase (SA-POD, 100 μ L) was transferred to the wells and incubated for 20 minutes on an ELISA plate shaker (for colorimetric confirmation of bound biotin) where it binds specifically to the biotin assisting in determining the amount of biotin in the wells. Followed by incubation, the excess SA-POD was washed off and 3,3',5,5'-tetramethylbenzidine (TMB, 100 μ L) was added and incubated at room temperature in the dark for 20 minutes without shaking resulting in the formation of blue colour. Stop solution (100 μ L) was then added to the wells and plates were left on the shaker for 5 seconds to stop the reaction and form yellow colour. The absorbance of the yellow

reaction mixture was read at 405 nm using BIO-RAD Model 680 XR microplate reader. The amount of antibodies in the wells was represented by the absorbance value. Sera positivity for the autoantibodies against the antigens of interest was determined using the positive controls provided by the manufacturer.

2.4. Development of IA-2, ZnT8R and ZnT8W MBP fusion protein ELISA assays

2.4.1. Generation of recombinant maltose binding fusion proteins

Soluble IA-2ic, ZnT8R and ZnT8W proteins comprising aa 601-969, ZnT8R-aa275-369 and ZnT8W-aa275-369 respectively, were expressed as maltose binding protein (MBP) fusion proteins. The ZnT8R and ZnT8W proteins were generated from pETMBP_1a plasmids (provided by Dr. Hanna Skarstrand, Lund University Diabetes care centre, Malmö, Sweden) and IA-2ic protein was produced from pMAL-c5X plasmid (provided by Dr. Massimo Pietropaolo, Department of Pathology, and Immunology, Baylor's college of Medicine, Houston, Texas, USA).

The Vectors incorporating ZnT8R, ZnT8W and IA-2 were transformed into BL21-Gold (DE3) competent *E. Coli* cells (Stratagene, San Diego, California, USA) using manufacturer's instructions. Briefly, competent DE3 BL21 cells were thawed on ice. The IA-2-MBP pMAL-c5X plasmid and ZnT8R and ZnT8W pETMBP_1a plasmids were diluted down to ~50ng/μL and stored on ice. The cells were then mixed gently and transferred (100 μL) to a pre-chilled Eppendorf tube. The diluted vectors (1 μL) were then added to the competent cells and gently swirled. To confirm the transformation efficiency, pUC18 control plasmid was also transformed into competent cells. The Eppendorf tubes were then incubated on ice for 30 minutes. Following incubation all tubes were transferred to the water bath (42°C) for 20 second heat pulse. Duration of the heat pulse was very critical to ensure optimal transformation efficiency. The transformation reactions were then placed on ice for 2 minutes. SOC media (900 μL, preheated at 42°C) was then transferred to each reaction tube and incubated at 37°C with shaking (~225 rpm) for 1 hour. The transformed cells were then concentrated by centrifugation at 200 x g for 4 minutes. Cells were then selected for antibiotic resistance

using Kanamycin and Ampicillin agar plates by transferring the cells on to agar plates with either Kanamycin, Ampicillin or plates without any antibiotics and incubated overnight at 37°C. The transformed cells thrived on the agar plates with the antibiotic they carried resistance to and plates without any antibiotics. In a second selection step, one of the colonies that thrived were selected and streaked on another agar plate which was treated with the antibiotic the colony was resistant to. After overnight incubation at 37°C, a colony was picked and cultured in 10 mL of Terrific Media (12 g/L tryptone, 24 g/L yeast extract, 0.04 mL glycerol).

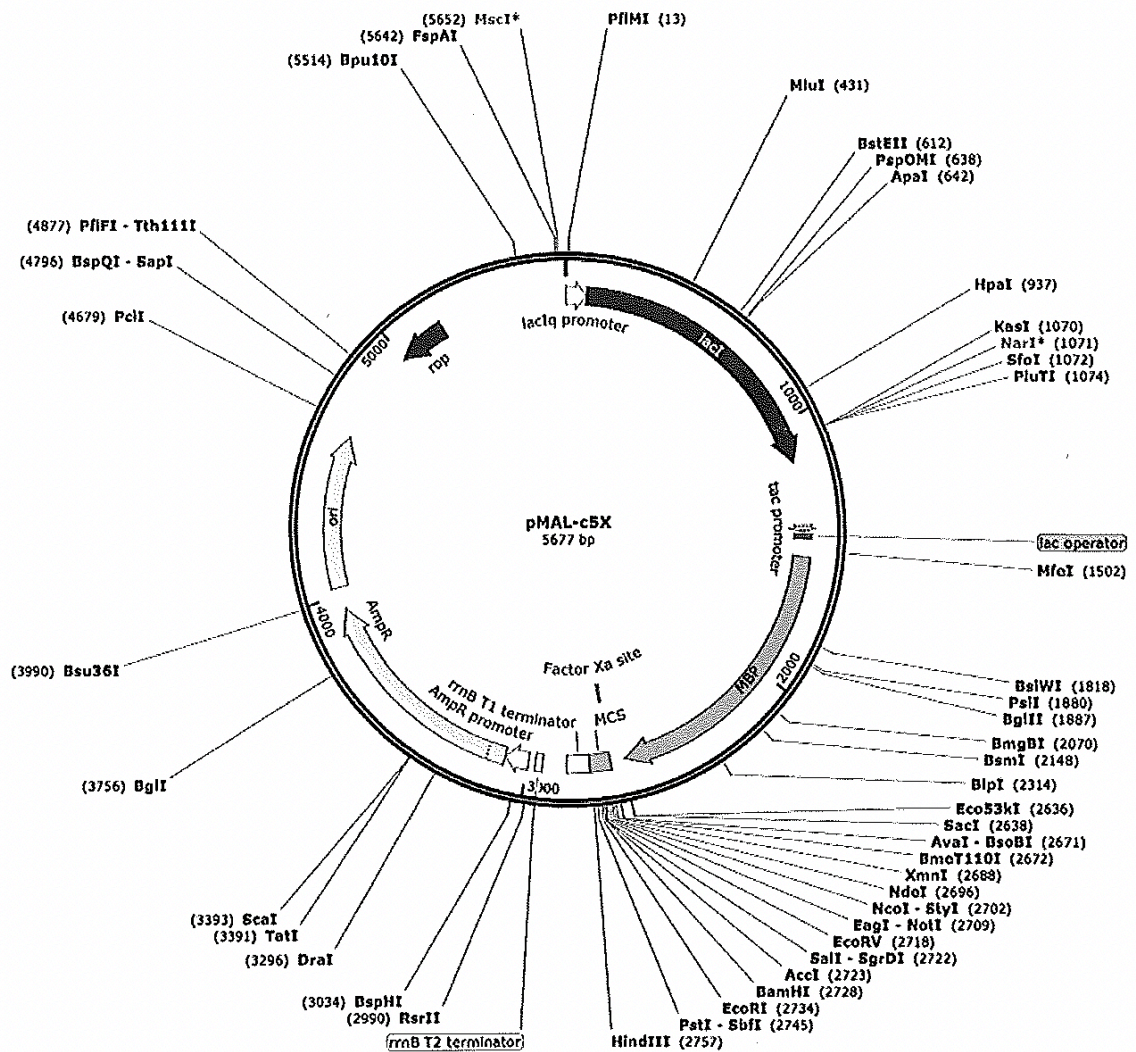


Figure 2.1. pMAL-c5X plasmid with the encoding for IA-2ic MBP fusion protein. The cDNA of aa 605-979 IA-2ic was cloned into the vector using the restriction enzymes BamHI and AvaI resulting in pMAL IA-2ic vector containing the encoding for maltose binding protein and Ampicillin resistance.

2.4.2. Miniprep of transformed cells

Briefly, selected colony was cultured in terrific media overnight at 37°C shaking at 220 rpm. Ten millilitres of the culture were transferred to 1L of fresh media. Once the optical density (OD) value of the culture was 1, Isopropyl β -D thiogalactopyranoside (IPTG, 0.1mM) was added to the culture to induce expression of the fusion proteins overnight shaking at 30°C. Cells were harvested by centrifugation at 4600 RPM for 20 minutes and washed with 0.9% NaCl and stored at -20°C.

2.4.3. Verification of Plasmid DNA

2.4.3.1 Plasmid DNA extraction from transformed E. Coli cells for agarose gel electrophoresis and Sanger sequencing.

Transformed bacterial cells were cultured and plasmid DNA was extracted in order to confirm the correct expression of fusion proteins. Overnight bacterial cultures (5mL) were spun down (8000 rpm, 3 minutes, room temperature) to collect cells. DNA from collected cells was extracted using the Qiagen DNA kit (Qiagen, Hilden, Germany). The cell pellet was resuspended completely in buffer P1 (250 μ L) provided in the kit. Briefly, buffer 2 (250 μ L) was added to the sample mix and the microcentrifuge was inverted 12 times until the solution turned blue. The reaction mix was incubated for five minutes to allow cell lysis. Buffer N3 (350 μ L) was added to the sample and the tube was inverted 12 times again until the solution turned colourless. The sample was centrifuged (13,000 rpm) for ten minutes to remove cell debris. The supernatant was transferred to the QIAprep spin column and centrifuged for 60 seconds. The flow through was discarded and the sample was washed by adding Buffer PB (500 μ L) and Buffer PE (750 μ L). The residual wash buffer was removed by centrifuging the sample for 1 minute. The spin column was placed in a fresh 1.5 mL microcentrifuge tube and DNA was eluted off the column by adding Buffer EB (60 μ L). After letting the column stand for one minute, the spin column was centrifuged to collect isolated DNA (1 min).

Concentration and purity of the DNA sample was determined using Nanodrop. Plasmid samples were then sent to IMVS sequencing facility for Sanger sequencing. Sequencing results showed the expression of amino acid sequences corresponding to the expected sequence for all 3 antigens of interest.

2.4.3.2 Plasmid DNA digestion for agarose gel Electrophoresis

Isolated plasmids were digested with enzymes and run through agarose gel electrophoresis to determine the DNA sequence that encodes the fusion proteins (Fig. 1). Extracted DNA (2 μL) was mixed with equal volumes of buffer (2 μL), enzyme (0.5 μL) and dH_2O (15 μL). The reaction mix was left on water bath at 37°C for 4 hours. Meanwhile, the agarose gel was prepared by weighing out 0.5 g of Agarose gel and mixing with 0.5 x TBE in a conical flask. Once the agarose was soaked, the mixture was microwaved for 2 minutes. The agarose gel was left on the bench for 1 minute to cool down and poured into the gel tray. Comb was left on the tray then the gel was left for 30 minutes to set. TBE (x0.5) was transferred to the tank with the gel. Light sensitive easy vision 3-DNA dye (4 μL) was transferred to each sample. Samples were mixed thoroughly and transferred to the gel along with a DNA ladder (1kDa). Gel electrophoresis was run at 100 V 32 mA for 45 minutes in the dark and imaged using Transilluminator.

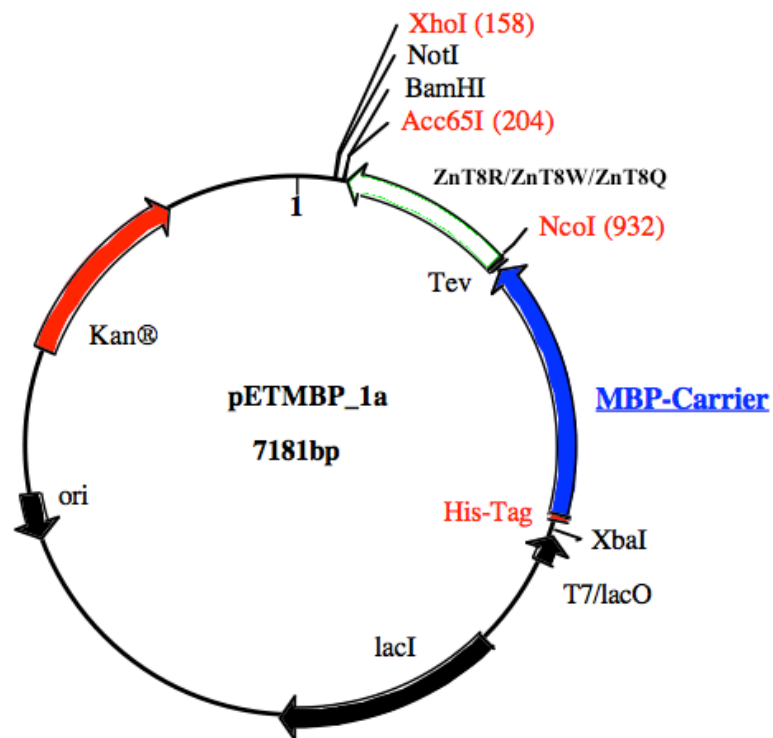


Figure 2.2. pETMBP_1a 7181 bp plasmid map with the encoding for ZnT8R/W/Q MBP fusion protein. The cDNA of aa ZnT8 C terminal aa 275-369 was digested into the plasmid using restriction sites XhoI and NcoI resulting in pETMBP_1 ZnT8R/W/Q containing the coding for the maltose binding protein, His tag and Kanamycin resistance. The arrows represent the respective 5' to 3' orientation.

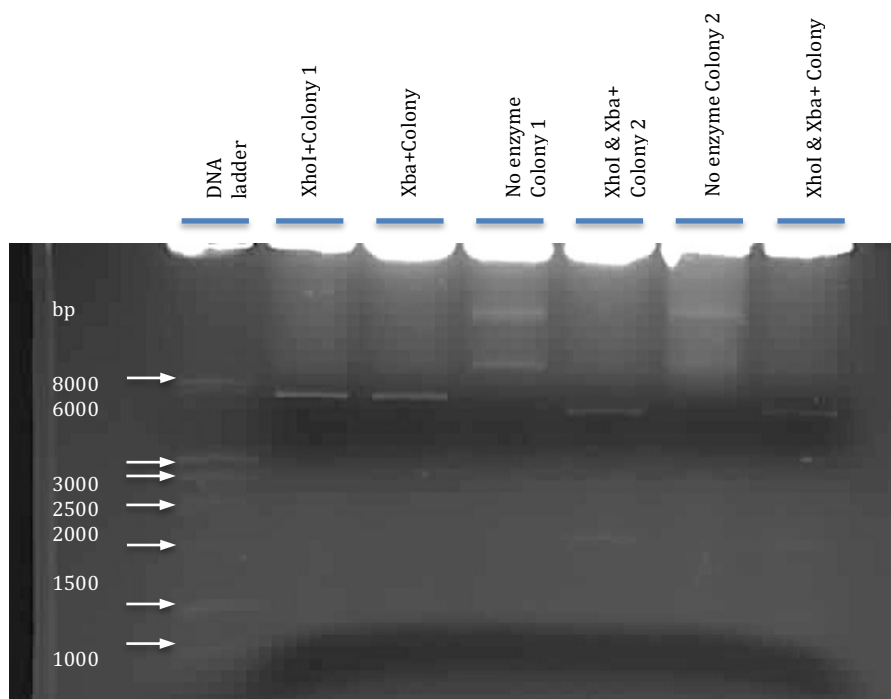


Figure 2.3. Agarose gel electrophoresis of digested pETMBP_1a 7181 bp ZnT8R/W/Q plasmid DNA. The plasmid DNA was purified from transformed DE3 BL21 E. Coli bacteria and digested with either XhoI or Xba enzymes or both. The full-length undigested vector runs at 7181 bp. When plasmid DNA from colony 1 and 2 was digested with XhoI and XbaI two bands ran at 5807 bp and 1374 bp.

2.4.4. Purification of fusion proteins using column chromatography

MBP fusion proteins (IA-2 and ZnT8R/W) were isolated from cell lysates by liquid column chromatography. Firstly, cells were re-suspended in ~30mL column buffer and sonicated (Misonix Sonicator Ultrasonic Liquid Processor) for 2 minutes with alternative sets of pulse sonication (100 Amplitude, 30 Watts, 878 Joules). Lysates were centrifuged at 9000 x g for 30 minutes and the resulting supernatants were loaded on amylose resin columns. Weakly bound and unbound proteins were washed off the column with 12 column volumes of column buffer (20mM Tris-HCl, 200 mM NaCl, 1 mM EDTA, pH 7.4). Bound fusion protein was eluted off the column with 5 column volumes of elution buffer per each concentration (10 mM and 20 mM Maltose in column buffer). The eluted proteins were pooled together and dialyzed using phosphate

saline buffer (PBS) in a 10K spin column (Ultra -15 Centrifugal filter, Amicon, Ireland).

The ZnT8-MBP fusion proteins were further purified by loading the sample into nickel-charged HiTrap chelating HP column (GE Healthcare, Uppsala, Sweden). The unbound proteins were washed with 40 column volumes of Nickel binding column buffer (Na_2HPO_4 , NaH_2PO_4 , NaCl). Subsequently fusion proteins were eluted using 10 column volumes of 200 mM Imidazole in column buffer (elution buffer) and 5 column volumes of 500 mM elution buffer. The eluted sample was pooled together and dialyzed using the spin column. Purified antigens were run in 1D SDS gel electrophoresis to determine the purity.

2.4.5. Protein concentration determination of the recovered fusion protein samples by Bradford or EZQ Protein quantification assay.

Protein concentration of the fusion protein samples was assessed using Bradford reagent assay and EZQ assay as followed, Bradford reagent was prepared with Coomassie Blue (10 % w/v), ethanol (20 %w/v) and 85 % Orthophosphoric acid (10 % w/v). Protein samples of unknown concentrations were added to 0.9 mL Bradford reagent and the OD value read at 595 nm (UV-160A UV-visible recording spectrophotometer, Shimadzu Corporation, Koyoto, Japan). OD values were used to derive protein concentration using the standard curve generated from bovine serum standards (Figure 2.4.).

2.4.6. EZQ protein quantification assay

BSA standards (2, 1, 0.5, 0.2, 0.1, 0.05, 0.02 and 0 mg/mL) were prepared in dH_2O . Standards, unknown samples, and blanks (1 μL) were transferred in triplicates to the assay paper on a microplate. Once the samples were dry, the paper was placed in a large weigh tray and immersed in methanol (~40 mL) for 5 minutes on a stirrer. The assay paper was dried using an easy breeze gel dryer. EZQ protein quantification reagent (~35

mL) was added to the paper and left on the stirrer for 30 minutes. The reagent was discarded, and the paper was rinsed three times with EZQ de-stain (~40 mL) for two minutes. Wet assay paper was imaged using the Typhoon scanner (Bio-rad Gel-Doc EZ imager). A polynomial graph was generated with the absorbance data retrieved for the standard BSA samples. Concentrations of the unknown samples were derived using the standard curve.

2.4.7. Verification of expressed fusion proteins via 1D SDS gel electrophoresis

1D SDS Gel electrophoresis was carried out to confirm the accurate production and purity of recombinant fusion proteins. Eluted protein samples were mixed with loading buffer with DTT (x4) and dH₂O and reduced by heating the samples for 10 minutes at 95°C. Samples were then vortexed, spun quickly and loaded on to precast gels (TGX-SDS, 4-20% acrylamide, Bio-rad, USA) along with unstained 1 KDA protein ladder and a dual stained 1 KDA protein ladder. Gel electrophoresis was conducted at 300 volts, 400 mA for 20 minutes and gels were removed from the case and imaged using stain free Gel Doc EZ Imager (Bio-Rad, Hercules, CA, USA).

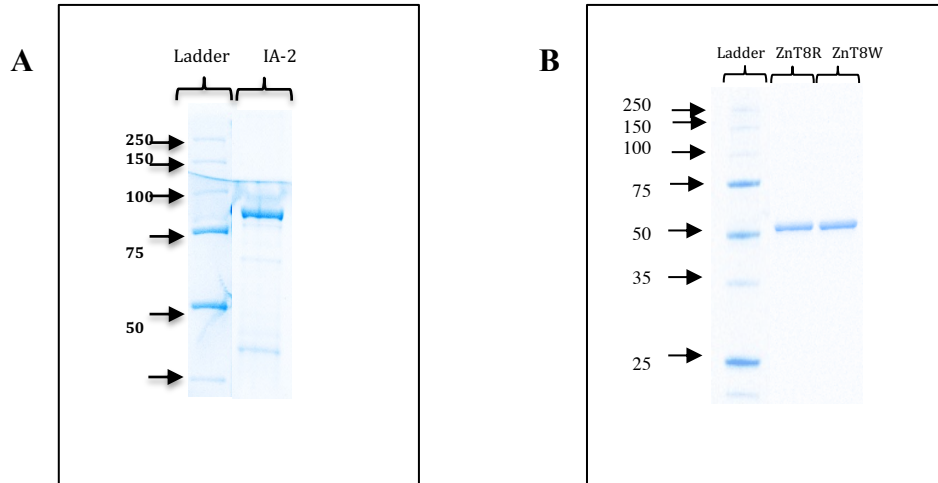


Figure 2.4. Confirmation of purity and integrity of the purified recombinant MBP fusion proteins by 1D SDS gel electrophoresis. **A.** MBP fusion protein of IA-2ic (~90 kDa) expressing the JM and PTP domains that contains the antigenic epitopes. **B.** MBP fusion proteins of ZnT8R and ZnT8W (~53 kDa) expressing the antigenic SNP at aa 325. Unstained 1kDa ladder was run alongside to determine the protein size.

2.4.8. The assessment of fusion proteins by western blotting

Purified proteins were immunoblotted with anti-MBP antibody in order to further verify the production of the fusion protein (Figure. 4). Nitrocellulose paper was soaked in methanol for 1 minute. The gel and nitrocellulose were equilibrated in 1x transfer buffer (25mM Tris, 190 mM Glycine, 20% Methanol) for 1 minute. Pre-soaked blotting paper was placed in Trans-Blot Turbo Tray then the nitrocellulose and the gel were placed on the blotting paper, respectively. A final layer of blotting paper was placed on the stack. The tray was transferred to the mini-Trans-Blot Electrophoretic Transfer Cell (Bio-Rad, Hercules, CA, USA) where the proteins were transferred from the gel on to the nitrocellulose membrane. Once the transfer was complete, nitrocellulose was blocked with 5% non-fat milk in TBS-T (20 mM Tris, 150 mM NaCl, 0.1% Tween-20, pH 7.5) for 1 hour at room temperature on stirrer and washed three times with TBS-T for 5 minutes. The nitrocellulose was then incubated in mouse monoclonal anti-MBP antibody (1:1000, New England Biolabs, Ipswich, Massachusetts, USA) in 1% skim milk TBS-T for 1 hour in room temperature on a stirrer. After another washing step, nitrocellulose was probed with anti-mouse IgG antibody conjugated with horseradish peroxidase (1:1000, Sigma-Aldrich, St. Louis, Missouri, USA). After washing the nitrocellulose, the anti-MBP antibody binding to the MBP fusion proteins was detected by incubating the nitrocellulose in chemiluminescent substrate for 5 minutes in the dark and imaging using LAS-4000 luminescent image analyser (Life Science, Fuji Film, Tokyo, Japan). Molecular mass of the proteins was determined using dual stained ladders (Bio-rad, USA).

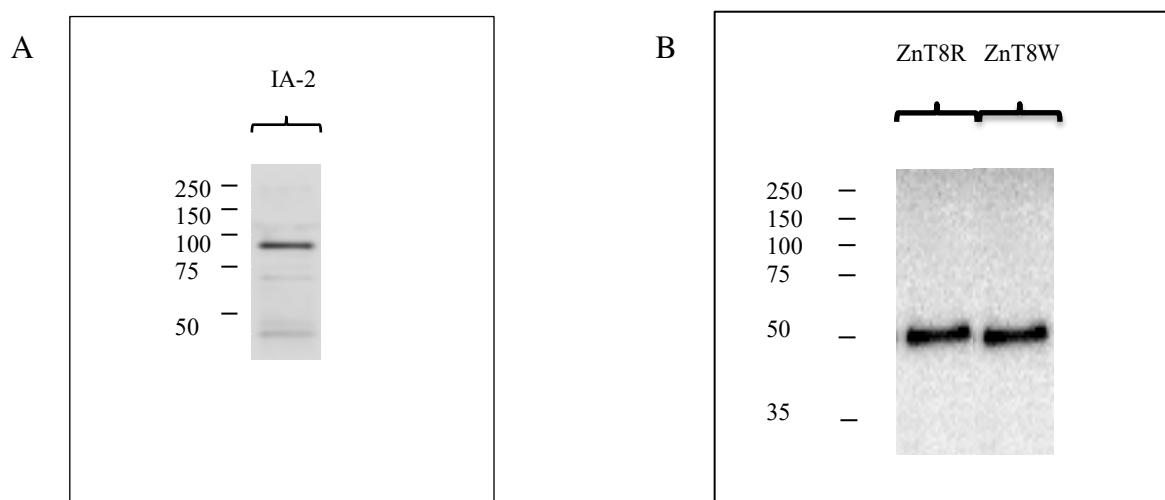


Figure 2.5. Confirmation of the integrity of the recombinant MBP fusion proteins by western blotting. **A.** MBP fusion protein of IA-2ic (~90 kDa). **B.** MBP fusion protein of ZnT8R and ZnT8W (~53 kDa). Fusion proteins were probed with monoclonal mouse anti-MBP antibody followed by anti-mouse HRP secondary antibody.

2.4.9. Maxiprep of transformed cells

Once plasmids were confirmed to be carrying the encoding of interest and the expression of the fusion proteins by was also verified, a colony was picked from an agar plate from the secondary selection step and cultured in 1L of Terrific media (Chapter 2.4.1.). Followed by the collection of transformed cells by centrifugation, *E.coli* cells were lysed and immunoblotted with Anti-MBP antibody to confirm the expression of the fusion protein. Once verified, the fusion protein was extracted from the cell lysate through column chromatography. Fusion protein sample was then pooled together, dialyzed, and quantified using EZQ assay. Before cell lysis 5 mL cell culture was spun down and re-suspended in glycerol storage media (15% glycerol, Tryptone soy broth include ingredients here) and stored in liquid nitrogen for later use.

2.4.10. ELISA plate coating and serum concentration Optimization

2.4.10.1. Optimization of coating concentration

The recovered fusion proteins were then used in ELISA assay to detect the presence of autoantibodies in the T1D patient sera. Firstly, to achieve optimal sensitivity, a range of IA-2 MBP fusion protein coating concentration was assessed in primary ELISA assays. Briefly, ELISA plates were coated with a series of IA-2-MBP, ZnT8R and ZnT8W fusion protein coating concentrations (0.06, 0.1, 0.6, 1, 2, 4, 6, 10 and 16 $\mu\text{g/mL}$) in 50 mM carbonate coating buffer (pH 9.6) were transferred to the ELISA plate and incubated overnight at 4°C. Following overnight incubation, non-specific sites were blocked with 1% BSA in PBS for 1 hour at 37°C and plates were washed with 0.05% Tween-20 in PBS. Anti-MBP antibody (New England Biolabs, Inc., US) diluted 1:1000 in 1% Skim milk in PBS and transferred to the wells and incubated at 37°C for 1 hour. The ELISA plates were washed three times again and the bound MBP antibody was detected by incubating wells with alkaline phosphatase conjugated anti-mouse IgG secondary antibody for 1 hour at 37°C. (1:1000). After repeating the washing step to remove unbound antibody, p-nitrophenyl phosphate substrate (Sigma, St Louis, MO, USA) in diethanolamine buffer (1 mg/mL, 90 mM, pH 9.6) was added to the wells. All samples were tested in duplicate. OD values were read at 405 nm.

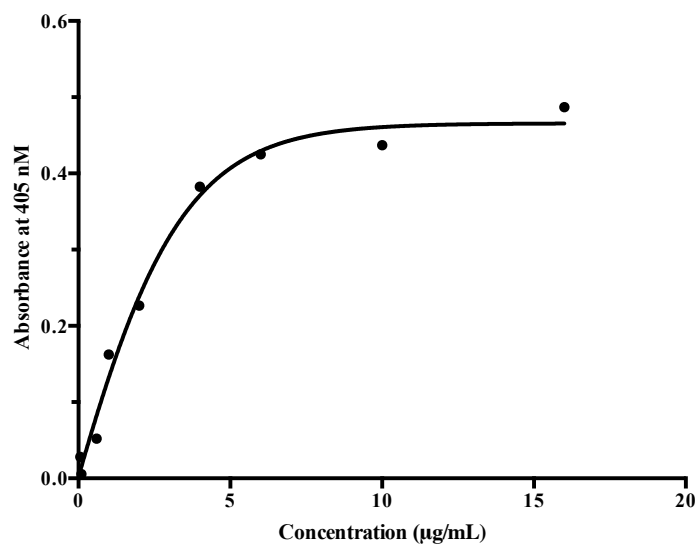


Figure 2.6. Assessment of IA-2ic MBP fusion protein coating concentration sensitivity. Coating concentrations ranging from 0.06 - 16µg/mL were tested with anti-MBP antibody in ELISA assay. The bound antibody was detected with anti-mouse alkaline phosphatase conjugated secondary antibody. Absorbance was read at 405 nM and normalized to the secondary antibody binding (n=2).

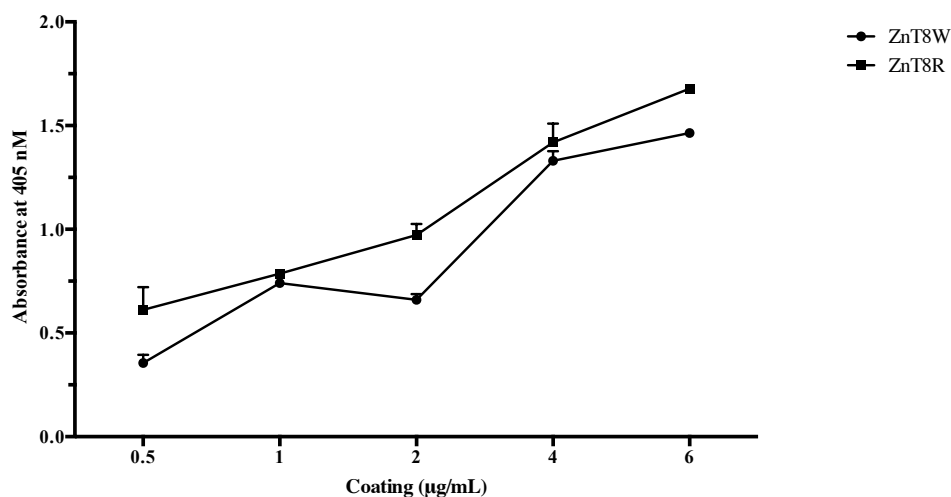


Figure 2.7. Assessment of ZnT8R/ZnT8W MBP fusion protein coating concentration sensitivity. Coating concentrations ranging from 0.5, 1, 2, 4 and 6 µg/mL were tested with anti-MBP antibody in ELISA assay. Anti-mouse alkaline phosphatase conjugated secondary antibody was used to detect the bound anti-MBP antibody. Absorbance was read at 405 nM and normalized to the secondary antibody binding (n=2).

2.4.10.2. Optimization of serum concentration

To identify the optimal sera concentration for the ELISA assay, sera from two healthy individuals were tested on several IA-2-MBP protein coating concentrations (0.06 to 16 µg/mL) to evaluate the background binding. Sera were diluted at 1:10, 1:20, 1:50 and 1:100 dilutions in PBS with 1% skim milk and transferred to the coated plate to be incubated at 37°C for 1 hour. Bound antibodies were detected with anti-human IgG conjugated with alkaline phosphatase and p-nitrophenyl phosphate substrate. OD values taken at 20 minutes were normalized to serum binding to wells without coating.

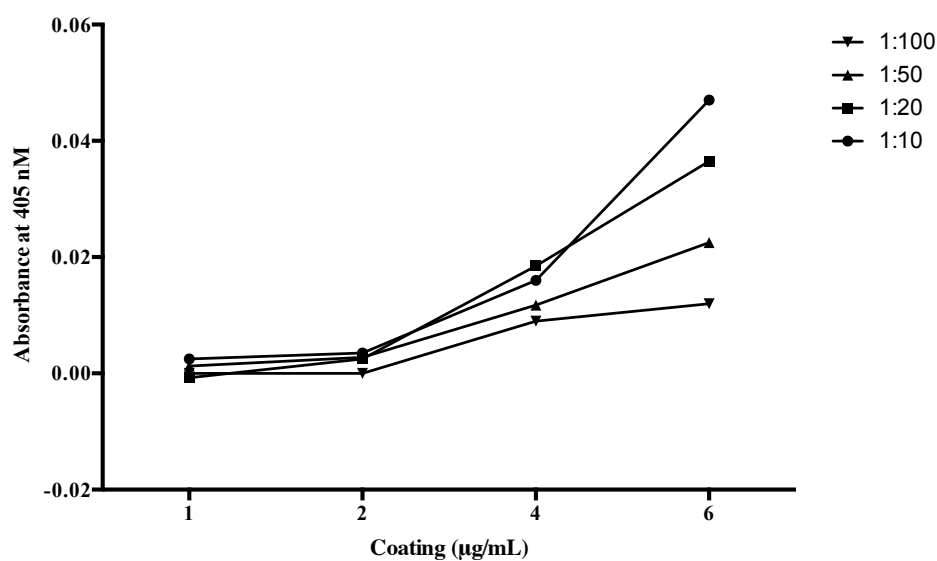


Figure 2.8. Evaluation of optimal serum concentration for the detection of true anti-IA-2 antibody binding by IA-2ic MBP fusion protein ELISA. Two healthy control sera at four serum dilutions (1/10, 1/20, 1/50, 1/100) were tested on coating concentrations ranging from 0.06 - 16 µg/mL to identify the optimal serum concentration for the ELISA assay. Bound antibody was detected using secondary anti-human alkaline phosphatase antibody. Results were expressed as a mean of duplicates. Data were normalized to background binding (n=2).

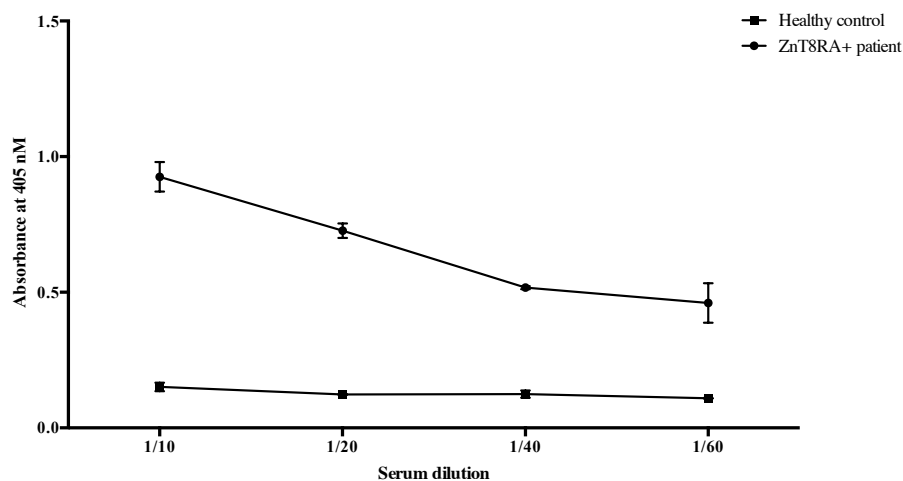


Figure 2.9. Evaluation of optimal serum concentration for the detection of true anti-ZnT8R antibody binding by ZnT8R MBP fusion protein ELISA. An Anti-ZnT8RA positive patient serum (T1D035) and a healthy control serum (CTR063) was tested at serum dilutions of 1/10, 1/20, 1/40 and 1/60 on ZnT8R MBP fusion protein at a coating concentration 4 $\mu\text{g}/\text{mL}$ to identify the optimal serum concentration for the ELISA assay. Bound antibody was detected using secondary anti-human alkaline phosphatase antibody. Results were expressed as a mean of duplicates. Data were normalized to background binding (n=2).

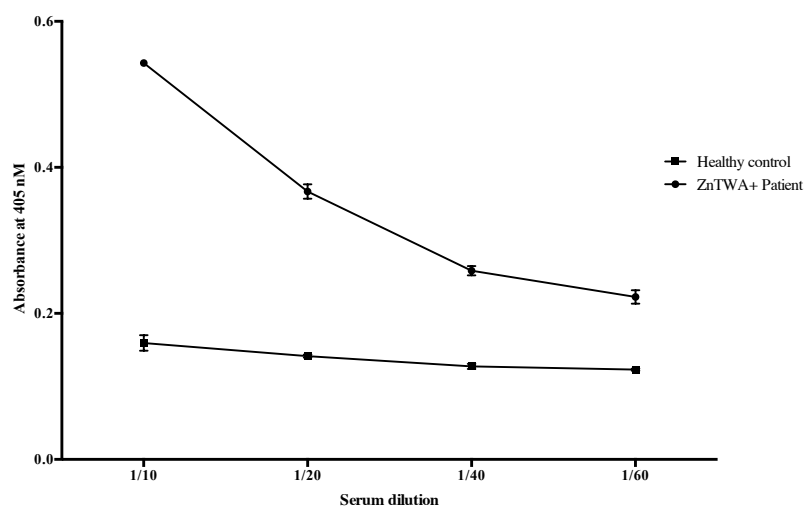


Figure 2.10. Estimation of optimal serum concentration for the detection of anti-ZnT8W antibodies by using ZnT8W MBP fusion in ELISA. Anti-ZnT8RA positive patient serum (T1D035) and a healthy control serum (CTR063) was tested at serum dilutions ranging from 1/10 - 1/60 on ZnT8W MBP fusion protein (4 $\mu\text{g}/\text{mL}$). Bound antibody was detected using secondary anti-human alkaline phosphatase antibody. Results were expressed as a mean of duplicates. Data were normalized to background binding (n=2).

2.4.11. Optimized ELISA

The subsequent ELISAs were performed by coating the ELISA plate (Maxisorp, Nunc, Rockslide, Denmark) with the optimized fusion protein coating concentration of 4 $\mu\text{g}/\text{mL}$ in 50 mM carbonate coating buffer (pH 9.6) overnight at 4°C. Next day, the plate was washed 3 times with PBS-T and non-specific sites were blocked with 250 μL of 1% BSA in PBS and incubated for 1 hour at 37°C. The samples of interest were then added to the plate and incubated at 37°C for 1 hour after washing the plate 3 times. The plate was then washed 4 times with PBS-T followed by incubation with secondary anti-human alkaline phosphatase conjugate antibody (Sigma, St Louis, MO, USA) at 1/1000 dilution in PBS-T for 1 hour at 37°C. In order to detect the bound antibodies, the plate was washed again with PBS-T and disodium p-nitrophenyl phosphate 1 mg/mL substrate in 90 mM diethanolamine (pH 9.6). All samples were tested in duplicates.

ELISA was read at 405 nm and the results were expressed as the mean of duplicates. Values were normalized to background binding.

2.5. Proteomic analysis of T1D specific autoantibodies

2.5.1 Elution of bound antibodies from fusion protein coated ELISA plates

Autoantibodies specific to fusion proteins were collected from T1D patient sera using inhouse ELISA method. Four ELISA plates were coated with each fusion protein in coating buffer (4 µg/mL, 100 µL per well, 1.59 g/L Na₂CO₃, 2.93 g/L NaHCO₃, 0.1% Sodium azide) overnight at 4°C. Following incubation, plates were washed 4 times with PBS and blocked with 1% BSA in PBS for 90 minutes at 37°C. Plates were washed 3 times again and incubated with patient sera (1/20 in PBS, thawed and spun at 8000 g for 5 minutes, 1% skim milk was not used in the serum sample as this interferes with the mass spectrometer) for 90 minutes at 37°C. Following incubation, the unbound sera were collected by inverting the plates over 2 large weigh trays and lightly tapping the plate to flick out any liquid. Plates were then washed 6 times with PBS to remove any unbound antibodies. Antibodies bound to the fusion protein were eluted off by incubating the wells with elution buffer (200 µL, 7.5 g/L Glycine, 29.2 g/L NaCl, pH 2.3) on the shaker for 5 minutes at room temperature. Eluted antibodies were collected by inverting the plates over two large new weigh trays and tapping lightly. The supernatant with eluted antibodies was neutralized to pH 7 by adding 1M-Tris (pH 8). The elution step was repeated two more times. The antibody sample was then concentrated from ~250 mL down to ~200 µL by centrifuging the supernatant in a 10K spin column (Merck Millipore, Massachusetts, US) for 8 minutes at 4600 rpm at room temperature. Flow through was collected and stored in -20°C. The concentrated antibody sample was washed with PBS/dH₂O by centrifugation at 4600 rpm for 15 minutes. The antibody sample was further concentrated by centrifugation at 14 000 g for 30 minutes in a 0.5 mL spin column (Merck Millipore, Massachusetts, US). Affinity purified antibody was tested for specificity by ELISA to determine the specificity and enrichment using a panel of antigens such as IA-2, ZnT8R, ZnT8W, Ro60, MBP and Calreticulin-GST.

2.5.2 Preparing the antibody sample for mass spectrometry

Affinity purified antibody samples were initially reduced with 100 mM DTT and heated at 100°C for 5 minutes. The samples were run on 1D gel electrophoresis in order to isolate heavy and light chains of the antibodies (Chapter 2.3.3.4). 1D gel (TGX-precast gel, Bio-Rad, Hercules, CA, USA) was removed from its cast and fixed in fixative buffer (20% Methanol, 7.5% Acetic acid) on an orbital shaker for 4 hours. 1D gel was then rinsed thoroughly with dH₂O and incubated in dH₂O for 1 hour on a shaker at room temperature. The gel bands were cut under UV light (365 nm) using a trans illuminator (Maestrogen, Xiangshan, Taiwan) and transferred to labelled low binding tubes (Axygen, Australia).

Gel bands were washed twice by incubating them in ammonium bicarbonate solution (500 µL, 50 mM, Sigma Aldrich, US) for 30 minutes at room temperature. Peptides within the gel pieces were then alkalized by 30-minute incubation in 10 µL of 100 mM Iodoacetamide (IAA, Bio-rad, US) and 150 µL of ammonium bicarbonate at room temperature in the dark. Gel pieces were washed twice again with ammonium bicarbonate and shrunk with 200 µL of Acetonitrile (100%, Hypergrade for LCMS LiChrosolv, Merck). Supernatant was discarded and trypsin in ammonium bicarbonate (~ 25 µL 12.95 ng/ µL, Trypsin Gold mass spectrometry grade, Promega, US) was transferred to the gel pieces where the peptides were digested overnight at 37°C. After brief centrifugation, trypsin solution with peptides was transferred to the MS vials (Thermo scientific, US).

2.5.3 Mass spectrometry

Digested peptides (~ 20 μ L) were analysed using Quadrupole-time of flight (QTOF) 5600+ mass spectrophotometer (AB Sciex, Framingham, MA, USA) coupled with Eksigent nanoLC 400 high performance liquid chromatography (HPLC). Peptides were transferred to a Protecol Trap Column (POLAR 120 A 3 μ m 10 mm x 300 μ m ID PK3, SGE Analytical Science, Australia) and were eluted off the trap using an acetonitrile gradient as followed, 5, 25, 40, 95, 5 and 5% for 35, 7, 12, 10, 2 and 29 minutes, respectively.

The spectrometer was operated on high sensitivity positive ion mode where ions with charges of +2 to +5 are selected. Followed by 20 MS scans with more than 300 counts per second MS/MS scans. TOF scans were collected from 350-1500 m/z ions over an accumulation time of 0.15s. Product ion scans were attained from 100-1500 m/z ions. All after 5 occurrences were excluded for 30 seconds. Ions were selected according to mass in Quadrupole 1 cell and transferred to collision cell (Quadrupole 2) to be fragmented by collision gas. Fragmented ions were further analysed by mass analysis in the TOF region and detected by the detector. The instrument displayed ion intensities for m/z values in a mass spectrum. All samples were tested in duplicates. The instrument was calibrated every 10 hours.

2.5.4 Proteomics data analysis

MS/MS spectra were received from mass spectrometer in the form of WIFF files. Raw data files were then loaded onto the Peaks studio software (Peaks Studio v8 software (Bioinformatics Solution Inc. Waterloo, ON, Canada) to analyse variable Ig peptide sequences. The parameters selected for the analysis were as follows, trypsin as the digestion enzyme; variable modification of oxidation of methionine, deamidation of asparagine and glutamine, and carboxymethylation of cysteine; 2 missed cleavages; precursor m/z tolerance of ≤ 15 ppm; product ion error tolerance of 0.02 Da; precursor charge state of +2 to +5; peptides were searched against IMGT database, NCBI

database (Need to check this again). The false discovery rate was set at 1% for database matching and the de-novo peptide average local confidence was set at ≥ 50 .

Gene families were assigned using the Peaks module, where the presence of unique peptides determined the gene family, which was supported by the presence of two, or more non-overlapping supporting germline peptides. Peaks module was also used to identify any aa mutations shared across samples and patients. All peptide matches were assessed for ion coverage, abundance, and spectra quality before adding to final data.

Chapter 3: Development of a MBP fusion protein ELISA method for the detection of IA-2, ZnT8R and ZnT8W autoantibodies in sera from patients with Type 1 diabetes

3.1 Introduction

The identification of autoantibodies and their cellular and tissue targets has facilitated considerable progress in autoimmunity. Specific autoantibody responses in individual patients now form key diagnostic and prognostic criterion for many autoimmune diseases which often share overlapping symptoms. Such is the case in systemic autoimmune diseases including Systemic Lupus erythematosus and Sjogren's syndrome which are both collagen vascular diseases associated with ANA antibodies, where the presence of anti-DsDNA antibodies is diagnostic of Lupus.

Similarly, for patients presenting with metabolic dysfunction consistent with diabetes, including elevated HbA1C and fasting blood glucose levels, assessment for the presence of islet autoantibodies can confirm a diagnosis of T1D. The emergence of these autoantibodies is also prognostic, with approximately 80% of at-risk children with two or more islet autoantibodies along with a HLA risk gene, develop T1D within 10 years, whereas only 15% of the children with one autoantibody develop the disease. While a direct pathogenic role for humoral autoimmunity has yet to be established in T1D, the temporal emergence of these autoantibodies appears indicative of progression to insulin dependency.

The correlation between the presence of high titre autoantibodies and progression to T1D strongly suggest a link with immunological beta cell loss. However, it is unclear whether the islet autoantibodies directly drive autoimmune mediated beta cell destruction or alternatively, the emergence of autoantibodies is a secondary by-product of beta cell loss. Addressing the relationship between the presence of autoantibodies and beta cell loss requires a greater understanding of the humoral autoimmune pathophysiological mechanism involved in T1D. Recently several studies combining the isolation of specific autoantibodies with proteomics by mass spectrometry reported that many autoimmune humoral responses appear to arise in individual patients from

common and highly restricted molecular pathways. For instance, it is now known that Ro60, Ro52 and La antibodies found in patients with Sjogren's syndrome and Lupus syndrome arise from shared public autoreactive B cell clonotypes (Lindop et al., 2011, Thurgood et al., 2013). A public clonotype is when a distinct B cell clone with a unique VDJ and VJ heavy and light chain variable region gene arrangement is shared across unrelated patients with the same disease. These findings imply that the pathogenic molecular pathways leading to autoimmunity in these systemic disorders are identical amongst patients. This understanding of shared pathophysiological pathway may give rise to novel therapeutic approaches to treat Sjogren's syndrome and other autoimmune diseases.

As mentioned in the introduction, autoantibodies to IA-2 and ZnT8 are strongly associated with disease progression and T1D onset when the putative autoimmune reactivity is at its peak (Chapter 1.2). Additionally, both IA-2 and ZnT8 antigens are found in insulin secretory vesicles are hypothesized to be associated with insulin secretion and beta cell growth. Therefore, presumably IA-2A and ZnT8A are suitable prototypical candidates for interrogating the origin of autoreactive B cells involved in autoimmune diabetes. As yet, the application of proteomics in studying humoral responses in organ specific diseases such as diabetes is not established. The first steps in answering these questions require expansion of methodological approaches used to investigate these T1D associated autoantibodies. Firstly, in order to isolate these antibodies, an in-house ELISA was developed incorporating recombinant fusion proteins of IA-2_{iC} (aa 601-979) and ZnT8R/W/Q (aa 268-369). These recombinant proteins were fused with maltose binding protein, which is a well-established affinity tag that improves solubility, correct folding and assists in affinity purification of recombinant fusion proteins (Rondard et al., 1997). Aim of this study was to examine self-reactive clonotypic IA-2 and ZnT8 autoantibodies isolated from polyclonal sera of patients with Type 1 diabetes utilizing the fusion protein ELISA assays.

3.2 Methods

3.2.1 Patient and control Sera

The collected sera as described in chapter 2.1 were tested by RSR ELISA as two separate cohorts. Sera coded T1D001-T1D051 (cohort 1) were tested for IA-2, ZnT8 and GAD by RSR ELISA assay. From cohort 1, 2 IA-2A positive T1D patients (T1D019, T1D035) and 2 healthy control sera (CTR063, CTR064) were used as prototype positive and negative controls in developing the IA-2 fusion protein ELISA. Two ZnT8A positive (T1D034, T1D054) and 2 healthy controls (CTR063, CTR064) were used to optimize the ZnT8 fusion protein ELISA. Subsequent to the establishment of the fusion protein ELISAs, cohort 2 (sera coded T1D051-T1D074) was collected and tested using the IA-2 RSR ELISA assay and screened using the optimized IA-2 fusion protein ELISA (Table 2.1 and 2.2).

3.2.2 RSR ELISA assay

RSR ELISAs were performed as described in chapter 2.2.

3.2.3 Fusion protein ELISA

Fusion proteins were generated and used in ELISA as described in chapter 2.3. The selected positive patients, healthy controls and negative patients were used to optimize the fusion protein ELISA. All T1D sera and healthy controls were then tested for IA-2A detection by validated fusion protein ELISA.

Individual experiments conducted for the detection of IA-2A, included 2 IA-2A positive patients and 2 healthy controls were performed across serum dilution ranges of between 1/10 to 1/100. Experiments conducted to optimize ZnT8A fusion protein ELISA included 2 ZnT8A positive patients and 2 healthy controls. The optimizing ELISA and the subsequent screening ELISA assays included the testing of each patient serum in duplicates and the experiments were repeated at least twice.

3.2.4 Statistical analysis

Two-way Friedmann ANOVA (non-parametric) testing was used for the analysis of any correlations between binding of IA-2A positive T1D patient sera and healthy control sera binding to IA-2 fusion protein coated ELISA. Tukey's multiple comparisons ANOVA test was used to test any correlation between serum binding of IA-2A positive patients and healthy controls at 1/20 serum dilution.

3.3 Results

3.3.1 Optimization of serum concentrations for IA-2 fusion protein ELISA

To determine whether IA-2 antigen expressed as MBP fusion protein can be bound by anti-IA-2 autoantibodies, selected patient sera characterized for IA-2A by RSR ELISA (Table 3.1) and sera from healthy individuals were used as positive or negative controls, in an ELISA approach as described in chapter 2.1.

Serum dilutions from two positive controls (T1D035, T1D019) and two healthy controls (CTR064, CTR063) were tested by IA-2 fusion protein ELISA across a serum dilution range of between 1/10 to 1/100 (Figure 3.1). Mean OD values of the two healthy control sera (CTR063, CTR064) ranged from 0.091 to 0.012 across the serum dilution range. There was no significant difference in OD values either within individual control serum dilutions or between individuals.

In contrast to the control serums, mean OD values of the two IA-2A positive T1D patients (T1D035, T1D019) were significantly higher, at between 0.416 to 0.244 across the dilution range. T1D019 serum binding was highest at 1/20 serum dilution (Mean OD of 0.401), which reduced significantly to a mean OD of 0.2535 at 1/100 ($P < 0.0001$, by ANOVA). T1D035 serum binding was highest at 1/10 (Mean OD of 0.386) and reduced significantly down to a mean OD of 0.272 at 1/100 ($P < 0.0001$ by ANOVA). OD values detected for each positive patient were significantly greater compared to the healthy controls tested across all serum concentrations ($P < 0.001$). However, there was no significant difference in binding between the individual positive controls across the dilution range. Interestingly both IA-2 RSR ELISA and IA-2 fusion protein ELISA identified both T1D035 and T1D019 as high IA-2A positive sera. Hence, the IA-2 fusion protein ELISA is consistent with IA-2 RSR ELISA.

Analysis of the OD values of the positive sera across the dilution range indicate that the maximal binding is achieved at between 1/10 and 1/20 serum concentration with significant increase over lower serum dilutions. Given T1D019 OD values were the highest at 1/20 as it is possible that IA-2 binding is saturated at around 1/20 for some patients. As mean OD values detected at 1/10 are not significantly different from values

at 1/20, there is little benefit in utilizing 1/10 serum dilution in comparison to 1/20 serum dilution. Therefore, 1/20 serum dilution was used for all subsequent T1D patient sera screening using IA-2 fusion protein ELISA, as this dilution is likely to provide high sensitivity to IA-2 fusion protein with reduced risk of background binding.

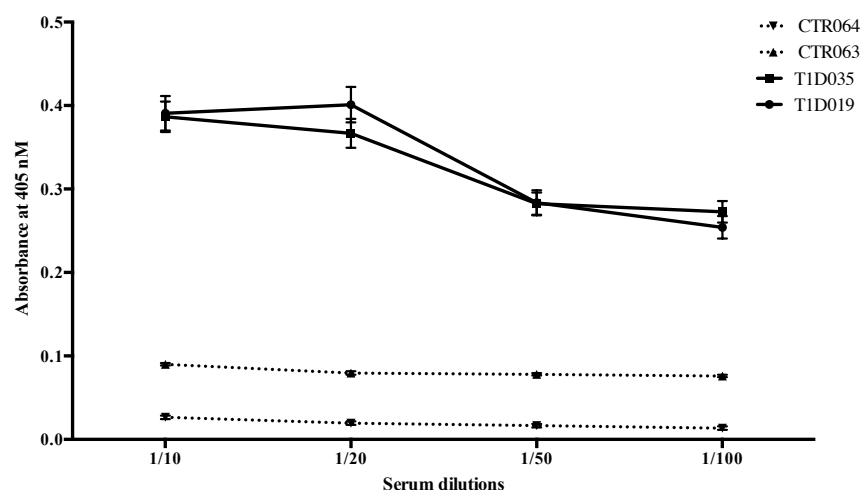


Figure 3.1. Additional assessment of optimal serum concentration required to detect anti-IA-2A antibodies by IA-2ic MBP fusion protein ELISA. Serum binding of two anti-IA-2A positive patients (T1D035, T1D019) and two healthy controls (CTR063, CTR064) across serum dilution ranges of between 1/10 to 1/100 on IA-2ic MBP fusion protein. Bound serum antibodies were detected by anti-human alkaline phosphatase conjugated secondary antibody. Results were expressed as a mean of duplicates. Data were normalized to background binding (n=2).

3.3.2. Optimization of serum concentrations for ZnT8R fusion protein ELISA.

Following the successful establishment of the IA-2 fusion protein ELISA, a ZnT8R fusion protein ELISA was developed using a similar approach (Figure 3.2). The same two T1D patients (T1D035, T1D019) as used in the IA-2 fusion protein ELISA were used for the optimization of the ZnT8R fusion protein ELISA. In terms of ZnT8 autoantibody positivity, T1D035 was identified ZnT8A positive and T1D019 was

negative by RSR ELISA while both patients were positive for IA-2A by RSR ELISA and fusion protein ELISA. This is of relevance as both IA-2 and ZnT8R fusion proteins carry a MBP affinity tag based on the same sequence. Therefore, using these patients allows the assessment of potential anti-MBP responses in T1D019 and positivity for MBP would result in positivity on the ZnT8R fusion protein ELISA.

In this ELISA mean OD values detected for T1D035 were significantly greater than the values detected for T1D019 across the serum dilutions. T1D035 mean OD values ranged from 1.124 at 1/10 dilution to 0.846 at 1/100 dilution. T1D019 mean OD values ranged from 0.210 to 0.141 across the dilution concentrations. Mean OD values of healthy controls ranged from 0.239 to 0.140 across the dilution range. T1D019 OD values were not significantly different from the two healthy controls across the dilutions of between 1/10-1/100. This indicated that ZnT8R fusion protein ELISA detects antigen specific serum binding in patient sera as confirmed by RSR ELISA.

Analysis of the OD values of the serum binding revealed that T1D035 binding is saturated at 1/20 serum dilution and there is no significant advantage in using 1/10 serum concentration. Furthermore, binding at 1/20 dilution is significantly greater than the binding at 1/50 (OD of 0.874, $P < 0.0001$) or greater dilutions. Therefore, as in IA-2 fusion protein ELISA, 1/20 serum dilution was used for all subsequent ZnT8R ELISA screening as it appears to provide optimal serum binding with reduced risk of background binding.

Following initial coating and serum optimization ELISA, ZnT8W MBP fusion protein ELISA was unable to detect any positive patient sera. Therefore, ZnT8W MBP fusion protein ELISA was not used for further experiments.

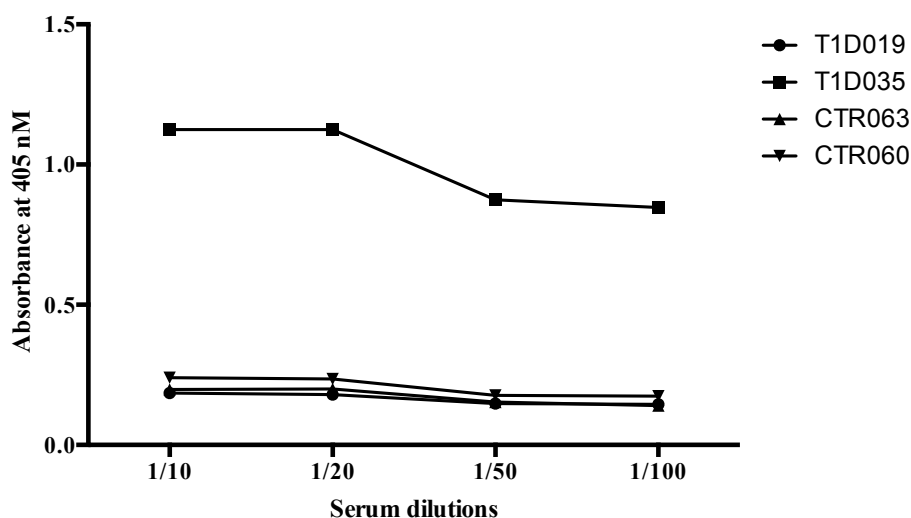


Figure 3.2. Further assessment of optimal serum concentration required for the detection of anti-ZnT8R antibodies by ZnT8R MBP fusion protein ELISA. Serum binding of one anti-ZnT8RA positive patient (T1D035), anti-ZnT8RA negative patient (T1D019) and two healthy controls (CTR060, CTR063) across dilution ranges of between 1/10 to 1/100 to ZnT8R fusion protein. Bound serum antibodies were detected by anti-human alkaline phosphatase conjugated secondary antibody. Results were expressed as a mean of duplicates. Data were normalized to background binding (n=2).

3.3.3. Confirmation of fusion protein ELISA specificity

To further confirm the specificity of the fusion protein ELISAs, the prototype T1D patients initially used to characterize the assays, were assessed alongside additional RSR validated positive and negative patients for antibody responses against IA-2 and ZnT8R.

For further validation of the IA-2 fusion protein ELISA, an additional RSR IA-2 positive patient (T1D019) with the highest OD value in RSR ELISA and two negative patients (T1D003, T1D040) were compared with T1D035 antibody binding against IA-2, MBP and GST-Calreticulin (Figure 3.3). As previously demonstrated, T1D035 presented binding values significantly higher than the healthy controls (CTR017,

CTR063). Negative controls with OD values ranging from 0.0165 to 0.1465, did not significantly differ from the healthy controls.

Furthermore, validated IA-2A positive serum (T1D035, T1D019) binding (OD of 0.37, 0.031 and 0.367, 0.367 respectively) to IA-2 fusion protein was significantly greater than the binding to free MBP (OD of 0.118, 0.092 and 0.053, 0.096) and GST-Calreticulin (OD of 0.061, 0.040 and 0.050, 0.056). However, negative control (T1D003, T1D040) binding (OD of 0.016, 0.210 and 0.038, 0.040) and healthy control sera (CTR017, CTR063) binding (OD of 0.049, 0.054 and 0.021, 0.007) binding to IA-2 fusion protein did not differ significantly from binding to free MBP (negative control ODs 0.041, 0.045 and 0.049, 0.031 respectively) (healthy control ODs 0.107, 0.113 and 0.070, 0.042). and GST calreticulin (negative control ODs 0.009, 0.009 and 0.003, 0.001 respectively). This indicated that the IA-2 fusion protein ELISA detects specific IA-2 antibodies in T1D patient sera.

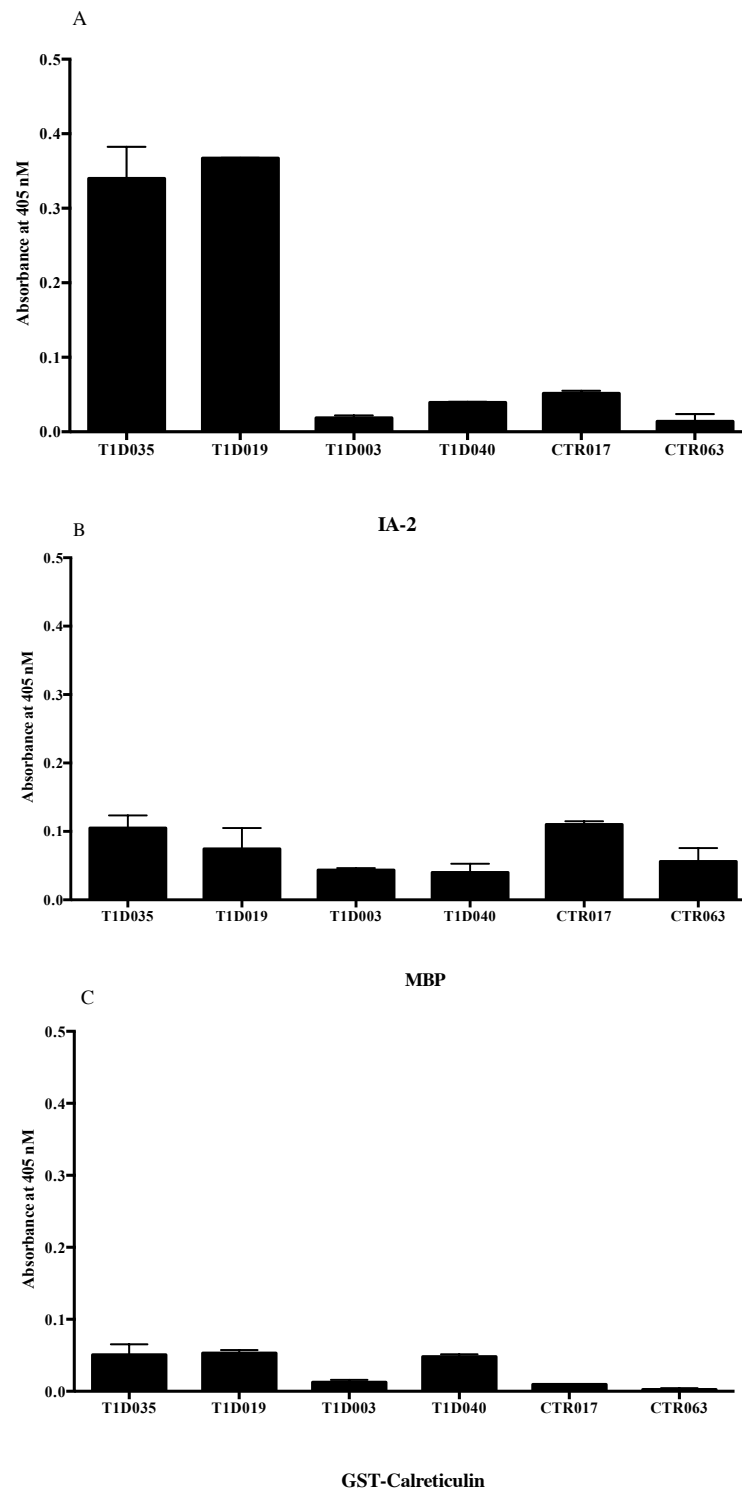


Figure 3.3. The specificity of the IA-2ic MBP fusion protein ELISA was further verified by testing the prototype positive, negative, and healthy control sera on MBP and GST calreticulin proteins. Bound serum antibodies were detected by anti-human

alkaline phosphatase conjugated secondary antibody. Results were expressed as a mean of duplicates. Data were normalized to background binding (n=2).

3.3.4. Prevalence of antibodies against islet antigen IA-2, GAD65 and ZnT8 in a cohort 1 of T1D patients

In order to characterize the prevalence of self-reactive islet autoantibodies by commercial RSR ELISA, sera from cohort 1 of T1D patients (15 females, 21 males, Average age of 35.78) were tested for the presence of IA-2, GAD65 and ZnT8 autoantibodies (Figure 3.4). As described in chapter 2, manufacturer's instructions were followed, and sera positivity was determined using positive controls provided by the manufacturer.

Assay results for GADA indicated that fourteen out of 36 patients were positive for GADA (5 females, 9 males, average age of 35.83), 7 were positive for IA-2A (2 females, 5 males, average age of 30.5) and 4 patients were positive for ZnT8A (1 female, 3 males, average age of 28.25). Two patients were positive for all 3 antibodies. These data demonstrate that the most prevalent antibody in this cohort is GAD65 autoantibodies followed by IA-2 antibodies and the least prominent antibodies were ZnT8A (Table 3.4).

Figure 3.4. Incidence of IA-2A, GADA and ZnT8A in cohort 1 (local cohort of T1D patients n=36) detected using RSR ELISA. **A.** IA-2A positivity determined using positive control (OD of 0.2287) provided by the manufacturer. Seven patients were positive for IA-2A. **B.** prevalence of GADA positive patients determined using GADA positive control with OD value of 0.4526. **C.** ZnT8A positive patients were characterized using positive control with OD value of 0.1601. All OD values were measured at 405 nM and results were presented as the mean of duplicates and normalized to background reading.

Table 3.1. Patient demographics matched to the positivity and negativity for islet autoantibodies IA-2A, GADA and ZnT8A by RSR ELISA (n=36).

Patient Code	Gender	Age	Autoantibody positivity		
			IA-2A	GADA	ZnT8A
T1D008	M		+	+	
T1D051	F	34	+	+	+
T1D035	M	19	+	+	+
T1D040	M	23	-	+	-
T1D041	M	28	-	-	-
T1D045	M	25	-	+	-
T1D046	M	26	+	-	-
T1D047	M	35	-	+	-
T1D030	M		-	-	-
T1D019	F		+	-	-
T1D011	M		+	-	-
T1D042	F	28	-	+	+
T1D049	M	28	-	+	-
T1D060	M		-	+	-
T1D034	M		-	+	-
T1D010	F	40	-	+	-
T1D002	F		-	+	-
T1D028			-	+	-
T1D050	M		-	+	+
T1D013	F	20	-	+	-
T1D043	M		-	-	-
T1D021	M	27	-	-	-
T1D016	F	60	+	-	-
T1D015	F		-	-	-
T1D004	M	63	-	-	-
T1D005	M		-	-	-
T1D003	F	55	-	-	-
T1D054	F		-	-	-
T1D037	F	40	-	-	-
T1D044	M	24	-	-	-
T1D022	F	18	-	-	-
T1D039	F		-	-	-
T1D038	M	22	-	-	-
T1D007	M	31	-	-	-
T1D048	M		-	+	-
T1D036	F	31	-	+	-

3.3.5. Selection of patients for the development of fusion protein ELISA

All sera positive patients and two sera negative patients along with two healthy controls, were selected as prototype controls to develop IA-2ic and ZnT8 fusion protein ELISA. High, mid, and low sera positive patients were tested in a range of dilutions in PBS with 1% skim milk in order to determine the optimal serum concentration with high affinity and low background binding (Chapter 2.4.10).

Table 3.2. Patients selected for the development of IA-2 MBP fusion protein ELISA. Concentration of antibodies were calculated using calibration curve that was generated using the standards provided by the manufacturer. Values lower than the detectable threshold of the assay is represented by (...).

Patients	IA-2	
	Positivity	u/mL
T1D008	+	2946.65
T1D051	+	681.92
T1D035	+	1829.44
T1D046	+	2728.17
T1D019	+	3009.37
T1D011	+	1333.98
T1D016	+	786.32
T1D034	-	14.21
T1D054	-	...
CTR063	-	...
CTR064	-	...
Positive Control	+	145.68

Table 3.3. Patients selected for the development of ZnT8R and ZnT8W MBP fusion protein ELISA.

Patients	ZnT8	
	Positivity	u/mL
T1D051	+	485.77
T1D035	+	951.86
T1D042	+	52.53
T1D050	+	320.52
T1D034	-	...
T1D054	-	...
CTR063	-	...
CTR064	-	...
Positive Control	+	47.11

3.3.6. Optimization of IA-2ic and ZnT8 MBP fusion protein ELISAs

Anti-MBP antibody that bound directly to the MBP portion of the fusion protein assisted in determining 4 $\mu\text{g/mL}$ as the optimal coating concentration with high sensitivity and low background binding for the fusion protein ELISA assays. Validated IA-2A and ZnT8A positive and negative patients assisted in identifying 1/20 serum dilution in 1% skim milk in PBS as the optimal serum concentrations with high affinity and low background binding for the fusion protein ELISA. In order to clarify true binding, all OD values were normalized to serum background binding. All sera were tested at least twice and mean of OD values from ELISA were presented in graphs.

The high IA-2A positive patients (T1D035 1829.44 $\mu\text{g/mL}$, T1D019 3009.37 $\mu\text{g/mL}$) were also identified as high positives by IA-2 fusion protein ELISA. Both negative patients (T1D034, T1D054) and healthy controls (CTR063, CTR064) were verified as IA-2A negative. Optimizing of ELISA confirmed that IA-2A can be detected by IA-2ic MBP fusion protein ELISA however, ZnT8A detection was not as successful. ZnT8R

MBP fusion protein ELISA detected one anti-ZnT8R antibody positive patient while ZnT8W MBP fusion protein ELISA was unable to detect any positive sera. All sera were then tested using the optimized fusion protein ELISA assays (Figure 3.5).

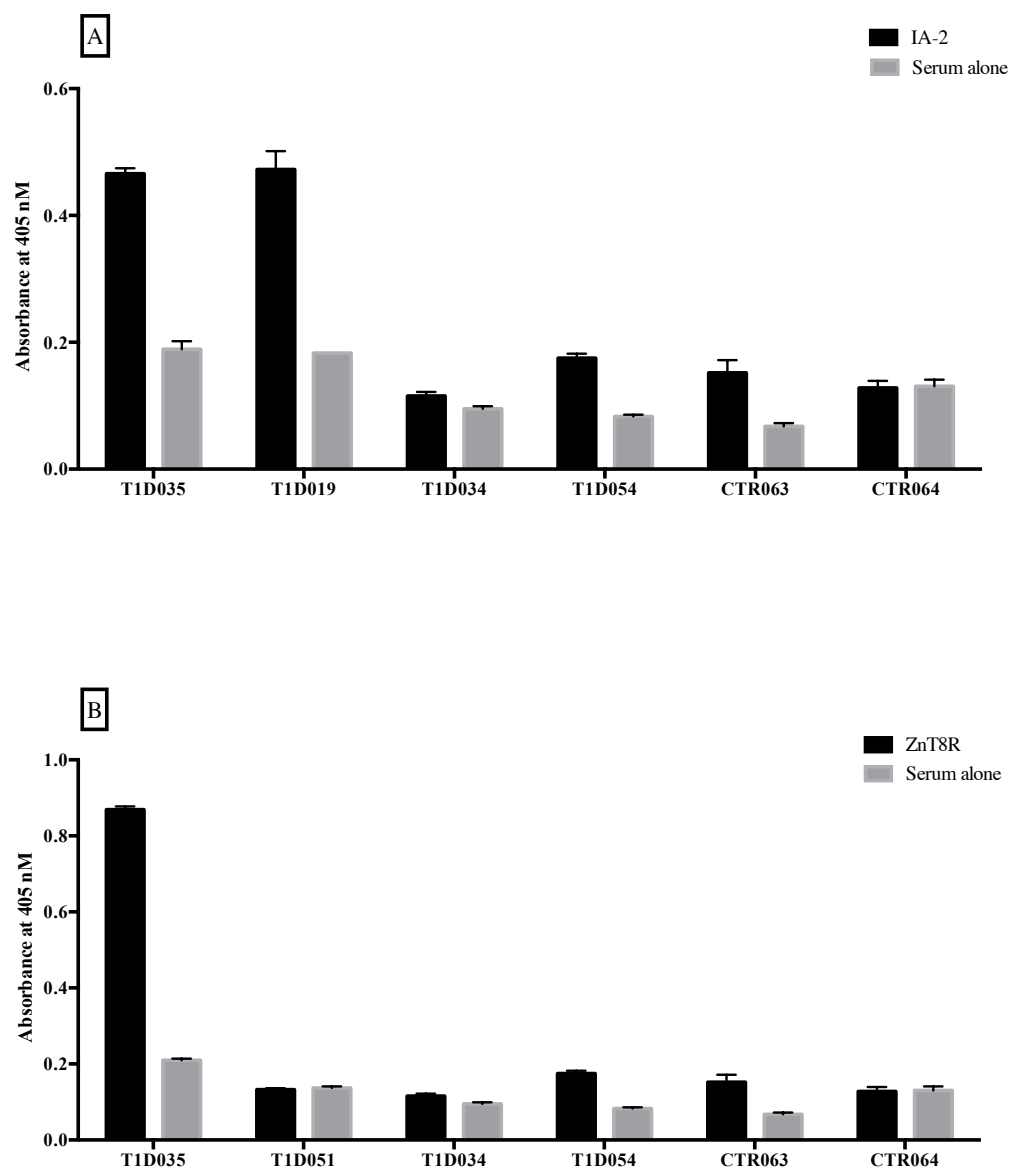


Figure 3.5. The validity of the MBP fusion protein ELISAs was tested by using prototype RSR positive and negative patient sera. **A.** Detection of anti-IA-2 antibodies by IA-2ic MBP fusion protein ELISA using validated IA-2A positive and negative T1D patient sera. **B.** Detection of anti-ZnT8 antibodies by ZnT8R MBP fusion protein

ELISA. All OD values were measured at 405 nM and results were presented as the mean of duplicates and normalized to background reading (n=2).

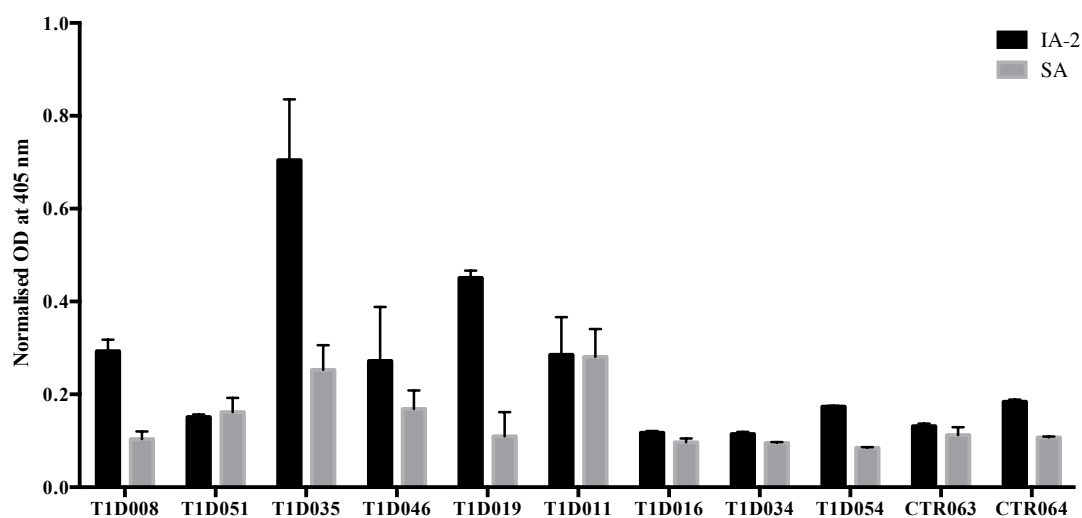


Figure 3.6. Anti-IA-2 antibody binding and background binding tested by IA-2ic MBP fusion protein ELISA. T1D008, T1D035, T1D019 to IA-2 fusion protein was significantly higher than sera background binding (Mann-Whitney t test P value, 0.0286). In contrast, the sera binding to fusion protein and background binding of negative controls and healthy controls were not significantly different (P value, 0.3333). Assay cut off for positivity, 0.271. All OD values were measured at 405 nM and results were presented as the mean of duplicates and normalized to background reading. (n=8).

3.3.7. Detection of anti-IA-2 antibodies in cohort 2 of T1D patients

Thereafter, sera from another 29 T1D patients were collected and tested using commercial ELISA in order to confirm antibody positivity. Three out of 30 patients (T1D019, T1D069, T1D056) were identified as IA-2A positive. The sera were then tested again using validated fusion protein ELISA to detect IA-2A. Two of the RSR ELISA positive patients (T1D019, T1D069) were also identified as positive by IA-2 fusion protein ELISA. The results were then compared to commercial ELISA results in order to determine the sensitivity and specificity of the IA-2 fusion protein ELISA (Table 3.4).

3.3.8. Comparison of RSR ELISA with MBP fusion protein ELISA

In comparison, RSR ELISA has detected the same number of sera (n=9) as IA-2A positive as the IA-2 fusion protein ELISA (n=9). However, the positive sera are not congruent. T1D035, T1D019 and T1D069 (1829.44 u/mL, 3009.37 u/mL, 4650 u/mL respectively) were identified as high IA-2A positive by RSR ELISA as well as fusion protein ELISA.

T1D008 was identified as high positive by RSR ELISA and IA-2A concentration was identified as 2946.65 u/mL by the ELISA. When tested by fusion protein ELISA, T1D008 was identified as negative as the background binding of this sera was also high negating the specific binding to IA-2. T1D011 was also identified as one of the high positive patients with anti-IA-2 antibody concentration of 1333.98 u/mL however, fusion protein ELISA identified T1D011 as negative also due to high background binding. Similarly, T1D046 was identified as a high positive by RSR ELISA with IA-2A concentration of 2728.17 u/mL, in contrast IA-2 fusion protein ELISA identified this serum as negative because of high serum background binding. T1D056 that was a mid-positive (1207 u/mL) in RSR ELISA was identified as negative by fusion protein ELISA. T1D051 and T1D016 which were RSR ELISA low positives which were detected as negatives by fusion protein ELISA. T1D001, T1D002, T1D010 and

T1D057 were recognized as IA-2A negative by RSR ELISA but IA-2A positive by fusion protein ELISA.

Two ZnT8A positive patients (T1D035, T1D051, confirmed by RSR ELISA) was tested by ZnT8 fusion protein ELISA and only T1D035 was identified as positive. Interestingly, anti-ZnT8R antibody negative patient serum, T1D002 as verified by RSR ELISA was detected positive by ZnT8R fusion protein ELISA. Two ZnT8A negative patients and two healthy controls were also identified as sera negative by fusion protein ELISA (Figure 3.5).

3.3.9. Screening of an additional cohort of T1D patient sera using RSR ELISA

Prior to screening additional patients using the IA-2ic and ZnT8R MBP fusion protein ELISAs, the cohort of RSR assessed patients was extended by testing a further group (cohort 2) of T1D patient sera (Chapter 2.1). Additional healthy controls were also tested by RSR ELISA. Sera positivity was determined using the positive controls provided by the manufacturer.

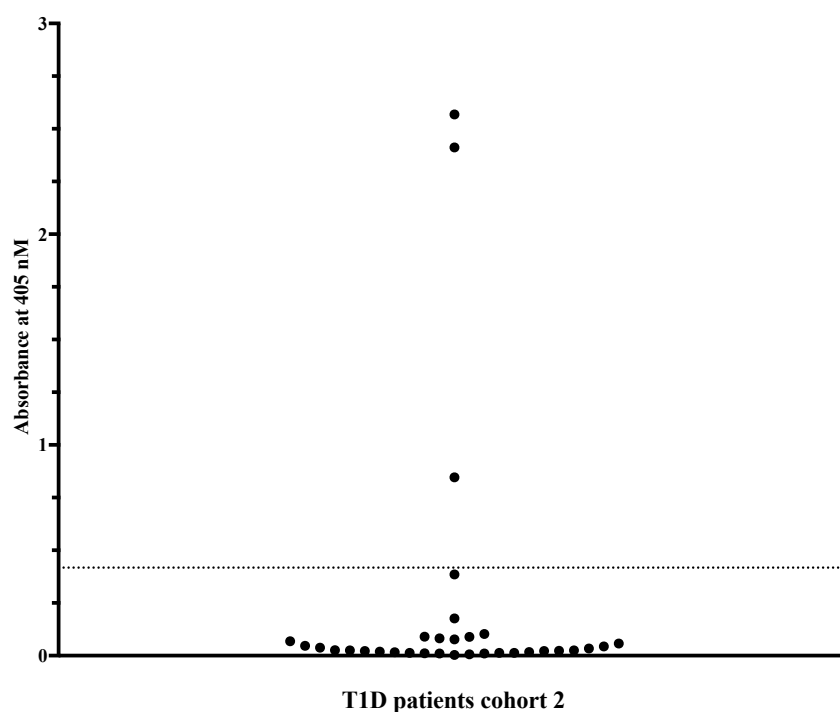


Figure 3.7. The Presence of anti-IA-2 antibodies in cohort 2 (T1D patients n=30) detected using RSR version 2 ELISA assay. Three out of 30 patients were detected as positive. Absorbance values were read at 405 nM. Assay cut off for positivity, OD of 0.4175. All data were normalized to mean background binding (0.0515).

3.3.10. Detection of high titre anti-IA-2 autoantibody sera using IA-2ic MBP fusion protein ELISA

As demonstrated in figure 3.9, IA-2ic MBP fusion protein ELISA appears to be capable of detecting high titre anti-IA-2 positive sera. Successful previous attempts to perform mass spectrometry on human derived autoantibodies have relied on the identification and subsequent affinity purification from high titre serum. Therefore, in order to select high IA-2 autoantibody titre sera and exclude suboptimal or negative IA-2A sera, a rigorous assay cut off was established by testing an additional pool of healthy controls (n=9) by IA-2 fusion protein ELISA. The mean OD value of all healthy controls was 0.0761 with a SD of 0.065. One or two standard deviations (0.129) above the mean OD of healthy controls did not exclude all individual healthy control sera. In order to avoid suboptimal samples, a cut off of mean + 3SD (0.195) was selected, which excludes all controls and lower titre anti-IA-2 positive sera but retaining high titre sera. Therefore, the assay cut off for anti-IA-2 positivity was established as 0.271. (Figure 3.9).

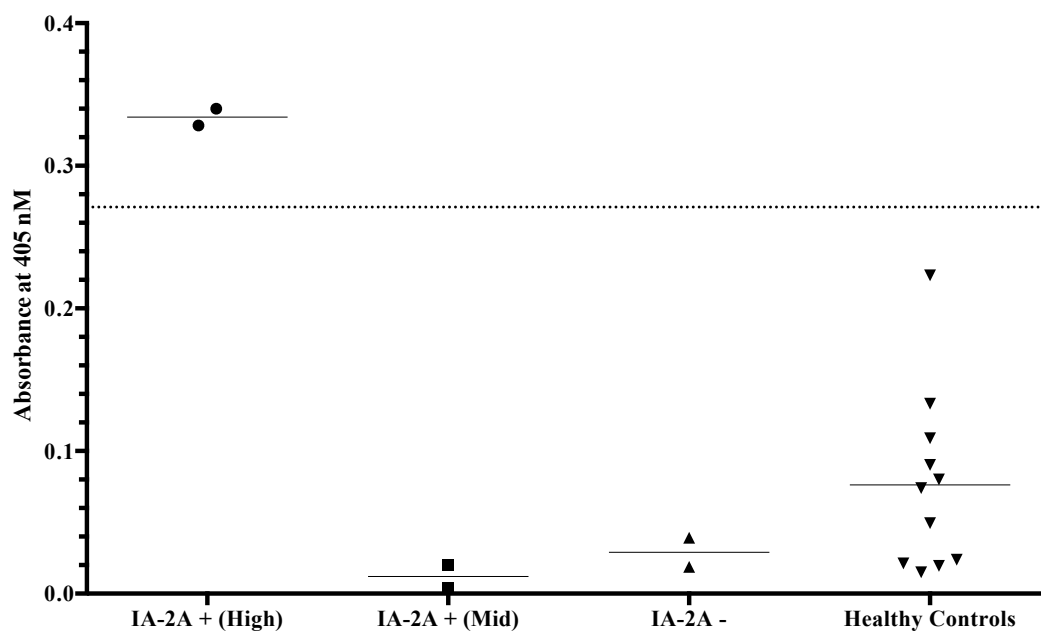


Figure 3.9. Establishment of assay cut off for the determination of high titre anti-IA-2 antibody positive serum. Two high titre anti-IA-2 antibody patient sera, two mid titre anti-IA-2 antibody positive sera and two anti-IA-2 antibody negative sera as verified by RSR ELISA was tested by IA-2 MBP fusion protein ELISA along with eleven healthy control serum. Mean OD of healthy sera binding was noted 0.0761. Assay cut off was established as the Mean OD + 3SD (0.271). Absorbance values were read at 405 nM and presented as mean of duplicates.

3.3.11. Detection of high titre anti-ZnT8R autoantibodies in T1D sera using ZnT8R MBP fusion protein ELISA

Similarly, as demonstrated in 3.10, the ZnT8R fusion protein ELISA appears to be suitable for detecting high titre anti-ZnT8R antibody positive sera, with one high titre anti-ZnT8R sera identified. A strategy similar to that used for IA-2 fusion protein ELISA was undertaken in an attempt to identify further high titre anti-ZnT8R positive patients. For this, an additional group of healthy controls (n=8) was tested by ZnT8R fusion protein ELISA, which resulted in a mean OD value of 0.059 with a SD of 0.0513 (Figure 3.10).

As with the IA-2 fusion protein ELISA, a stringent cut off for anti-ZnT8R antibody positivity was required for progression to proteomics analysis. Thus, three standard deviations above the mean OD value of healthy controls were used in subsequent ELISAs as the assay cut off (OD value of 0.212). This cut off value excluded all negative controls and healthy controls while retaining the validated positive sera (T1D035).

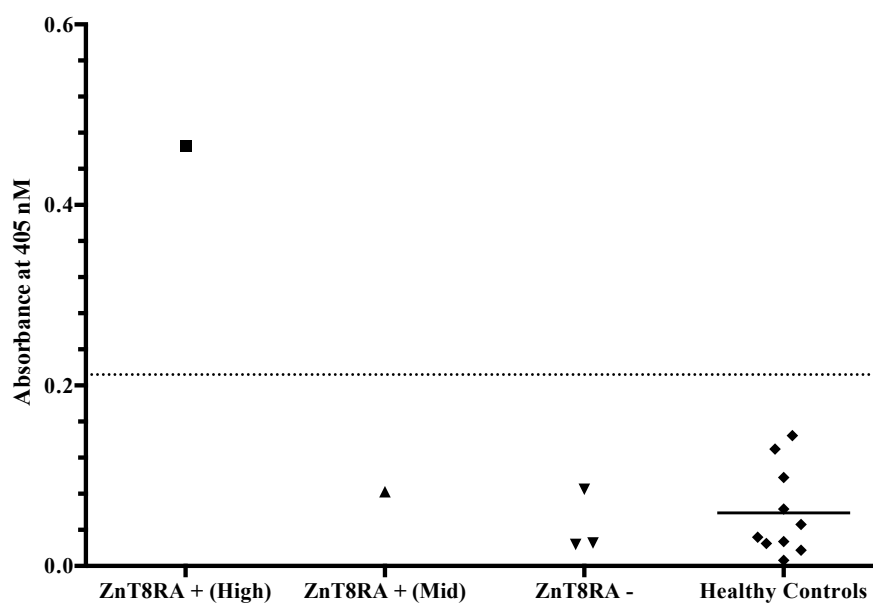


Figure 3.10. Establishment of assay cut off for the determination of high titre anti-ZnT8R antibody positive serum. One high titre anti-ZnT8R antibody patient sera, one mid titre anti-ZnT8R antibody positive sera and three anti-ZnT8R antibody negative sera as verified by RSR ELISA was tested by ZnT8R MBP fusion protein ELISA along with ten healthy control serum. Mean OD of healthy sera binding was noted 0.059. Assay cut off was established as the Mean OD + 3SD (0.212). Absorbance values were read at 405 nM and presented as mean of duplicates.

3.3.12. Detection of anti-IA-2 antibodies and anti-ZnT8R antibodies by IA-2ic MBP fusion protein and ZnT8R fusion protein in Cohort 1 and Cohort 2

T1D Cohort 1 and Cohort 2 were screened by IA-2ic MBP fusion protein ELISA. Eight out of sixty patients were above the established assay cut off (0.271) for anti-IA-2 antibody positivity. Of those, three (T1D019, T1D035, T1D069) were positive by IA-2 RSR ELISA. Similarly, total patient pool was tested by ZnT8R fusion protein ELISA. Seven out of sixty-two patients were detected as positive for anti-ZnT8R antibodies. Three (T1D035, T1D066, T1D069) of those patient sera were also found positive by ZnT8 RSR ELISA.

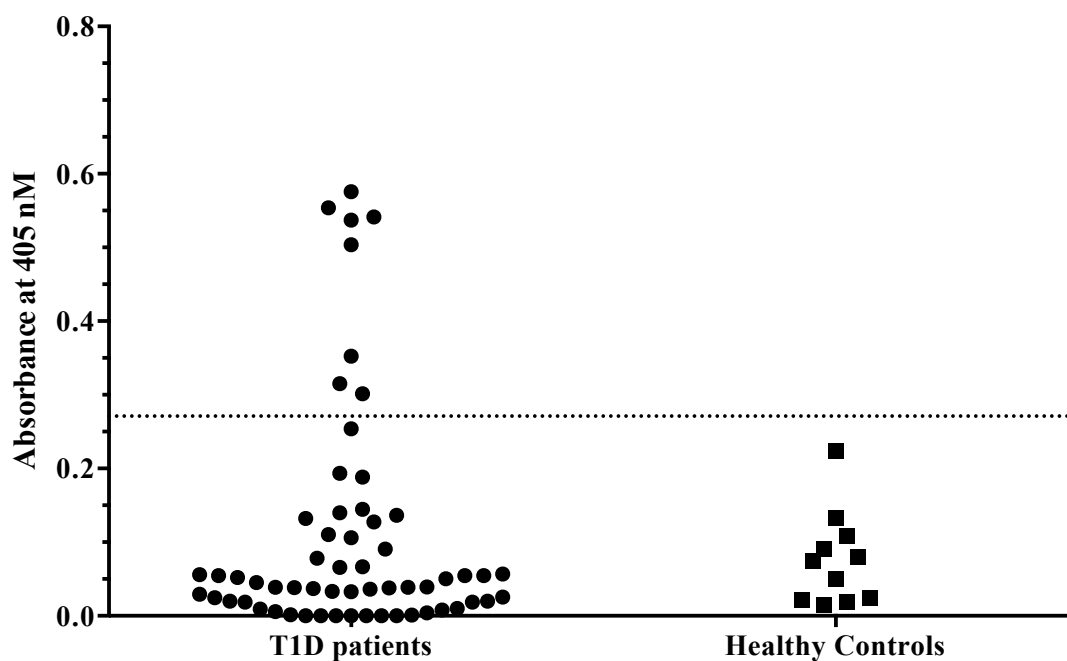


Figure 3.11. The presence of anti-IA-2 autoantibodies in T1D patient sera (Cohort 1 and 2) and healthy controls sera detected using IA-2ic MBP fusion protein ELISA. Sixty T1D patients and 11 healthy individuals were screened. Patients with OD values above 0.271 ($3SD + \text{Mean of controls}$) were considered as positive for antibodies against IA-2 antigen. 13% (8 out of 60 patients) were positive for IA-2 autoantibodies. Mean: 0.1078. SD: 0.1544. All OD values were measured at 405 nM and results were presented as the mean of duplicates and normalized to background reading.

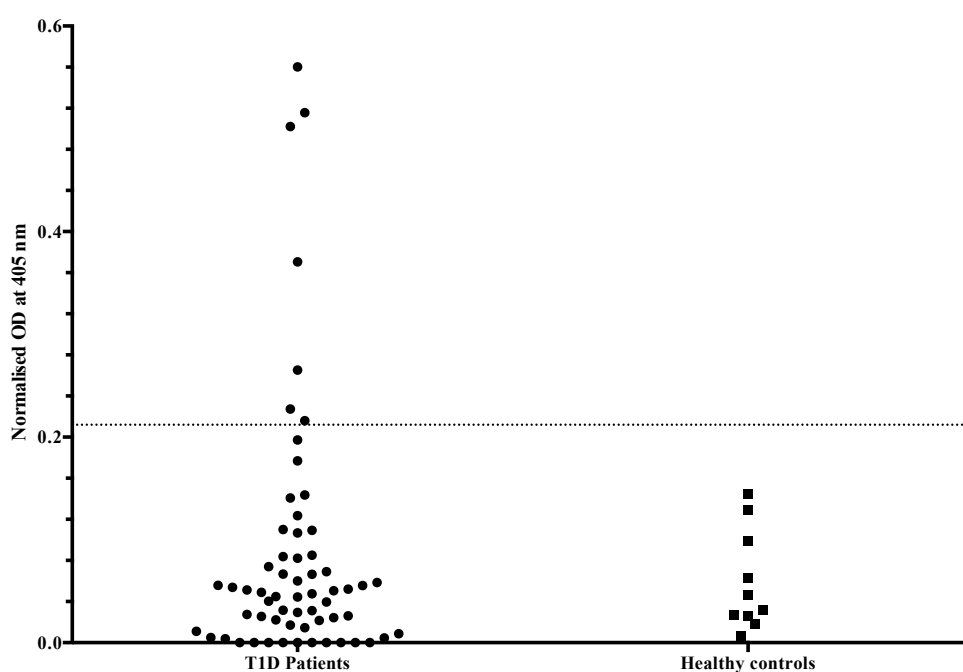


Figure 3.12. The presence of anti-ZnT8R autoantibodies in T1D patient and healthy control sera detected using ZnT8R MBP fusion protein ELISA. Sixty-two T1D patients and 10 healthy individuals were screened. Patients with OD values above 0.212 ($3SD + \text{Mean of controls}$) were considered as positive for antibodies against IA-2 antigen. Approximately 11% (7 out of 62 patients) were positive for anti-ZnT8R autoantibodies. All OD values were measured at 405 nM and results were presented as the mean of duplicates and normalized to background reading.

3.3.13. Confirmation of fusion protein ELISA specificity

To further confirm the specificity and utility of the fusion protein ELISAs, antibody positivity detected by MBP fusion protein ELISA was compared to that of RSR ELISA. Nine out of sixty patients were found positive for anti-IA-2ic antibodies by RSR ELISA. Seven out of sixty patients were found positive by IA-2 MBP fusion protein ELISA. Three patient sera (T1D035, T1D019, T1D069) were found positive for anti-IA-2 antibodies by both RSR and IA-2ic MBP fusion protein ELISA.

Similarly, seven out of sixty-two patients were positive for anti-ZnT8R antibodies by RSR ELISA. The two prototype T1D patients (T1D035, T1D019) were then used for the initial characterization of the ZnT8R fusion protein assays alongside additional RSR validated patient sera for antibody responses against IA-2 and ZnT8R.

3.3.13.1. Additional characterization of the IA-2ic MBP fusion protein ELISA.

Interestingly, RSR mean OD values for the IA-2A positive patients T1D019, T1D035 and T1D016 were 1.67, 1.08 and 0.56 by RSR ELISA (absorbance at 405 nM) respectively. While mean OD value obtained from IA-2ic MBP fusion protein ELISA for these patient sera were 0.315, 0.537 and 0.020 respectively (Table 3.3). It is therefore likely that the IA-2 fusion protein ELISA lacks sensitivity relative to the RSR ELISA method and may only detect high titre anti-IA-2 antibody responses. Another possibility is that the RSR ELISA presents a broader range of antigenic epitopes for serum binding compared to fusion protein.

Table 3.4. Comparison of Anti-IA-2 antibody positivity and mean OD values as detected by RSR and IA-2ic MBP fusion protein ELISA in cohort 1 and 2 of T1D patients.

No.	Code	RSR ELISA		IA-2 Fusion Protein ELISA	
		Positivity	OD at 405 nM	Positivity	OD at 405 nM
1.	T1D008	+	0.870	-	0.146
2.	T1D051	+	0.469	-	0.230
3.	T1D035	+	1.083	+	0.537
4.	T1D046	+	1.532	-	0.038
5.	T1D019	+	1.673	+	0.315
6.	T1D011	+	0.835	-	0.000
7.	T1D016	+	0.561	-	0.020
8.	T1D001	-	0.010	+	0.541
9.	T1D002	-	0.047	+	0.553
10.	T1D010	-	0.042	+	0.503
12.	T1D057	-	0.082	+	0.352
13.	T1D065	-	0.089	-	0.254
14.	T1D069	+	2.568	+	0.575
15.	T1D056	+	0.846	-	0.004
16.	T1D063	-	0.385	-	0.052
17.	T1D014	-	0.006	-	0.000

3.3.13.2. Characterization of the ZnT8R MBP fusion protein ELISA

As with IA-2 fusion protein ELISA, further testing of patient sera was conducted with the ZnT8 fusion protein ELISA. For the ZnT8R MBP fusion protein ELISA, additional RSR validated positive sera (T1D051 and T1D054) and patient sera negative for ZnT8A (T1D034) by RSR ELISA were compared to the positive control (T1D035) (Table 3.4).

In this ELISA, OD values for T1D035 was above the assay cut off (0.212) consistent with the previous ELISAs. Interestingly, OD values for all other sera samples were below the assay cut off. These values did not significantly differ from OD values obtained from the 2 control sera included in the ELISA or when compared to pooled control OD values (mean OD of 0.11) at serum dilution of 1/20.

As with the IA-2 results, RSR OD values for T1D035 is 1.23 whereas values for T1D050 is 0.54, while mean OD values obtained from ZnT8R MBP fusion protein ELISA were 0.56 and 0.082 suggesting that the ZnT8R fusion protein ELISA also lacks sensitivity in comparison to the RSR ELISA, and only detects high ZnT8RA patient sera. Furthermore, there are 3 types of autoantibody isotypes that target the polymorphic residues at aa position 325 of the C-terminal of the ZnT8 protein giving rise to either anti-ZnT8R, ZnT8W and ZnT8Q antibodies. Therefore, in addition to the lower sensitivity, it is likely that the lower number of ZnT8A positive patients detected by this ZnT8R fusion protein ELISA is due to the presence of the other two autoantibody variants that are not detected by ZnT8R MBP fusion protein ELISA in the patient sera.

Interestingly, T1D patients positive by ZnT8R fusion protein ELISA (T1D002, T1D010, T1D068, T1D059) with mean OD values of 0.502, 0.515, 0.227 and 0.216 respectively were negative by ZnT8 RSR ELISA with mean OD values of 0.024, 0.035, 0.006, 0.003 respectively. It was concluded that this is due antibodies against the MBP portion in the sera or high background binding to the fusion protein due to high viscosity.

Table 3.5. Comparison of anti-ZnT8R antibody positivity and mean absorbance values as detected by RSR ELISA and ZnT8R MBP Fusion protein ELISA for T1D patient cohort 1 and 2.

No.	Code	RSR ELISA		ZnT8R MBP fusion protein ELISA	
		Positivity	OD at 405 nM	Positivity	OD at 405 nM
1.	T1D051	+	0.720	-	0.000
2.	T1D035	+	1.232	+	0.560
3.	T1D042	+	0.174	-	0.000
4.	T1D050	+	0.538	-	0.082
5.	T1D002	-	0.024	+	0.502
6.	T1D010	-	0.035	+	0.515
7.	T1D066	+	0.530	+	0.265
8.	T1D068	-	0.006	+	0.227
9.	T1D069	+	0.728	+	0.370
10.	T1D074	+	0.460	NS	NS
11.	T1D009	+	0.266	-	0.083
12.	T1D054	+	0.220	-	0.040
13.	T1D059	-	0.003	+	0.216

3.4. Discussion

Recent advances in proteomics methods have facilitated the study of variable region peptide signatures of autoantibodies. Arising from these studies is the concept that the autoimmune B cell and autoantibody repertoires in systemic autoimmune diseases such as Sjogren's syndrome and SLE arise from common pathophysiological pathways in individual patients. For example, it has been shown that anti-Ribosomal P antibodies associated with SLE and anti-Ro60 responses in SS are kappa restricted and contain public, unique heavy and light chain pairings (Al Kindi et al., 2016). Prior to these studies it was assumed that the generation of autoreactive B cells was relatively a random process. However, the evidence emerging that the generation of autoantibodies of the same clonal family with identical heavy and light chain variable regions with identical antigen specificity in numerous unrelated individuals is remarkable. This implies that the autoimmune pathway of the humoral response against many autoantigens is identical from patient to patient in systemic autoimmune diseases. Such findings may open opportunities for the development of novel therapies to address autoimmune diseases.

A similar proteomics approach was taken in the current project to interrogate the origin and role of autoantibodies generated against islet antigens in T1D. To date autoantibodies against islet antigens such as IAA, IA-2, GAD and ZnT8 are readily used diagnostic markers for autoimmune T1D. However, their origin and role in the disease process remains ambiguous as characterising autoantibodies in organ specific autoimmune diseases such as T1D face a variety of challenges. For instance, the autoantibody titres in sera of patients with T1D is much lower in comparison to the autoantibody levels seen in patients with systemic autoimmune diseases, hindering the generation of high yield antibody samples required for proteomics analysis.

Additionally, some autoantibody responses are relatively brief in duration and are prominent in early stages of disease. The major T1D autoantibodies, GAD and IA-2 presenting a prevalence of approximately 90% at diagnosis dropping to 40% in the first year of the disease. For example, in terms of anti-IA-2 responses, the intracellular domain has been described as the most antigenic region for the detection of IA-2

autoantibodies from T1D sera. This region contains the JM and PTP domains, both of which contain autoantigenic epitopes commonly targeted at diagnosis and appear to comprise the bulk of the anti-IA-2 response (Bearzatto et al., 2002).

These limitations notwithstanding, the current study utilized a recombinant MBP fusion protein approach in an attempt to isolate anti-IA-2 and anti-ZnT8 autoantibodies for proteomic analysis using the IA-2ic and two individual ZnT8 fusion proteins comprising the antigenic SNP at aa 325 encoding R/W.

In the first instance, IA-2 fusion protein was utilized in an ELISA immunoassay in an attempt to detect IA-2 autoantibodies by testing two high positive and two negative sera validated by RSR ELISA. This was met with success, as the two high positives showed OD values greater (10-fold) than the OD values of the two healthy controls by fusion protein ELISA. After establishing that the fusion protein ELISA was able to detect IA-2 autoantibodies from T1D sera, a larger pool of healthy control sera was tested to set up an ELISA assay cut off to exclude autoantibody negative sera (Lardeaux et al. 2016, Ridge et al. 1993). The mean OD values of the validated autoantibody positive sera (0.334) was over three-fold higher than the mean OD value of the pool of healthy control sera. Therefore, the assay cut off for positivity for IA-2 autoantibodies was set at 3SDs above the mean OD value of healthy controls, following standard practice for establishing assay cut offs for serological assays (Ridge et al. 1993).

Subsequently once the cut off was set up where all validated negative and healthy sera were below the assay cut off, the remaining 56 T1D patient sera were tested for the presence of IA-2 autoantibodies. In comparing the IA-2ic MBP fusion protein ELISA results to IA-2 RSR ELISA results, three (T1D019, T1D035, T1D069) out of nine RSR positives were detected as positives by IA-2ic MBP fusion protein ELISA.

The disparity in the ability of the MBP fusion protein ELISA and RSR ELISA in the detection of IA-2 antibodies is highly likely due to the difference in the antigen presentation in the assays. The RSR ELISA utilizes a recombinant IA-2ic protein from which the GST affinity tag has been cleaved off, whereas the IA-2ic MBP fusion protein ELISA utilizes a recombinant MBP fusion protein of IA-2ic antigen with the

affinity tag still intact. The presence of a large MBP affinity tag (~45 kDa) is likely to affect the tertiary structure of the fusion protein and therefore the epitope presentation for antibody binding (Costa et al. 2014). It is possible that the removal of the affinity tag from the protein prior to the use in ELISAs would change the folding of the IA-2ic protein, potentially increasing the presentation of epitopes or further inhibiting antigen presentation. However, this approach would add another layer of complexity that is beyond the scope of this project. As the IA-2ic MBP fusion protein detects 3 out of the 9 RSR high binders indicating >50% success rate of detecting high titre sera required to produce high yield antibody samples for mass spectrometry. Therefore, IA-2 fusion protein ELISA appears suitable for isolating IA-2 autoantibodies from T1D sera.

Once the protocol for IA-2ic MBP fusion protein ELISA was developed, a similar strategy was applied to the ZnT8 fusion protein ELISAs. As explained in chapter 3.3.2. the recombinant ZnT8R fusion protein was successfully generated while ZnT8W and ZnT8Q fusion proteins were unsuccessful. Therefore, only ZnT8R fusion protein ELISA was developed as explained below.

Firstly, ZnT8R MBP fusion protein was tested in an ELISA assay to detect anti-ZnT8R autoantibodies using two high positives and two negative sera validated by ZnT8 RSR ELISA. One of the positives was also detected as anti-ZnT8R antibody positive by fusion protein ELISA. The detected positive was the highest binder in RSR ELISA and showed a mean OD value approximately 7-fold greater than the mean OD values of the healthy control sera. Therefore, it appeared that the fusion protein ELISA was able to detect anti-ZnT8R antibodies in T1D sera. Hence, as with IA-2 ELISA, a pool of healthy control sera was tested by ZnT8R ELISA to establish an ELISA assay cut off to determine ZnT8R autoantibody positivity and exclude negative sera.

Subsequently, T1D cohort 2 was also tested by ZnT8R fusion protein ELISA for the presence of anti-ZnT8R antibodies. When comparing RSR ELISA results to ZnT8R fusion protein ELISA results, the first positive sera which presented the highest OD values by RSR ELISA, remained the highest positive detected by both ZnT8R fusion protein ELISA and RSR ELISA. Two additional patient sera were also detected as positive (T1D066, T1D069). As the ZnT8R fusion protein ELISA utilized only one

variant limiting the detection to anti-ZnT8R antibodies alone, it was expected that the number of positives detected by fusion protein ELISA would be lower compared to RSR ELISA which uses all three variants.

Moreover, similar to IA-2 fusion protein ELISA, ZnT8R fusion protein ELISA also utilizes a recombinant MBP fusion protein of ZnT8R protein. Therefore, as suspected in IA-2 fusion protein ELISA, it is likely that the presence of the large affinity tag may have an adverse effect on the tertiary structure of the small aa 369 protein fragment hence affecting the epitopes available for antibody binding.

This is supported by Wenzlau et al who reported that 80% of the ZnT8A positive T1D patients have antibodies that targets the ZnT8 C terminal domain (aa 268-369) which consists of the SNP at aa 325 along with aa 332, 333, 336 and 340. These are identified as an important part of a conformational epitope and the epitope presentation may not be preserved in exactly the same form in the fusion protein as the native antigen (Wenzlau et al. 2008, Araujo et al. 2004). Therefore, it is possible that the large affinity tag incorporated into the ZnT8R fusion protein interacts with the small ZnT8R construct such that not all epitopes are available for serum antibody binding.

In conclusion, as the ZnT8R fusion protein ELISA was unable to detect high titre anti-ZnT8R positive patient sera required for proteomic analysis likely due to the reasons discussed above hence, the ZnT8R fusion protein ELISAs were not utilized for the following affinity purification experiments.

Chapter 4. Affinity purification of antibodies that target epitopes within IA-2ic antigens with the use of a novel ELISA plate purification method

4.1. Prologue to chapter 4

4.1.1. Prologue to affinity purification of anti-IA-2 antibodies

To establish a rationale for proteomic analysis of clonality, preliminary ELISAs were performed to look at the distribution of kappa and lambda light chains in the anti-IA-2 responses as determined by IA-2 fusion protein. It is reported that the kappa and lambda expression ratio in healthy individuals ranges from 0.85-1.86 (Smith et al. 2016). This reflects the ratio of functional V gene segments at the two loci. This ratio is reported to be altered and reach up to >10:1 during antigenic selection (Langman & Cohn, 1995). For instance, antibodies against EBV protein EBNA-1 and diphtheria toxin mutant CRM197 are reported to be kappa dominant, showing a kappa to lambda ratio of 4.52 – 9.72 (Smith et al. 2016). Similarly, Al Kindi et al. reported that anti-Rib-P autoantibody proteome in SLE autoimmune response is IgG1 kappa restricted (Al Kindi et al. 2016). Therefore, in order to investigate whether a similar light chain skewing is present in the anti-IA-2 response in T1D, a preliminary kappa and lambda ELISA was conducted by using anti-human kappa and lambda antibodies on T1D serum IgG bound to the IA-2 fusion protein coated on the ELISA plate (Figure 4.1).

4.1.2. Methods

4.1.2.1 Kappa and lambda distribution ELISA

As described in chapter 2.3.3.6, ELISA was carried out using the optimized coating and serum concentrations. Assessment of potential clonality for the bound serum antibodies was assessed using rabbit kappa and lambda anti-human antibodies (A0191, A0193, Dako, Agilent, CA, USA) which were detected by using a Goat anti-Rabbit alkaline

phosphatase secondary antibody (Sigma, Merck, New Jersey, USA). All samples were tested in duplicates. Results were graphed as the mean of duplicates.

4.1.3. Results

4.1.3.1. Anti-IA-2 antibodies against epitopes within the IA2 MBP fusion protein have altered kappa lambda distribution

Mean OD of the bound patient sera antibodies probed with anti-kappa antibody was 1.9 while mean OD of anti-lambda antibody reactivity on anti-sera antibodies was 0.632. Therefore, the kappa to lambda IgG ratio in the bound patient IgG population was 3.2:1. Whereas the anti-kappa antibodies tested on healthy control sera gave an OD of 0.539 and anti-lambda antibodies showed an OD of 0.4065, kappa to lambda antibody ratio in the bound healthy control IgG is 1.32:1.

This disparity in kappa to lambda antibody ratio in the bound patient sera and healthy control sera suggest a clonal restriction. Therefore, in order to further study the clonality of the anti-IA-2 antibodies in individual T1D patients more closely, monospecific antibody samples were produced by ELISA plate affinity purification for mass spectrometry.

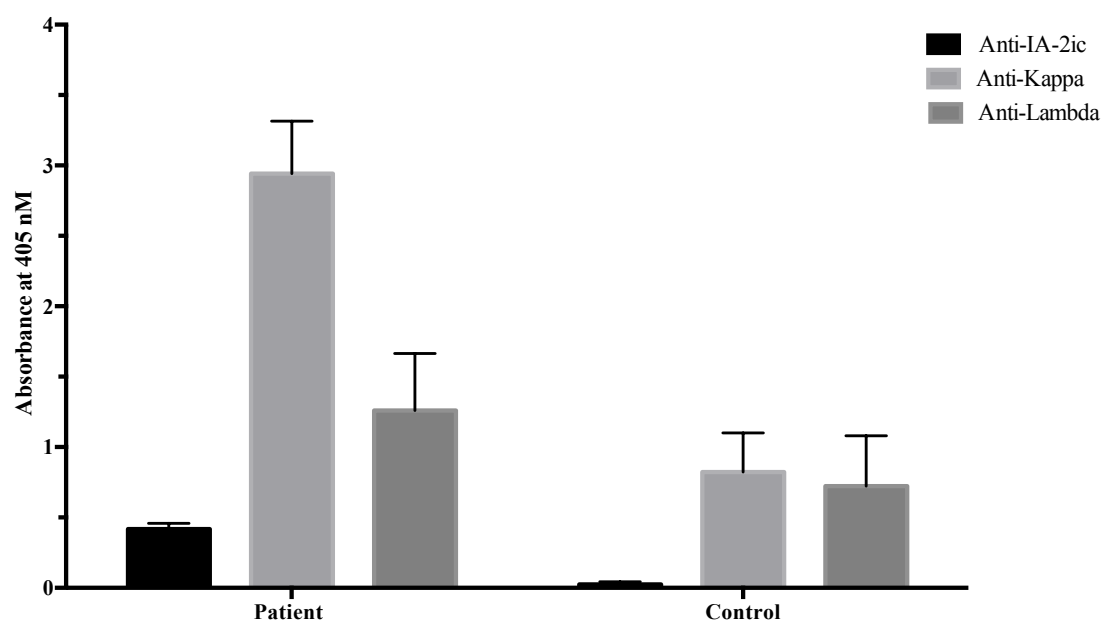


Figure 4.1. Kappa and lambda light chain distribution in the anti-IA-2ic affinity purified antibody sample generated from T1D069 sera. Bound kappa and lambda antibodies were probed with secondary anti-rabbit HRP conjugated antibody. Absorbance values were read at 405 nM and values were presented as means of triplicates.

4.2. Introduction

Chapter 3 describes an ELISA method to detect IA-2 autoantibodies from T1D sera using recombinant MBP fusion protein of IA-2ic. This ELISA method successfully detected sera with high titres of IA-2 antibodies, which are suitable for generating purified high yield antibody samples required for mass spectrometry analysis.

For this project, several methods were considered to affinity purify IA-2 antibodies from the selected high IA-2A titre sera. Alkindi et al. 2012 developed an ELISA plate affinity purification method to purify anti-SmD antibodies from complex SLE patient sera using antigen coated ELISA plates. They reported that the method superseded the more complex and time-consuming column chromatography previously used by the same group to affinity purify anti-SmD antibodies.

They also reported that this ELISA plate method is as efficient as the column chromatography method in affinity purifying antibodies from complex sera. This efficiency was achieved from serum volumes of 1 mL and fusion protein concentrations of 20 micrograms in comparison to 5 ml sera and 7 mg of recombinant fusion protein used in column chromatography. Therefore, IA-2 fusion protein ELISA plate method was utilized to affinity purify anti-IA-2 antibodies from the selected high anti-IA-2 titre sera in order to produce suitable samples for mass spectrometry analysis.

4.3. Materials and Methods

4.3.1. Selection of patient and control sera for affinity purification experiments

As described in chapter 3, three sera with high anti-IA-2A titres detected by both IA-2 fusion protein ELISA and RSR ELISA (T1D019, T1D035, T1D069) were selected for ELISA plate affinity purification to isolate IA-2 antibodies. However, T1D035 was not used for further experiments due to lack of sera resources, and the participant was unable to be contacted. Therefore, only T1D019 and T1D069 were used for the affinity purification experiments.

Two T1D patients (T1D001, T1D002) were selected based on IA-2A RSR ELISA negative results. These samples showed high OD values against IA-2 and ZnT8R by fusion protein ELISA due to possible background binding to the MBP component of the fusion proteins. This is likely as the sequence for the MBP portion of both fusion proteins is identical (Chapter 3.3.6.2). These patients were therefore used as controls for true IA-2A binding.

In addition, two healthy control sera (CTR062, CTR063) were used as prototype negative controls.

4.3.2. Affinity purification of IA-2 antibodies

Affinity purification experiments were performed as described in chapter 2.4.1 with the use of IA-2 fusion protein ELISA. The selected positive patients, negative patient controls and healthy controls, as described above, were tested by ELISA in parallel at the time of each affinity purification experiment as a positive control to confirm success of the ELISAs and confirm adequate titres of anti-IA-2 antibodies binding to the fusion protein. The same reagents were used in the parallel ELISA and in the affinity purification experiment for accurate verification. Affinity purification experiments were carried out at least four times per individual serum. Two such purification experiments were used for determination of specific enrichment of anti-IA2 antibodies,

with the final two purification rounds used to produce antibody samples for mass spectrometry analysis.

4.3.3 Quantification of purified IgG by western blot densitometry analysis

Protein yields from affinity purification experiments were assessed prior to reactivity ELISAs to allow adjustment of serum and affinity purified immunoglobulin for the specificity ELISA experiment. Quantification was not performed on the IgG samples for proteomics.

In order to quantify the yield of the affinity purification experiment, SDS PAGE densitometry analysis was performed. The eluted fraction (5 μ L) was run along with serial dilutions of control caprylic IgG samples of 2, 1, 0.5, 0.25, 0.125, 0.0625, 0.03125, 0.01562, 0.0078, 0.0039, 0.00097, 0.000244, 0.000061 and 0.000000001 ug/mL concentrations as standards (Figure 4.2). The completed electrophoresis gel was imaged using Bio-Rad Gel Doc EZ imager (Bio-Rad, Australia). Following SDS gel electrophoresis, western blotting was carried out with anti-human IgG antibody and the immunoblot image was imaged using ChemiDoc Imaging system (Bio-Rad, Australia). Individual patient sample lanes were analysed and compared to each other based on densitometry using image lab software (Bio-Rad, Hercules, CA, USA). The intensity values of all samples were normalized to the background. The normalized values were used for densitometry calculations.

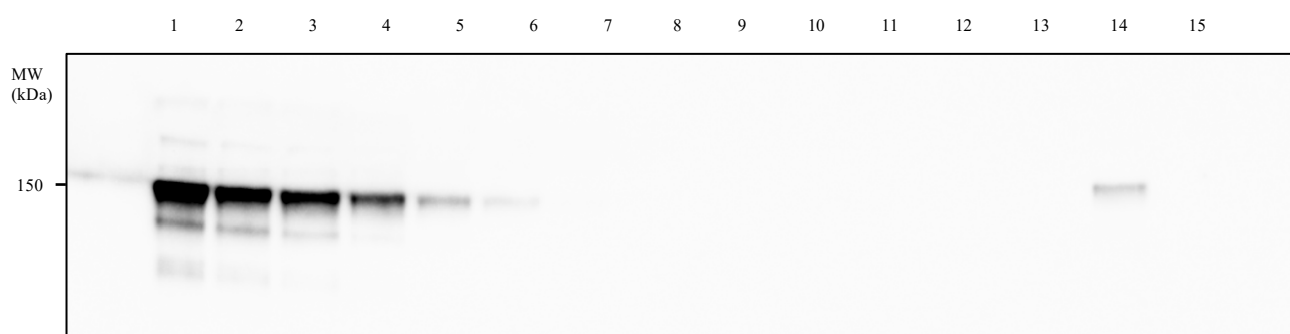


Figure 4.2. Representative western blot used for densitometry analysis. The immunoblot was used in Bio-Rad Image Lab software to calculate the concentration of immunoglobulin in the affinity purified antibody sample generated from T1D sera using ELISA plate affinity purification method.

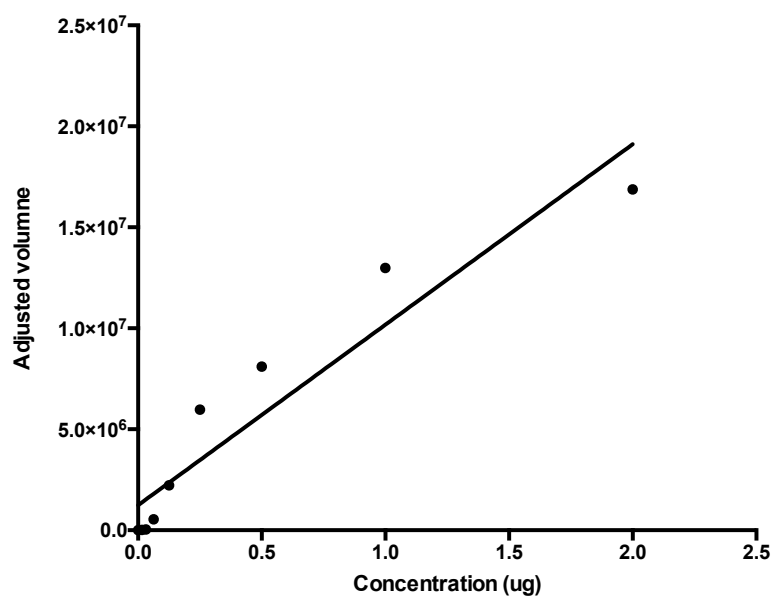


Figure 4.3. Representative linear regression standard curve. The standard curve was generated using densitometry absorbance values of IgG standards of known concentrations using image Lab software.

Table 4.1. Representative table of the protein intensity data. The western blot image of the caprylic IgG standard was analysed by generating a linear regression curve to calculate the concentration of IgG in the affinity purified antibody sample using Bio-Rad image lab software.

No.	Label	Type	Volume (Int)	Adj. Vol. (Int)	Mean Bkgd. (Int)	Abs. Quant. (ug)
1	U1	AP AB T1D019	792,583.00	331,582.00	692.193694	0.031137
2	B1	Background	461,001.00	0	692.193694	N/A
3	2 ug	Standard	17,337,863.00	16,876,862.00	692.193694	2
4	1.0 ug	Standard	13,451,516.00	12,990,515.00	692.193694	1
5	0.5 ug	Standard	8,564,132.00	8,103,131.00	692.193694	0.5
6	0.25 ug	Standard	6,434,422.00	5,973,421.00	692.193694	0.25
7	0.125 ug	Standard	2,682,592.00	2,221,591.00	692.193694	0.125
8	0.062 ug	Standard	996,811.00	535,810.00	692.193694	0.062

Table 4.2. Representative yields of affinity purified antibodies produced from approximately 1 mL sera. Affinity purified antibody samples were generated using IA-2A positive, IA-2A negative and healthy control sera using IA-2 fusion protein ELISA plate affinity purification method.

	Patient	Yield (ug)
1.	T1D019	1.25
2.	T1D069	2.80
3	T1D001	2.89
4.	T1D014	8.40
5.	CTR063	8.60
6.	CTR062	3.04

4.3.4. Reactivity ELISA

Following successful affinity purification and parallel ELISAs, the specificity of the eluted affinity purified antibody samples was confirmed by testing the individual eluted antibody sample against IA-2, ZnT8R fusions proteins and serum alone on ELISA plate (1/6 dilution), along with starting serum (1/20 dilution), unbound serum, adjusted sera (sera diluted so the total IgG in the eluted fraction is identical to the total IgG in the sera) and healthy control serum by ELISA as described in chapter 2.3.3.7.

4.3.5. SDS-PAGE gel electrophoresis of eluted IgG for isolation of heavy and light chains for mass spectrometry

SDS-PAGE electrophoresis of eluted IgG fractions was carried out as described in chapter 2.4.2 to confirm the purity of affinity purified antibody sample. Each purified antibody sample was run in parallel with a caprylic IgG of known concentration as a positive control. This sample was cut out and processed as described in chapter 2.4.2 for mass spectrometry analysis.

4.4. Results

4.4.1. Affinity purification of anti-IA-2 antibodies targeting the epitopes within the fusion protein IA-2

4.4.1.1. Confirmatory ELISA conducted in parallel to each affinity purification process

To confirm the integrity of the reagents and the plate purification reaction, a parallel ELISA was carried out for each affinity purification process for the two validated IA-2A positive patients (T1D019, T1D069), two validated negative patients (T1D001, T1D002) and two healthy controls (CTR062, CTR063) (Figure 4.2). Each serum was tested on IA-2 fusion protein and ZnT8R fusion protein.

IA-2A positive T1D patients

The parallel confirmatory ELISAs conducted in conjunction with the four affinity purification experiments using T1D019 sera on IA-2 fusion protein showed mean OD values of 0.241, 0.475, 0.399 and 0.331, in the 4 experiments, respectively. Three of which were above the assay cut off (0.27) for anti-IA-2 antibody positivity while the first confirmatory ELISA showed slightly lower ODs (Table 4.1), which would have potentially affected the yield in that purification round.

This indicated that the ELISA reaction worked successfully on the day, giving positive OD values over healthy control binding (0.145, 0.018, 0.012 and 0.010 respectively) for anti-IA-2 antibodies (Figure 4.2). The mean ODs of T1D019 sera binding to ZnT8R fusion protein were 0.087, 0.080, 0.123 and 0.000 in the confirmatory ELISAs, respectively. These OD values were below the assay cut off for anti-ZnT8R antibody positivity (mean OD of 0.341), as described in Chapter 3.3.4.

Similarly, the binding against the IA-2 fusion protein in the four T1D069 parallel ELISAs were 0.831, 0.840, 0.408 and 1.031 which were above the assay cut off (0.27), with OD values of the healthy control sera 0.012, 0.005, 0.007 and 0.043, respectively. The mean ODs of T1D069 serum binding to ZnT8R fusion protein were 0.497, 0.246,

0.081 and 0.565, respectively. Three out of 4 of the ELISAs showed OD values positive for anti-ZnT8R antibodies. The mean OD values obtained from the confirmatory ELISAs, representing T1D069 serum binding to IA-2 fusion protein, were not significantly different from the OD values obtained from previous ELISAs (mean OD of 0.739) (Chapter 3.2.2).

IA-2A negative T1D patients

To account for potential anti-MBP responses in comparison to true IA-2 responses, T1D001 and T1D002 patient sera were also used in the same 4 round affinity purification approach as the true IA-2A positive patients.

The confirmatory ELISAs gave high OD values for both T1D001 and T1D002, with T1D001 patient giving mean OD values of 0.918, 0.961, 0.070, 0.486 in each of the four confirmatory ELISAs.

The mean OD values of T1D001 serum binding against ZnT8R fusion protein were also above the assay cut off for positivity for anti-ZnT8R antibodies (0.345, 0.412, 0.002, 0.476). These high OD values observed against both fusion proteins were likely due to background binding to the non-specific MBP portion of the fusion protein. This was further investigated in the following reactivity ELISA.

The two antibody samples generated by the first two affinity purification experiments were used for specificity ELISAs. The third sample was not utilized given the confirmatory ELISA showed low OD values across IA-2 and ZnT8R fusion proteins suggesting that the affinity purification experiment was not successful on the day. Therefore, only the fourth sample was used for proteomic analysis. Unfortunately, there was not sufficient serum samples to repeat a 4-plate affinity purification experiment.

The mean OD values of T1D014 of serum binding on IA-2 fusion protein in the confirmatory ELISAs were 0.030, 0.036, 0.898 and 0.026. The mean OD values representing serum binding to ZnT8R fusion protein were 0.005, 0.011, 0.076 and 0.020.

Healthy control sera

The mean ODs of CTR062 serum binding on IA-2 fusion protein, were 0.084, 0.062, 0.029 and 0.111. Mean ODs of CTR062 serum binding on ZnT8R fusion protein, were 0.158, 0.051, 0.002 and 0.098.

Similarly, mean ODs of CTR063 serum binding on IA-2 fusion protein was 0.026, 0.003, 0.016 and 0.009 and the mean ODs of serum binding on ZnT8R fusion protein were 0.028, 0.034, 0.012 and 0.051. The mean OD values were not significantly different from the pooled mean OD value of the respective control sera binding against the IA-2 fusion protein (0.076).

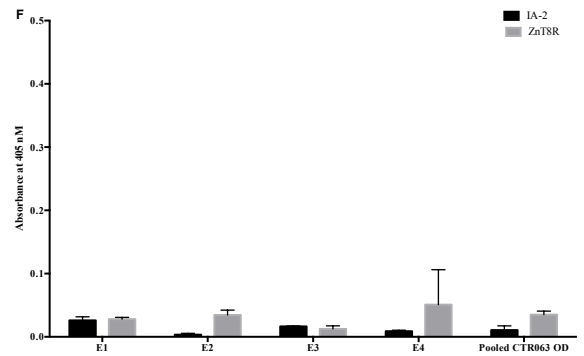
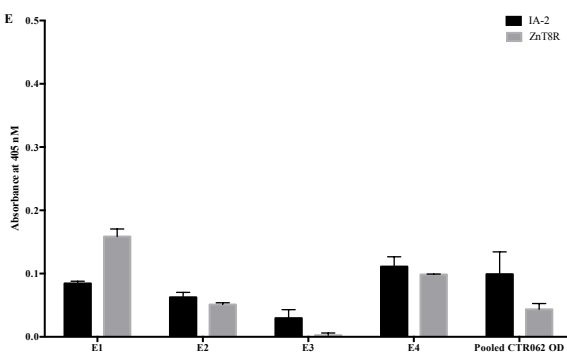
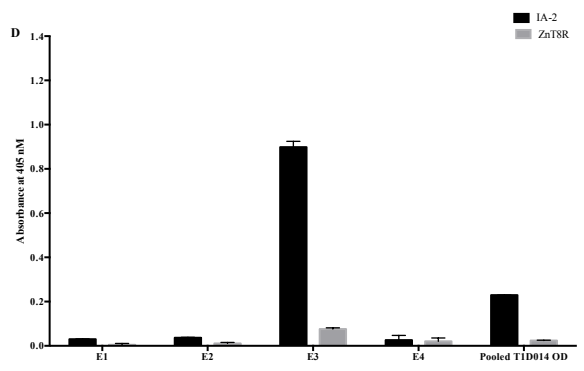
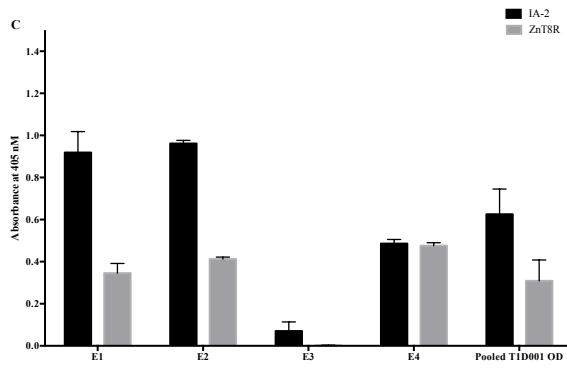
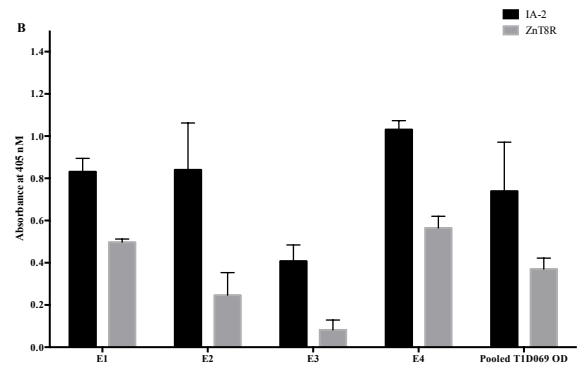
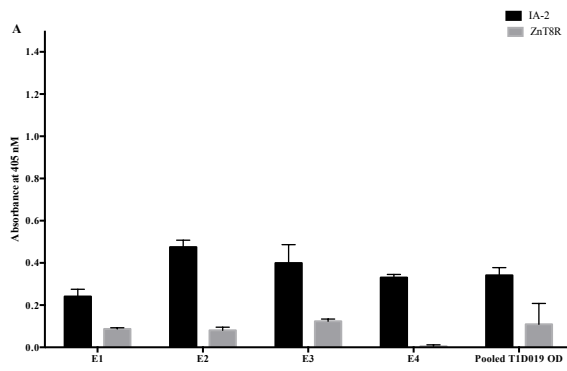


Figure 4.4. ELISA carried out in parallel to affinity purification process to confirm the integrity of the reaction. **A.** Mean OD of T1D019 serum binding in parallel ELISAs conducted per each affinity purification experiment compared to the mean OD of the sera binding from previous ELISAs. **B.** Mean OD of T1D069 serum binding in parallel ELISAs conducted per each affinity purification compared to the mean OD from previous ELISAs. **C.** Mean OD of T1D001 serum binding to IA-2 and ZnT8R fusion proteins in parallel ELISA compared to mean OD from previous ELISAs. **D.** Mean OD of T1D014 serum binding to IA-2 and ZnT8R fusion proteins in parallel ELISA compared to mean OD from previous ELISAs. **E.** Mean OD of CTR062 serum binding to IA-2 and ZnT8R fusion proteins in parallel ELISA compared to mean OD from previous ELISAs. **F.** Mean OD CTR063 serum binding to IA-2 and ZnT8R fusion proteins compared to binding from previous ELISAs. The antibody samples generated from the first two affinity purification experiments was used for specificity ELISA and the last two were used for mass spectrometry analysis.

4.4.2. Specificity ELISA

Following round one and two affinity purification experiments, eluted antibodies were assessed for specificity and enrichment of anti-IA-2 antibodies by reactivity ELISA for anti-IA-2 and anti-ZnT8R antibody positivity and the ratio of the two was compared to the serum binding in the same experiment (Chapter 4.2.4).

4.4.2.1. Affinity purification enriches the binding of T1D019 serum to IA-2 fusion protein

To determine enrichment for anti-IA-2 antibodies, the eluted antibody sample was first compared to the starting serum for anti-IA-2 reactivity by fusion protein ELISA (Figure 4.3.5). In this experiment the starting serum yielded a mean OD value of 0.30 while the affinity purified sample yielded a mean OD of 0.65. Both OD values were above the assay cut off for positivity (0.271). When the starting serum was adjusted ($\sim 1/63$

dilution) for IgG concentration to match the affinity purified antibody sample, binding against IA-2 was reduced to 0.033, effectively eliminating positivity for IA-2.

This suggests that the antibody sample is enriched with anti-IA-2 antibodies.

A second round of affinity purification experiments confirming these bindings, yielding mean OD values of 0.476, 0.248, 0.619 and 0.254 for starting serum, unbound serum, affinity purified antibody sample and adjusted serum against IA-2 fusion protein.

4.4.2.2. T1D069 affinity purified antibody sample binding to IA-2 and ZnT8R fusion proteins

Similarly, as expected T1D069 starting serum binding to IA-2 fusion protein showed mean OD value of 0.749 which was above the assay cut off (0.271). As with T1D019, T1D069 affinity purified antibody sample showed mean OD of 0.801, which was also above the assay cut off. In contrast, when IA-2A positive T1D069 serum was adjusted (~1/300) to match the total IgG in the affinity purified antibody sample, the positivity to anti-IA-2 antibodies was again eliminated. Therefore, it appeared that the affinity purification method was successful in generating an enriched antibody sample specific to IA-2 fusion protein.

Further clarification of purification was achieved by the analysis of binding to ZnT8R fusion protein. T1D069 starting serum binding on ZnT8R fusion protein (mean OD of 0.500) was above the assay cut for positivity (0.212) as observed in previous ELISAs (0.212). Comparatively, the affinity purified antibody sample binding to ZnT8R fusion protein showed OD values (mean OD of 0.042) that were below the assay cut for anti-ZnT8R antibodies. The adjusted serum binding to ZnT8R fusion protein was also below the detection levels.

In addition, the ratio of affinity purified antibody sample binding IA-2 and ZnT8R fusion protein was ~19:1 which was higher than the binding ratios of the starting serum which was ~1.5:1 and the binding ratios of adjusted serum which was ~5.6:1. This supported that an IA-2 specific antibody sample was generated using T1D069 serum.

The second round of affinity purification experiments confirmed these bindings giving mean OD values of 0.474, 0.274, 0.318 and 0.081 for the starting serum, unbound serum, affinity purified antibody sample and adjusted serum sample against IA-2 fusion protein.

4.4.2.3. T1D001 affinity purified antibody sample binding on IA-2 and ZnT8R fusion proteins

As expected, T1D001 patient starting serum, which was negative for IA-2 antibodies showed high OD values on IA-2 (0.666) and ZnT8R (0.366) fusion proteins. The affinity purified antibody sample also showed high OD values on IA-2 (0.916) and ZnT8R (0.801) fusion proteins. The antibody binding ratio of the starting serum was (~2:1) did not drastically differ from the ratio of affinity purified antibody binding to IA-2 and ZnT8R fusion protein was (~1:1). This shows that the antibody sample was not enriched with IA-2 specific antibodies and as discussed in chapter 3, the high ODs of starting serum and affinity purified antibody sample binding to both IA-2 and ZnT8R fusion proteins is likely due to reactivity to the non-specific MBP portion of the fusion proteins.

The second-round affinity purification experiment confirmed the binding giving OD values of 0.786, 0.857, 1.120 and 0.750 for starting serum, unbound serum, affinity purified antibody sample and adjusted serum sample against IA-2 fusion protein.

4.4.2.4. T1D014 affinity purified antibody sample binding on IA-2 and ZnT8R fusion proteins

Similarly, IA-2A negative T1D014 patient starting serum showed high OD values on IA-2 (0.086) and ZnT8R (0.037) fusion proteins, consistent with previous ELISA results. The affinity purified antibody sample also showed low OD values on IA-2 (0.103) and ZnT8R (0.030) fusion proteins. The binding OD values were below the assay cut for positivity (0.76).

Second round of affinity purification experiments also showed similar mean OD values of 0.05, 0.024, 0.019 and 0.015 for starting serum, unbound serum, affinity purified antibody sample and adjusted serum against IA-2 fusion protein.

4.4.2.5. CTR062 affinity purified antibody samples against IA-2 and ZnT8R fusion proteins

The mean OD of CTR062 starting serum (0.179) and eluted antibody sample (~0.216) were below the assay cut for anti-IA-2 antibody positivity. Similarly, the mean OD of starting serum (0.185) and affinity purified antibody (0.027) sample binding to ZnT8R fusion protein were also below the assay cut for anti-ZnT8R antibody positivity. Similarly, second round of affinity purification experiment gave similar mean OD values of 0.0925, 0.047, 0.1275 and 0.041 for starting serum, unbound serum, affinity purified antibody and adjusted serum against IA-2 fusion protein.

4.4.2.6. CTR063 affinity purified antibody samples against IA-2 and ZnT8R fusion proteins

The mean OD of starting serum binding (0.090) and affinity purified antibody sample binding (0.067) of CTR063 were also below the assay cut off for anti-IA-2 antibody positivity. The mean OD of CTR063 starting serum (0.056) and affinity purification antibody sample binding (0.081) to ZnT8R fusion protein were also below the assay cut off.

The second-round affinity purification experiments showed mean OD values of 0.072, 0.02, 0.059 and 0.031 for starting serum, unbound serum, affinity purified antibody sample and adjusted serum against IA-2 fusion protein. Neither CTR062 nor CTR063 affinity purified antibody samples showed anti-IA-2 antibody enrichment therefore, these were suitable healthy controls for the affinity purification experiments.

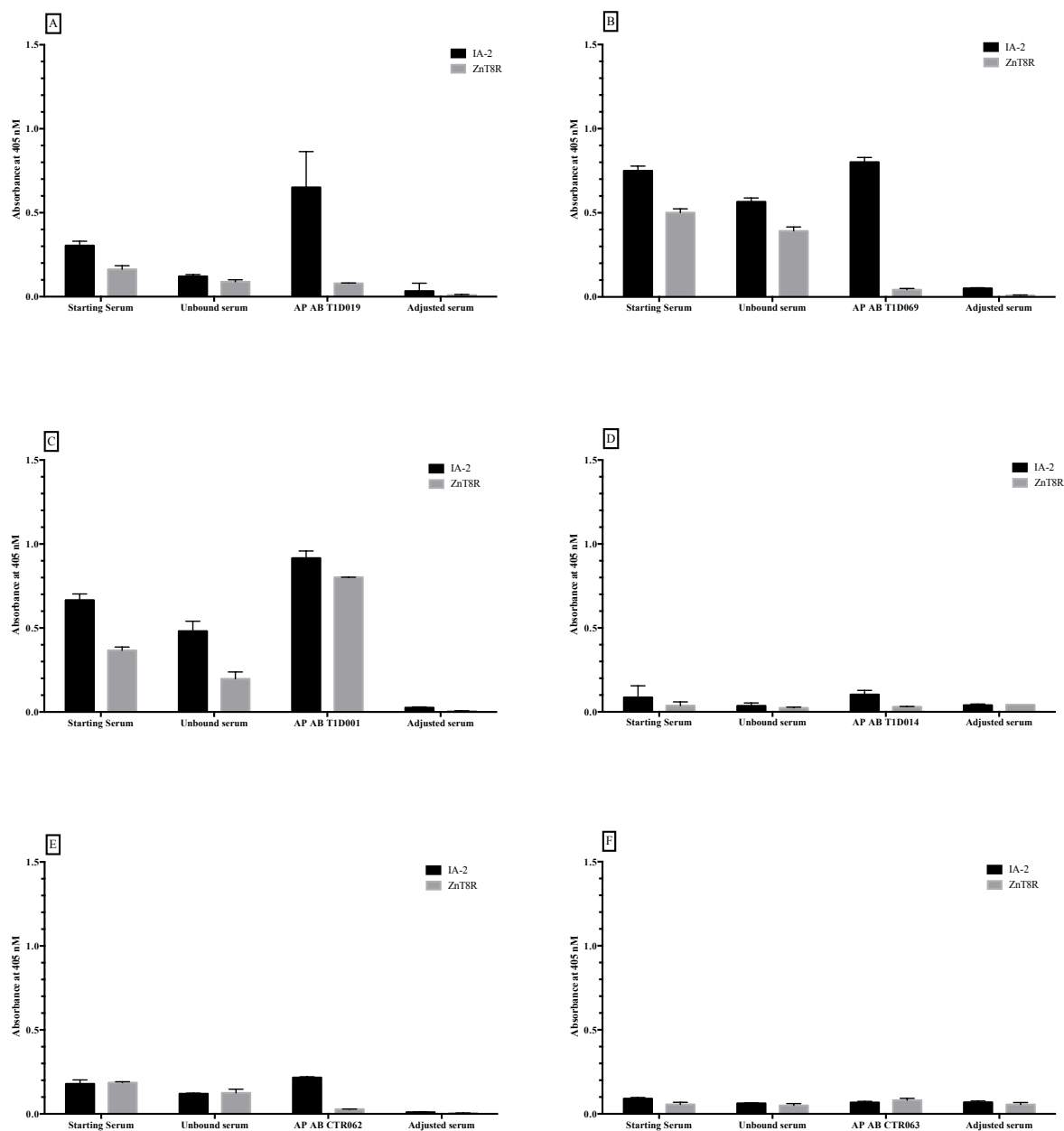


Figure 4.5. Reactivity ELISA of the affinity purified antibody samples generated using the IA-2ic MBP fusion protein ELISA plate affinity purification method. **A.** Affinity purified antibody sample prepared from T1D019 sera binding to IA-2 and ZnT8R fusion protein. **B.** Affinity purified antibody sample prepared from T1D069 sera binding to IA-2 and ZnT8R fusion protein. **C.** Binding of affinity purified antibody sample generated from T1D001 sera on IA-2 and ZnT8R fusion protein. **D.** Binding of affinity purified antibody sample generated from T1D014 sera against IA-2 and ZnT8R fusion protein. **E.** Binding of affinity purified antibody sample generated from CTR062

tested on IA-2 and ZnT8R fusion proteins. **F.** Binding of affinity purified antibody sample generated from CTR063 tested on IA-2 and ZnT8R fusion proteins.

4.4.3. SDS gel electrophoresis of eluted IgG fraction

After confirming the successful enrichment of anti-IA-2 antibody samples, two more rounds of affinity purifications were carried out to generate antibody samples for mass spectrometry analysis. The antibody samples were concentrated using 100 kDa spin columns and SDS gel electrophoresis was carried out to facilitate the isolation of heavy and light chains of the affinity purified antibodies. A caprylic IgG from a healthy control serum was run alongside the purified antibody sample. The thicker band running at 50 kDa molecular weight corresponds to the size of heavy chains. The fainter band running at 25 kDa corresponds to the size of light chains. These bands were cut out and transferred to a labelled Eppendorf tube. The gel bands were processed as described in chapter 2.4.2 and introduced to the mass spectrometer.

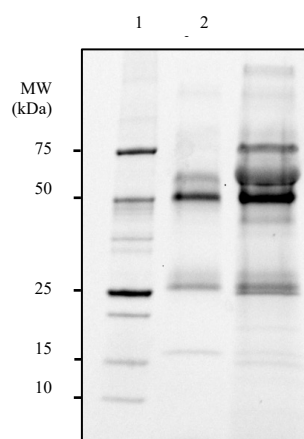


Figure 4.6. Representative gel image of 1D SDS gel electrophoresis of an affinity purified antibody generated by IA-2ic MBP fusion protein ELISA plate affinity purification method. The affinity purified antibody sample was run alongside a caprylic IgG sample from a healthy control to isolate heavy and light chain populations required for mass spectrometry analysis. Lane 1. Marker. Lane 2. Healthy control caprylic IgG sample. Lane 3. Affinity purified antibody sample generated from IA-2A positive sera by IA-2 fusion protein affinity purification plate method.

4.5. Discussion

The pathophysiological lineage of the B cells giving rise to the autoantibodies in autoimmune diseases have remained relatively obscure until recently. In an attempt to address this question, groups such as Alkindi et al. 2015, have attempted to look at the clonality of autoantibodies in systemic autoimmune diseases using a proteomic approach.

In this study, Alkindi and colleagues showed that anti-SmD autoantibodies in unrelated patients with SLE are mainly kappa restricted IgG1 (Alkindi et al. 2015). Further proteomic analysis of the antibody population in this study revealed that the variable regions of the immunoglobulin are encoded by only two heavy chains, IGHV3-7, IGHV1-69 and two light chains, IGKV3-20, IGKV2-28 (Alkindi et al. 2015). This common usage of heavy and light chains implies that an identical molecular pathway is present in the humoral response in unrelated patients with SLE. This restriction in B cell usage has subsequently been confirmed in other diseases such as diphtheria and EBV and appears to be associated with antigenic selection (Smith et al. 2016). Understanding the variable region gene usage and therefore the pathophysiological mechanisms that drives self-directed humoral responses in these autoimmune diseases could lead to the development of new immunotherapies.

As previously stated, the aim of this project is to determine whether T1D, an organ confined autoimmune disease, has similar restricted immunoglobulin variable region gene usage, driving antibody production as described in systemic autoimmune diseases.

In the current study, the successful establishment of an ELISA for anti-IA-2 antibodies (Chapter 3.2.1), allowed further testing of the hypothesis that restricted clonality in B cells gives rise to anti-IA-2 antibodies. As described in the prologue, these antibodies show skewing in kappa expression which suggests clonality. Hence, this chapter describes efforts to affinity purify anti-IA-2 antibodies in preparation for proteomic analysis.

Given the efficacy of using the multiple plate purification method described previously (Al Kindi et al. 2015), this relatively simple method was used as the first approach to affinity purify antibodies from selected patient sera. This involved four-affinity purification rounds per patient or control sera. A fraction of the antibody sample generated by the affinity purification process was first used for quantification by 1D gel electrophoresis densitometry. The first two rounds of affinity purification were done to confirm that this process could generate specific and enriched anti-IA-2 antibody samples. As shown in chapter 4.3.2, this was achieved for the two positive patients (T1D019, T1D069), where the specificity ELISAs demonstrated an enrichment had occurred over the starting serum. The last two rounds were carried out to generate antibody samples for mass spectrometry analysis.

Estimates of the IgG yields from the affinity purification rounds were calculated using western blot densitometry. Interestingly, this process showed that the yields are between 1-3 ug of specific IA-2 antibodies per 1 mL of patient serum for the two positive patients assessed. Given the low yield, the entire antibody sample generated from one affinity purification round was required for the ELISA to confirm enrichment. Based on nephelometry estimates of total IgG per mL for the two positive patients, it appeared that the anti-IA-2 antibody population makes up between 0.009 and 1.6% of the total IgG population in T1D019 and T1D069 patient sera, respectively. However, this may not represent the entirety of the anti-IA-2 antibodies present in the T1D patients, as the IA-2 fusion protein ELISA may be presenting a restricted set of epitopes and is not 100% efficient.

While the Ig yields were relatively low, the reactivity ELISAs carried out using the affinity purified antibody samples showed outstanding enrichment. When comparing the OD values of affinity purified antibody sample to adjusted serum on IA-2 fusion protein, it showed that the affinity purified antibody sample of T1D019 was enriched by approximately 20-fold while the antibody sample of T1D069 was enriched by approximately 15-fold.

Furthermore, the second patient (T1D069), who was positive for both anti-IA-2 and anti-ZnT8R antibodies, generated affinity purified antibody samples that showed

reactivity specifically to the IA-2 fusion protein. This lack of reactivity of T1D069 antibody sample to the ZnT8R fusion protein and raised binding OD values of affinity purified antibody samples of both T1D019 and T1D069 to IA-2 fusion protein confirmed that the ELISA plate method was able to generate specific and enriched anti-IA-2 antibody samples.

This study has developed a novel method that is able to generate purified, specific, and enriched anti-IA-2 antibody samples from IA-2A positive T1D patient sera. To date this is the first attempt that has successfully isolated humoral autoreactive anti-IA-2 autoantibodies. A previous study describing attempts to isolate IA-2 antibodies by B cell isolation from T1D sera, using EBV transformation of isolated B cells to produce anti-IA-2 antibodies, is the closest other groups appear to have come to the current study (Kolm-Litty et al. 2000). This, however, does not ensure that the autoreactive autoantibodies identified are derived from the autoantibody secreting plasma cells contributing to the pathogenic humoral autoantibodies.

Therefore, the bottom end approach described in this study of isolating humoral autoreactive antibodies that target IA-2 antigen is potentially a superior method to purify anti-IA-2 antibodies to study the pathophysiological relevance of the autoantibodies in T1D immune response.

Chapter 5. Proteomic analysis of clonally restricted IA-2 autoantibody response in T1D

5.1 introduction

As described in chapter 4, to our knowledge, the establishment of the novel IA-2 fusion protein affinity purification technique facilitates the isolation of true autoreactive humoral antibodies from T1D patient sera for the first time. The availability of affinity purified autoreactive humoral anti-IA-2 antibodies from T1D sera, allows further investigation of the pathophysiological origin of the antibody in the disease process, by understanding the clonality and variable region gene usage of anti-IA-2 antibodies. Proteomic analysis of the purified anti-IA-2 antibodies allows the investigation of variable gene usage and clonality of this autoantibody producing B cells.

To date, the proteomic analysis of autoantibody and B cell repertoires in systemic autoimmune diseases have revealed two public clonotypes encoded by H chains IGH3-7 and IGHV1-69 and light chains IGKV3-20 and IGKV2-28, which represents the antibody response against clinically relevant Sm autoantigen in patients with SLE (Al Kindi et al. 2015). A similar study looking at the clonality of anti-Ro60peg (aa 193-236) in patients with Sjogren's syndrome responses indicates that one single clonal family of antibodies encoded by V_H 3-23 paired with V_K3-20 represents the entire anti-Ro60peg antibody response (Lindop et al. 2011). In addition, it has also been revealed that two autoantibody clonotypes encoded by IGHV3-7.JH6/IGKV3-20.JK2 and IGHV1-3.JH4/IGKV1-39.JK4 dominates the humoral response against Ribosomal P antigen in SLE (Al kindi et al. 2016). These findings have led to speculations on the origins of the B cells giving rise to the autoantibodies in systemic autoimmunity. For instance, Harley et al in his editorial commenting on the findings on anti-Ro60peg antibody response, proposed that the presence of antibodies of the same clonal family with the same heavy and light chain variable regions in several unrelated patients suggests that the pathophysiological pathway from the stimulus to autoantibody production must be identical in all patients (Harley et al. 2013). Therefore, investigating

the clonality of the autoantibodies and B cells may provide insights into the role they play in the pathophysiological mechanisms that drives the disease process which can lead to new therapeutic interventions.

In this study we focused on investigating the clonality and variable region gene usage of B cells giving rise to anti-IA-2 antibodies. As mentioned previously, anti-IA-2 antibodies are highly specific to T1D and are one of the major biomarkers used in clinical settings. Therefore, understanding the origin and proteome of anti-IA-2 antibodies may help us understand their relevance in the T1D humoral response. In order to achieve this, we characterized the clonality and variable region gene usage of affinity purified anti-IA-2 antibodies by mass spectrometry analysis.

5.2. Methods

5.2.1. Patients and samples

As described in chapter 4.2.1, the patient pool of two anti-IA-2 antibody positives (T1D019, T1D069), two anti-IA-2 antibody negatives (T1D001, T1D014) and two healthy controls (CTR062, CTR063) were advanced into the proteomics analysis. See table 3.1 for patient demographics and serological findings.

5.2.2. Samples analysed

As described in chapter 4.3.1, the purified antibody samples from the affinity purifications 3 and 4 were used for mass spectrometry analysis.

5.2.3. Sample preparation

As described previously, SDS-PAGE 1D gel electrophoresis was carried out with the antibody samples in order to isolate heavy and light chains (Chapter 2.4.2). The in-gel digests were subjected to Quadrupole-time of flight (QTOF) 5600+ mass spectrophotometer for sequencing to further investigate clonality and variable region subfamily gene usage (Chapter 2.4.4).

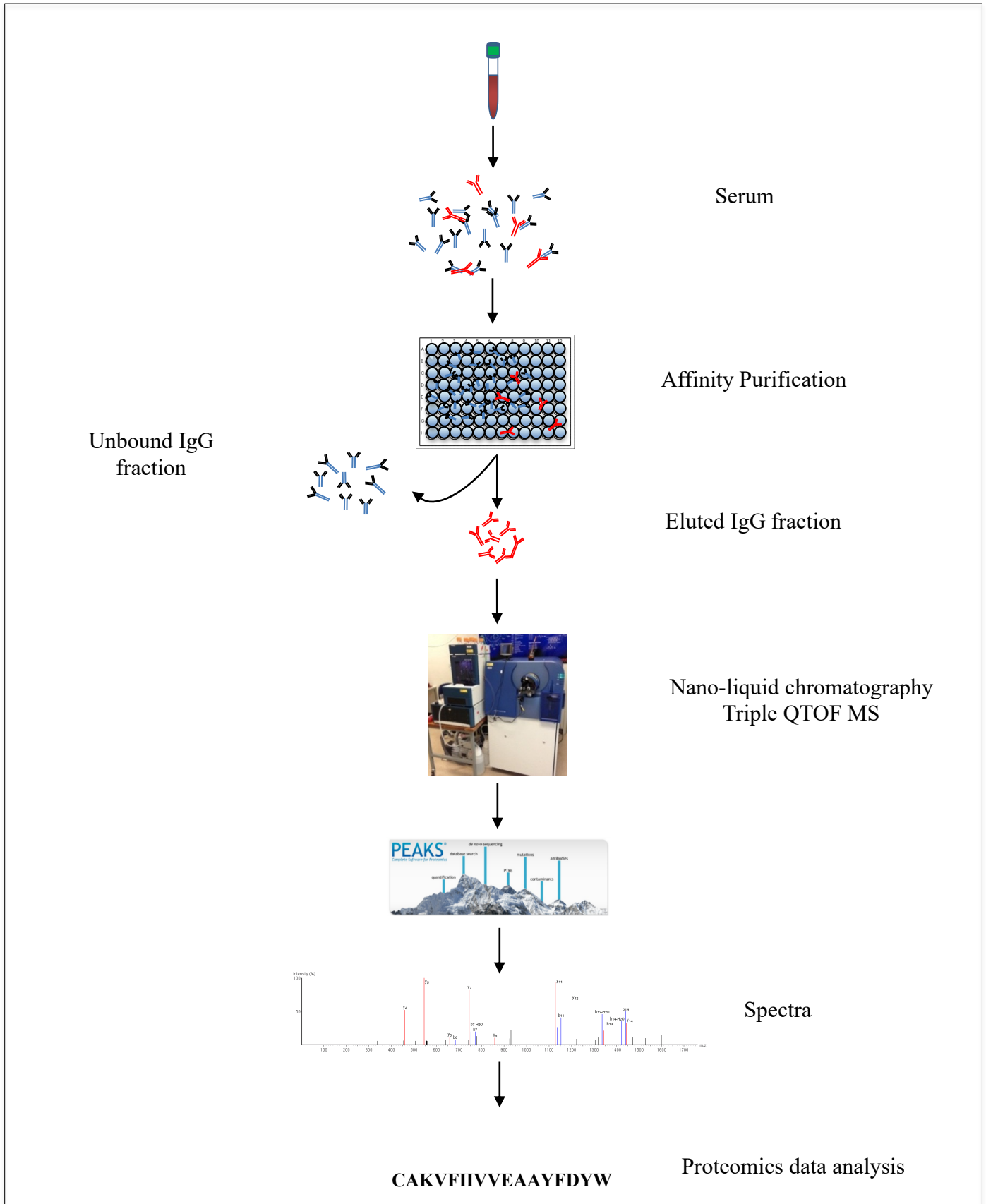


Figure 5.1. Proteomics workflow for the investigation of clonality of secreted anti-IA-2 antibodies affinity purified from T1D sera.

5.2.4. Proteomic analysis

Mass spectrometry data were then matched to the selected databases to derive the peptides present within the antibody samples (Chapter 2.4.4).

5.3. Results

5.3.1. Quantification of affinity purified antibody

This study attempted to characterize the clonotypes of the secreted self-reactive anti-IA-2 antibodies present in T1D sera. Anti-IA-2 antibodies were affinity purified using IA-2 fusion protein ELISA plate affinity purification method from the selected two IA-2A positive T1D patients, two negatives and healthy controls (Chapter 4.3.1).

1D gel electrophoresis of affinity purified antibody samples was carried out to confirm the purity of the antibody sample as well as to separate and isolate the heavy and light chains of the affinity purified antibody. The relative antibody yield for each sample was calculated by densitometry analysis of the gel bands and comparison with control caprylic IgG samples of known concentration run alongside of the affinity purified antibody. The relative loading concentrations which ranged from 0.95-39 ug is shown below in table 5.1.

Table 5.1. Relative quantities of the affinity purified antibodies run on 1D gel prior to introduction to the mass spectrometer.

	Sample	Quantity of Affinity purified antibody (μg)
1.	T1D069 sample 1	3.00
2.	T1D069 sample 2	2.28
3.	T1D019 sample 1	2.89
4.	T1D019 sample 2	7.00
5.	T1D014	2.00
6.	T1D001	39.0
7.	CTR063	4.00
8.	CTR062	0.95

5.3.2. Confirmation of peptide digestion and sample integrity

Following 1D electrophoresis, the heavy and the light chain bands of the affinity purified antibody samples were then cut out, processed, and analysed by the mass spectrometer (Chapter 2.4.2).

The instrument was operated at the selected optimal standards described in chapter 2.4.3. The successful generation of spectra relied on adequate digestion. To assess sufficient digestion, the spectra obtained from the runs were briefly analysed to ensure high volume of digested peptides were present.

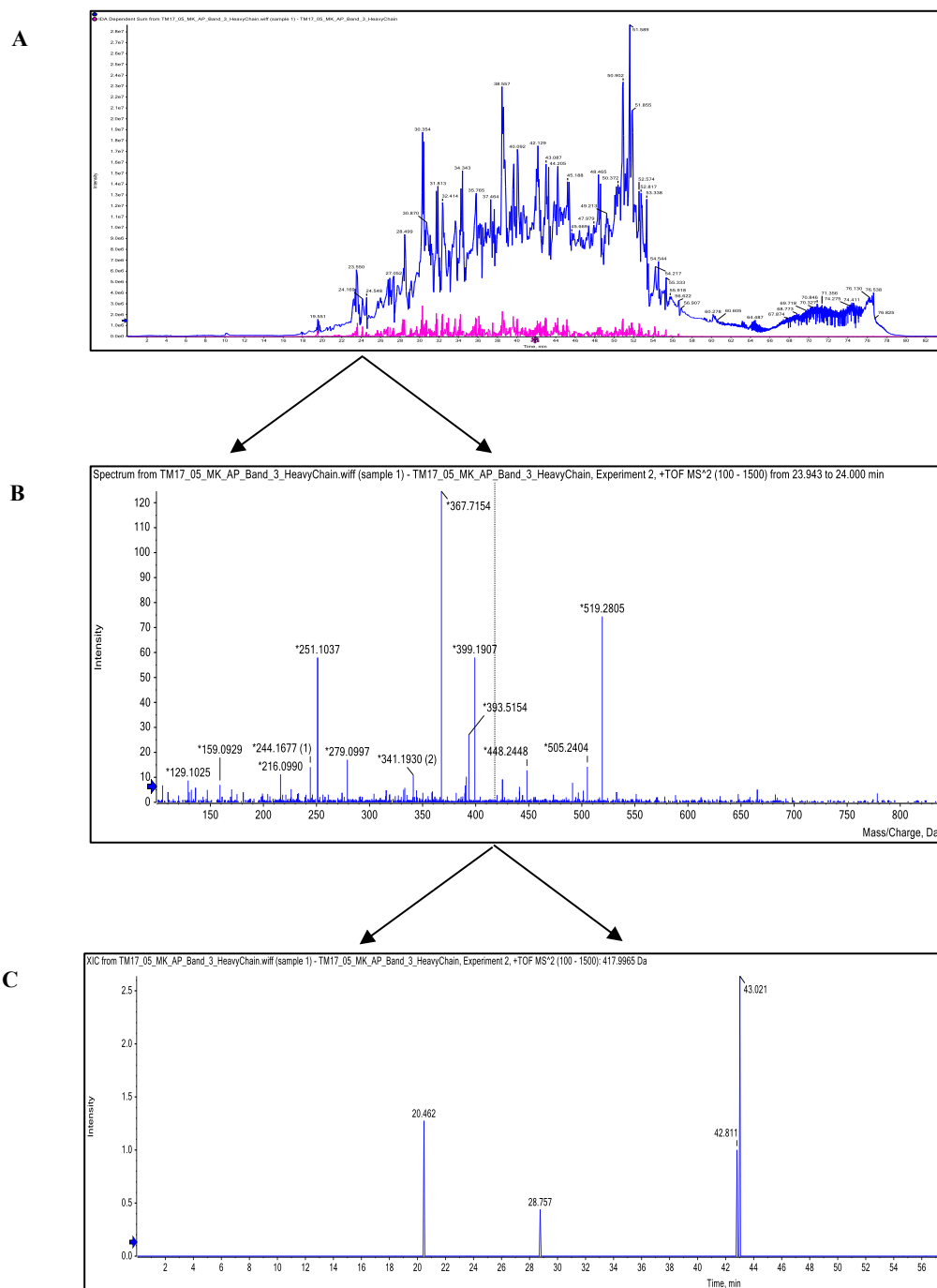


Figure 5.2. Representative figure of total iron current spectra obtained from the mass spectrometer for each heavy and light chain sample. **A.** Total iron current spectra obtained from the mass spectrometer for the heavy chain of the third T1D019 affinity purified antibody sample. This represents the volume of digested peptides eluting off

the column over a period of 80 minutes. **B.** MS spectra obtained for the heavy chain of the third T1D019 affinity purified antibody sample showing the peptides eluted off at 24 minutes. **C.** MS/MS spectra obtained for the heavy chain of the third T1D019 affinity purified antibody sample showing the precursor ions detected for the peptides of ~417 Da.

5.3.3. Protein sequence data analysis

Following confirmation of sample integrity, the peptides were analysed and assigned to gene families by a two-stage process. Firstly, the peptides were matched to the IMGT database by the peaks software. Secondly, the peptide matches were manually confirmed by looking at de-novo data for correct ion match, spectral counts, intensity, and manual search in the IMGT database to search whether peptides were unique or supporting peptides to a specific gene family.

5.3.4. Gene family assignment using proteomics analysis of variable region gene family usage in anti-IA-2 antibody repertoires

The proteomic analysis revealed the presence of multiple clonal repertoires with common expression of heavy and light chain gene families shared across the selected anti-IA-2 antibody samples from patients and controls (Table 5.3). As described in chapter 2.4.4., the selection criteria of inclusion for gene family assignment required the presence of one or more unique peptides as well as supporting peptides.

5.3.4.1. Light chain variable region gene family analysis

5.3.4.1.1. Identification of common light chain gene family IGKV 3-20 in patient and control samples

The analysis of gene family assignment identified IGKV 3-20 gene family in both replicates of positive, negative, and healthy control affinity purified antibody samples.

IGKV 3-20 gene family assignment in affinity purified antibody samples from anti-IA-2 positive patients

The anti-IA-2 antibody positive patient T1D019 sample 3 and 4 were analysed by Peaks software and manual confirmation. The presence of the IGKV 3-20 unique peptide “LLIYGASSR” and the presence of supporting peptides, “ATGIPDR, FSGSGSGTDFTLTISR, TLSLSPGER, LLIYGASR”, fulfilled the criteria for assignment of IGKV 3-20 gene family in the first affinity purified antibody sample run through the mass spectrometer. The analysis of the second affinity purified antibody sample run through the mass spectrometer for the same patient also indicated the presence of IGKV 3-20 gene family. The second sample confirmed the presence of IGKV 3-20 by the presence of unique peptides “LLIYGASSR” and “LLIYGASSRA” and supporting peptides, “ATGIPDR, FSGSGSGTDFTLTISR, TLSLSPGER, GSGTDFTLTISR”, fulfilling the criteria of inclusion.

Similarly, the analysis of the 1st sample of patient T1D069 also showed the presence of IGKV 3-20 by the presence of unique peptide “LLIYGASR” and supporting peptides, “ATGIPDR, ASQSVSSSYLAWYQQKPGQAPR, GSGSGTDFTLTISR”. The 2nd affinity purified antibody sample of T1D069, also showed the presence of IGKV 3-20 by complying to the inclusion criteria.

The presence of IGKV 3-20 in anti-IA-2 negative patient and control antibody samples

After confirming the presence of IGKV 3-20 in the anti-IA-2 antibody positive patient samples, the negative and healthy control antibody samples were analysed. The analysis of the T1D001 affinity purified antibody sample showed the presence of IGKV 3-20 by the presence of unique peptide, “LLIYGASSR” and the presence of supporting peptides, “TSLSPGER, FSGSGSGTDFTLTISR, ATGIPDR, FSGSGSGTDFTLTISR”. The analysis of affinity purified antibody samples from T1D014, CTR062 and CTR063 also identified the presence of IGKV 3-20 by the inclusion criteria while presenting some differences in the peptides present.

Table 5.2. Representative table of peptide comparison across the antibody samples for high quality. Quality of the IGKV 3-20 unique peptide present in the affinity purified antibody samples from the anti-IA-2 antibody positive patients, negative patients, and healthy controls.

	Sample	3-20 Coverage (%)	3-20 Unique peptide	Details
1	T1D019 Sample 2	52	LLIYGASSR	All but 1 ion matched. Intensity 6E2. Two spectrums.
			LLIYGASSRA	Only 6 ions matched. Intensity 2E3. Two spectrums.
2	T1D019 Sample 1	77	LLIYGASSR	All but 2 ions matched. Intensity 3E2. Two spectrums. 8 more peps.
3	T1D069 Sample 2	35	LLIYGASSR	All ions matched. Intensity 1.4E3. Five spectra.
4	T1D069 Sample 1	75	LLIYGASSR	All ions matched. Intensity 8E3 spectra. Five more peps.
5	T1D001	52	LLIYGASSR	All ions matched. Intensity 7E3. Eight spectrums.
6	T1D014	26	LLIYGASSR	All ions matched. Intensity 5E2. Two spectrums.
7	CTR063	52	LLIYGASSR	All ions matched. Intensity 8.2E3. Nine spectrums. Seven more peptides.
			LLIYGASSRATGIPDR	Ten ions matched. Intensity 9.6E1.
			LLIYGASSRA	Seven ions matched. Intensity 1.5E2. One spectrum.
8	CTR062	49	QAPRLLIYGASSR	Ten ions matched. Intensity 1.3E3. One spectrum.
			LLIYGASSR	All ions matched. Intensity 1E3. Two spectrums.

5.3.4.1.2. Expression of the unique light chain gene family IGKV 1-9 in the anti-IA-2 positive affinity purified antibody samples

Following the assignment of IGKV 3-20 to all samples regardless of anti-IA-2 positivity, further analysis of light chain gene family sequences confirmed the presence of IGKV 1-9 family in anti-IA-2 antibody positive samples only.

Analysis of light chain gene family assignment of T1D019

The proteomic analysis revealed a difference in expression of the IGKV 1-9 light chain. The first affinity purified antibody sample of T1D019 showed the presence of the IGKV 1-9 by the presence of unique peptides, DIQLTQSPSFLSASVGDR and LTQSPSFLSASVGDR as well as the presence of supporting peptides, VTITCR, AASTLQSGVPSR, STLQSGVPSR, LQSGVPSR fulfilling the criteria of inclusion for

IGKV 1-9 gene family assignment. Similarly, the 2nd affinity purified antibody sample from the same patient also revealed the presence of IGKV 1-9 by the presence of unique peptides, DIQLTQSPSFLSASVGDR and LTQSPSFLSASVGDR and presence of supporting peptides, VTITCR, LIYAASTLQSGVPSR, AASTLQSGVPSR, STLQSGVPSR, LQSGVPSR.

Analysis of light chain gene family assignment of T1D069

Similar to patient T1D019, both affinity purified antibody samples of T1D069 contained both unique and supporting peptides, for example, the 1st antibody sample of T1D069 indicated the presence of IGKV 1-9 by the presence of unique peptide “DIQLTQSPSFLSASVGDR” and supporting peptides, “ASQGISSYLAWYQQKPGK and SYLAWYQQKPGK. While the supporting peptides were different, the 2nd affinity purified antibody sample of T1D069 also fulfilled the criteria of IGKV 1-9 gene family assignment by the presence of unique peptide, “DIQLTQSPSFLSASVGDR” and supporting peptides, “AASTLQSGVPSR, STLQSGVPSR, LSASVGDR, VTITCR, LESGVPSR”.

Analysis of light chain gene family assignment of controls

After confirmation of the IGKV 1-9 gene family assignment in the anti-IA-2 antibody positive samples, the negative samples and healthy control samples were also analysed which revealed that IGKV 1-9 gene family was absent in all negative controls and healthy controls. This suggested that IGKV 1-9 is unique to the anti-IA-2 antibody response in T1D patients.

5.3.4.1.3. Detection of other common light chain gene family members in the patient and control antibody samples

The common expression of light chain IGKV 1-12, 1-33, 4-1, 2-24, IGLV 1-47 and IGLV 3-19 was observed in all four anti-IA-2 antibody positive samples. IGKV 1-12, 1-33, 4-1, IGLV 1-47 and IGLV 3-19 was present in one negative control (T1D001)

and one healthy control (CTR063). While IGKV 2-24 was present in one negative control sample (T1D001).

5.3.4.2. Heavy chain variable region gene family analysis

5.3.4.2.1. Identification of IGHV 3-23 heavy chain gene family in patient and control antibody samples

Gene family analysis revealed the presence of IGHV 3-23 in all positive, negative, and healthy control affinity purified antibody samples.

Analysis of the heavy chain gene family assignment of anti-IA-2 positive antibody samples

The heavy chain gene family analysis of the 1st affinity purified antibody sample from T1D019 revealed the presence of IGHV 3-23 unique peptides, “YYGDSVK and EVQLES GGGLVQP GGSLR” and the presence of supporting peptides, “LLES GGGLVQP GGSLR, LVQP GGSLR, NSKNTLYLQMNSLR, NTLYLQMN, AEDTAVYYCAK” fulfilled the criteria for IGHV 3-23 gene family assignment. The 2nd affinity purified antibody sample also showed the presence of the IGHV 3-23 by the presence of unique peptide, “EVQLES GGGLVQP GGSLR” and supporting peptides, “LVQP GGSLR, NTLYLQMN, AEDTAVYYCAK”.

Similarly, 1st antibody sample of T1D069 indicated the presence of IGHV 3-23 by the presence of unique peptide, EVQLES GGGLVQP GGSLR and supporting peptides, LLES GGGLVQP GGSLR, NTLYLQMN, YYADSVK and AEDTAVYYCAK. The 2nd affinity purified antibody sample of T1D069 also showed the presence of IGHV 3-23 by the presence of unique peptides, “YYGDSVK and EVQLES GGGLVQP GGSLR” and the presence of supporting peptides, “TYADSVK, AEDTAVYYCAK, NTLYLQMN, LVQP GGSLR”.

Analysis of the heavy chain variable region gene family assignment of controls

Following confirmation of the presence of IGHV 3-23 in the anti-IA-2 antibody positive samples, the negative and the healthy control samples were analysed for the presence of IGHV 3-23 heavy chain gene family. This analysis of negative antibody sample from T1D001 identified the presence of IGHV 3-23 heavy chain gene family by the presence of “YYGDSVK and EVQLLESGGGLVQPGGSLR” and supporting peptide, “NTLYLQMNSLR”. Similarly, while there were some differences in the peptides the IGHV 3-23 heavy chain gene family was found in the antibody samples from T1D014 and CTR063.

5.3.4.2.2. Detection of other heavy chain variable region gene families in the patient and control antibody samples

While IGHV 3-23 was the only gene family present in all positive patient samples, IGHV 3-7 was found in one of the replicates of both T1D019 and T1D069 anti-IA-2 antibody sample, one anti-IA-2 negative sample (T1D001) and one healthy control sample (CTR063).

5.3.4.3. Light chain joining region gene family analysis

5.3.4.3.1. Identification of IGKJ2 joining region light chain gene family in patient and control samples

The analysis of the joining region gene family assignment identified IGKJ2 joining region gene family in patient and control antibody samples.

Analysis of the IGKJ2 light chain joining region gene family assignment of anti-IA-2 positive samples

The analysis of the 1st affinity purified antibody sample of T1D019 showed the presence of IGKJ2 by the presence of unique region, “YTFGQGTK”. The 2nd antibody sample of T1D019 also indicated the presence of IGKJ2 by the presence of the unique peptide, “YTFGQGTK”.

The analysis the 1st affinity purified antibody sample of T1D069 also showed the presence of IGKJ2 by the presence of unique peptide, “YTFGQGTK”. The 2nd antibody sample also indicated the presence of IGKJ2 by the presence of the same unique peptide.

Analysis of the IGKJ2 light chain joining region gene family assignment of controls

The joining region gene family assignment revealed that IGKJ2 joining region is present in one negative control (T1D001) and both healthy controls (CTR062, CTR063) by the presence of the unique peptide, “YTFGQGTK”.

5.3.4.3.2. Identification of IGKJ4 joining region gene family in patient and control antibody samples

The joining region gene family assignment identified IGKJ4 joining region gene family in the patient antibody samples and one healthy control sample.

Analysis of the IGKJ4 joining region gene family assignment of ant-IA-2 positive patient samples

The gene family assignment of the 1st affinity purified antibody sample of T1D019 showed the presence of IGKJ4 by the presence of unique peptide, “LTFGGGK”. The same unique confirmed the presence of IGKJ4 gene family in the 2nd antibody sample.

Joining region gene family analysis of the 1st affinity purified antibody sample indicated the presence of IGKJ4 by the presence of unique peptide, “LTFGGGK”. The same peptide of IGKJ4 joining region family was also present in the 2nd antibody sample.

Analysis of the IGKJ4 joining region gene family assignment of controls

Analysis of the joining region gene family assignment in the control samples indicated that IGKJ4 gene family is present in one healthy control (CTR063) by the presence of unique peptide, “LTFGGGT” while being absent in the other healthy control (CTR062) and both negative controls (T1D001, T1D014).

5.3.4.3.3. Detection of other light chain joining region gene families in the patient and control antibody samples

The analysis of gene family assignment also revealed the presence of other light chain joining region gene families. IGKJ3 joining region gene family was present in both antibody samples from T1D019 and one healthy control antibody sample (CTR063) indicated by the presence of the unique peptide, “FGPGK”. IGKJ5 joining region gene family unique peptide, “TFGQGTR” was present in both replicates of T1D019, one negative control (T1D001), and one healthy control antibody sample (CTR063).

5.3.4.4. Heavy chain joining region gene family analysis

5.3.4.4.1. Identification of IGHJ6 joining region gene family in the patient and control antibody samples

The analysis of joining region gene family assignment identified the presence of IGHJ6 gene family in patient and control antibody samples.

Analysis of the IGHJ6 heavy chain joining region gene family assignment of anti-IA-2 positive antibody samples

The gene family assignment of the 1st antibody sample of T1D019 indicated the presence of IGHJ6 by the presence of unique region, GTTVTVSS. The analysis of the 2nd antibody sample also showed the presence of IGHJ6 by the presence of unique peptide, “TTVTVSS”.

Similarly, the analysis of the 1st affinity purified antibody sample of T1D069 showed the presence of IGHJ6 by the presence of unique region, “TTVTVSS”. The 2nd affinity purified antibody sample of the same patient also showed the presence of IGHJ6 by the presence of “GTTTVTVSS”.

Analysis of the IGHJ6 heavy chain joining region gene family assignment of controls

The joining region gene family assignment of the negative and healthy controls also revealed the presence of IGHJ6 joining region in all the negative and healthy control samples by the presence of unique region “TTVTVSS”.

Table 5.3. Heavy chain variable region gene expression in the anti-IA-2 affinity purified antibody samples from T1D019 and T1D069 patient sera.

	Gene families	T1D019 2				T1D019 1				T1D069 2				T1D069 1			
		Coverage %	No. of Unique Peptides	No. of Supporting Peptides	Total No. of peptides	Coverage %	No. of Unique Peptides	No. of Supporting Peptides	Total No. of peptides	Coverage %	No. of Unique Peptides	No. of Supporting Peptides	Total No. of peptides	Coverage %	No. of Unique Peptides	No. of Supporting Peptides	Total No. of peptides
1.	H 3-23	42	1	6	6	55	1	16	17	61	1	6	7	49		7	7
2.	H 3-30						1	13	14	57		7	7	18		5	5
3.	H 3-64					35	1	10	11	46	1	6	7				
4.	H 3-7	38		5	5	58	1	6	7	69	1	3	4	58		1	1
5.	H 3-53	31		2	2	55		7	7	51		4	4				
6.	H 3-69	31		2	2			6	6	61		5	5				
7.	H 3-13							7	7	35	1	3	4	31		2	2
8.	H 3-15						4	5	9	46	1	2	3	9		1	1
9.	H 3-33						1	2	3	57		7	7	39	1	2	3
10.	H 4-4					37		6	6	54		5	5	37		2	2
11.	H 3/OR 16-10	31		4	4			4	4	39		4	4				
12.	H 3-43D							6	6	30		4	4	18		2	2
13.	H 4-61					60		4	4	43		5	5	38		3	3
14.	H 3-43	11		1	1		1	5	6	38		3	3	18		1	1
15.	H 3-9					45		8	8	38		3	3				
16.	H 3-48					53		5	5	60		4	4	49		1	1
17.	H 3-74					49		7	7	33		3	3				
18.	H 4-34					32	1	5	6	32	1	3	4				
19.	H 3-21							7	7					49		2	2
20.	H 3/OR 16-13							7	7					31		2	2
21.	H 4-39	14		1	1	53		3	3	51		5	5				
22.	H 4-39	14		1	1	53		3	3	51		5	5				
23.	H 3-72							5	5	56		2	2	30	1		1
24.	H 5-10			1	1	28		3	3	33		3	3				
25.	H 1-46									41		3	3	32	1	2	3
26.	H 4-30									35		5	5	6		1	1

Table 5.4. Heavy chain variable region gene family expression in the affinity purified antibody samples generated from negative control and healthy control serum samples.

	Gene families	Negative Controls								Healthy controls							
		T1D001				T1D014				CTR063				CTR062			
		Coverage %	No. of Unique Peptides	No. of Supporting Peptides	Total No. of peptides	Coverage %	No. of Unique Peptides	No. of Supporting Peptides	Total No. of peptides	Coverage %	No. of Unique Peptides	No. of Supporting Peptides	Total No. of peptides	Coverage %	No. of Unique Peptides	No. of Supporting Peptides	Total No. of peptides
1.	H 3-23	38	2	1	3	27	1	1	2	52	2	10	12	-	-	-	-
2.	H 3-7	47	1	4	5	27	-	2	2	58	1	6	7	38	-	3	3
3.	H 3/or 16-10													38		3	3
4.	H 5-10													12		1	1

Table 5.5. Light chain variable region gene family expression across the affinity purified anti-IA-2 antibody samples from T1D019 and T1D069 patient sera.

	Gene families	T1D019 2				T1D019 1				T1D069 2				T1D069 1			
		Coverage %	No. of Unique Peptides	No. of Supporting Peptides	Total No. of peptides	Coverage %	No. of Unique Peptides	No. of Supporting Peptides	Total No. of peptides	Coverage %	No. of Unique Peptides	No. of Supporting Peptides	Total No. of peptides	Coverage %	No. of Unique Peptides	No. of Supporting Peptides	Total No. of peptides
1.	K 1-39	58		11	11			9	9	37		6	6	55	+(1)	8	8
2.	K 1-6	71	+(1)	11	12			8	8	51	+(1)	4	5	42	+(1)	7	8
3.	K 3-20	52	+(2)	8	10	77	+(1)	7	10	35	+(1)	3	4	75	+(1)	7	8
4.	K 1-9	41	+(2)	7	9	38	+(2)	6	8	55	+(1)	7	8	61	+(1)	2	3
5.	K 1-12	58	+(1)	8	9	37	+(1)	5	6	51	+(1)	5	6	42	+(1)	6	7
6.	K 1-33	36	+(5)	3	8	36	+(4)	4	8	36	+(2)	5	7	36	+(2)	2	4
7.	K 1-17	54		10	10	75		10	10		-			44		5	5
8.	K 1-NL1		+(1)	5	6	61	+(1)	6	7	34		5	5	42	+(1)	3	4
9.	K 1-37	58	+(2)	3	5	51	+(1)	5	6	37		5	5	42	+(2)	3	5
10.	K 4-1	68	+(6)	2	8	53	+(3)	2	5	30	+(2)	-	2	53	+(4)	1	5
11.	K 1/OR 2-108	58		8	8	37		5	5		-	-	-	33		7	7
12.	L 1-47	57	+(2)	6	8	52	+(1)	5	6	42	+(1)	1	2	42	+(1)	2	3
13.	K 1-13	59	+(2)	5	7	75	+(1)	6	7	54		5	5		-	-	-
14.	K 3-7	59	+(1)	6	7	45	+(1)	3	4	23		2	2	35	+(1)	3	4
15.	L 3-19	69	+(5)	1	6	20	+(2)	2	4	18	+(1)	2	3	10	+(1)	1	2
16.	K 2-24	29	+(2)	2	4	20	+(1)	1	2	44	+(2)	4	6	20	+(1)	2	3
17.	L 1-51	44	+(2)	3	5	44	+(1)	5	6		-	-	-	34	+(1)	2	3
18.	L 3-21	40	+(1)	4	5	41	+(1)	3	4	36		1	2	44	+(1)	1	2
19.	K 1D-43		-	-	-	31		4	4	25		4	4	29		4	4
20.	K 1-16	58	+(1)	3	4		-	-	-		-	-	-	63	-	7	7
21.	L 2-11	40	+(2)	2	4	16	+(1)	-	1	16	+(2)	1	3	16	+(2)	-	2
22.	K 2-28	56	+(2)	1	3	43		5	5		-	-	-	13		1	1
23.	K 2D-29		-	-	-			6	6	29		3	3		-	-	-
24.	L 1-40	43	+(1)	3	4	38	+(1)	3	4		-	-	-		-	-	-
25.	L 3-13			2	2	41	+(1)	4	5	12		1	1		-	-	-
26.	L 3-10	43	+(1)	4	5		-	-	-	19		2	2		-	-	-
27.	L 3-1	33	+(1)	3	4	8	+(1)	2	3		-	-	-		-	-	-
28.	K 2-18	20	+(2)	-	2	7	+(1)	-	1	7	+(1)	1	2	7	+(1)	-	1
29.	L 7-46	18	+(1)	1	2	26	+(1)	2	3		-	-	-		-	-	-
30.	L 2-14	24	+(1)	3	4	8		1	1		-	-	-		-	-	-
31.	K 7-3	27	+(2)	-	2	9	+(1)	-	1		-	-	-	9	+(1)	-	1
32.	K 2-30		-	-	-	49	+(1)	3	4		-	-	-		-	-	-
33.	L 8-61	22	+(1)	1	2		-	-	-		-	-	-	22	+(1)	1	2
34.	L 6-57	39	+(1)	1			-	-	-	8	+(1)	-	-		-	-	-
35.	L 5-45	18	+(1)	-	1	10	+(1)	-	1	6		-	-		-	-	-

Table 5.6. Light chain variable region gene family expression across the affinity purified antibody samples generated from negative control and healthy control serum samples.

	Gene families	Negative Controls								Healthy controls							
		T1D001				T1D014				CTR063				CTR062			
		Coverage %	No. of Unique Peptides	No. of Supporting Peptides	Total number of peps	Coverage %	No. of Unique Peptides	No. of Supporting Peptides	Total number of peps	Coverage %	No. of Unique Peptides	No. of Supporting Peptides	Total number of peps	Coverage %	No. of Unique Peptides	No. of Supporting Peptides	Total number of peps
1.	K 3-20	28	1	6	7	26	1	1	2	52	3	8	11	49	2	3	5
2.	K 1-9	-	-	-	-	-	-	-	-	-	-	-	-	-	-	-	-
3.	K 1-12	37	1	3	4	-	-	-	-	45	1	5	6	-	-	-	-
4.	K 1-33	36	2	2	4	-	-	-	-	36	4	5	9	12	1	1	2
5.	K 1-17	40	-	6	6					40	2	4	6				
6.	K 1-NL1	34	-	4	4	-	-	-	-	45	3	7	10	-	-	-	-
7.	K 1-37	37	1	4	5	-	-	-	-	37	1	5	6	-	-	-	-
8.	K 4-1	53	5	-	5	-	-	-	-	60	6	1	7	-	-	-	-
9.	K 1/OR 2-108	-	-	-	-	-	-	-	-	40	1	6	7	-	-	-	-
10.	L 1-47	47	1	3	4	-	-	-	-	47	1	2	3	-	-	-	-
11.	K 1-13	27	-	4	4	-	-	-	-	45	1	7	8	-	-	-	-
12.	K 3-7	47	1	4	5	9		1	1	58	1	6	7	-	-	-	-
13.	L 3-19	10		3	3	-	-	-	-	9	1	-	1	-	-	-	-
14.	K 2-24	20	1	1	2	-	-	-	-	-	-	-	-	-	-	-	-

Table 5.7. Assignable heavy chain gene family shared across the affinity purified anti-IA-2 antibody samples generated from anti-IA-2 antibody positive sera.

	Gene families	T1D019 2				T1D019 1				T1D069 2				T1D069 1			
		7 ug of AP AB				2.89 ug of AP AB				2.28 ug of AP AB				3 ug of AP AB			
		Coverage %	No. of Unique Peptides	No. of Supporting Peptides	Total No. of peptides	Coverage %	No. of Unique Peptides	No. of Supporting Peptides	Total No. of peptides	Coverage %	No. of Unique Peptides	No. of Supporting Peptides	Total No. of peptides	Coverage %	No. of Unique Peptides	No. of Supporting Peptides	Total No. of peptides
1	H 3-23	42	1	6	6	55	1	16	17	61	1	6	7	49		7	7

Table 5.8. Assignable light chain gene families shared across the affinity purified anti-IA-2 antibody samples generated from anti-IA-2 antibody positive sera.

	Gene families	T1D019 2				T1D019 1				T1D069 2				T1D069 1			
		7 ug of AP AB				2.89 ug of AP AB				2.28 ug of AP AB				3 ug of AP AB			
		Coverage %	No. of Unique Peptides	No. of Supporting Peptides	Total No. of peptides	Coverage %	No. of Unique Peptides	No. of Supporting Peptides	Total No. of peptides	Coverage %	No. of Unique Peptides	No. of Supporting Peptides	Total No. of peptides	Coverage %	No. of Unique Peptides	No. of Supporting Peptides	Total No. of peptides
1.	K 1-9	41	+ (2)	7	9	38	+ (2)	6	8	55	+ (1)	7	8	61	+ (1)	2	3

5.3.5. Analysis of peptide maps derived from IA-2 specific V regions reveals idiotypic and shared amino acid (aa) substitutions

Following gene family assignment, the V region peptides of both heavy and light chains were interrogated for the presence of idiotypic or shared amino acid replacements.

5.3.5.1. Peptide pool comparison between patients and control antibody samples

Previous studies have identified public and shared mutations in affinity purified antibodies against other self-antigens, for instance, shared mutational signatures were found in the dominant IGKV 3-20 that encoded for the L-chain of the anti-Ro and La responses derived from patients with Sjogren's syndrome (Wang et al., 2016). In order to analyse whether the peptide pool derived from the affinity purified anti-IA-2 antibodies from T1D patients and controls also have mutations, the peptides that were matched to the major heavy (IGHV 3-23) and light chains (IGKV 3-20, IGKV 1-9) were then compared to the germline sequence for the appearance of mutations. This revealed that peptide set for each V region gene family was more extensive in the patient antibody samples than the peptide set in the control samples. Similarly, the aa replacement analysis showed that more aa mutations were present in the peptides in the patient samples compared to controls, details of which is presented below.

Analysis of peptide sets that matched to IGHV 3-23 in the patient and control samples

Positive patients

For IGHV 3-23, 18 peptides were present in the 1st affinity purified antibody sample. Of the 18 peptides in the 1st antibody sample of T1D019, 10 had amino acid mutation replacements, while eight matched the germline sequence. Six peptides were present in the 2nd affinity purified antibody sample of T1D019. Of the six peptides in the 2nd antibody sample, 3 had mutation replacements and 3 matched the germline sequence.

Twelve peptides were matched to the IGHV 3-23 germline sequence in the 1st affinity purified antibody sample of T1D069, while 19 were matched in the 2nd affinity purified antibody sample. Of the 12 peptides that matched IGHV 3-23 in the 1st affinity purified antibody sample of T1D069, seven peptides had aa mutations, while 5 matched the germline sequence. In the 2nd antibody sample, out of the 19 peptides, 12 peptides had aa mutation replacements.

Negative patients and healthy controls

Seven peptides were found in the T1D001 sample. Out of the seven peptides, three had amino acid replacements, while the other 4 matched the germline. Three peptides were present in the T1D014 sample, and only one had an aa replacement. Eleven peptides were found in the CTR063 antibody sample, and three of the peptides had amino acid replacements while others matched the germline sequence.

Analysis of peptides that matched to IGKV 3-20 in the patient and control samples

Positive patients

For IGKV 3-20, fifty-one peptides were present in the 1st affinity purified antibody sample. Seventy-seven peptides were present in the 2nd antibody sample of T1D019. Out of the 51 peptides, 42 peptides had aa replacements, while 9 were germline. Of the 77 peptides in the 2nd antibody sample, 66 peptides had aa replacements, while 11 matched the germline sequence. Thirty peptides were found in the 1st antibody sample of T1D069. Out of the 30, 22 peptides had aa replacements and 8 matched the germline sequence. Ten peptides were found in the 2nd antibody sample of T1D069. Out of ten peptides, 7 had aa replacements, and 3 were germline sequences.

Negative patients and healthy controls

Eighteen peptides were present in T1D001. Out of the 18 peptides, 12 peptides had aa mutations. Four peptides were present in T1D014, and 2 of those had aa replacements. Forty-eight peptides were present in CTR063. Out of the 48 peptides, 38 peptides had

aa replacements, while 10 matched the germline. Four was present in CTR062, and of those, one had an aa replacement.

Analysis of peptide sets that matched to IGKV 1-9 in the patient and control samples

For IGKV 1-9, 36 peptides were present in the 1st antibody sample of T1D019. Twenty-seven of those have aa replacements, while eight matched to the germline sequence. Forty-six peptides were present in the 2nd antibody sample of T1D019. Of those, 36 peptides had aa replacements, while ten matched to the germline sequence. Forty-five peptides were present in the 1st antibody sample of T1D069. Thirty-eight of those peptides had aa replacements, while 7 matched to the germline sequence. Thirty-one peptides were present in the 2nd antibody sample of T1D069. Of the 31 peptides, 21 peptides had aa replacements and 10 peptides to the germline.

5.3.5.2. Common aa replacements are present in the IGHV3-23 V region peptides across the affinity purified anti-IA-2 antibody samples

Amino acid replacements found in all anti-IA-2A positive samples

In the IGHV 3-23 heavy chain, the most common aa substitution was Alanine (A) to threonine (T) at 97 position which was in all 4 anti-IA-2A positive antibody samples. This mutation was also present in one of the negative antibody samples (T1D001).

Amino acid replacements found in three anti-IA-2A samples

The next most common aa substitution was from Lysine (K) to Arginine (R) that was present at the 98 aa positions of IGHV 3-23 heavy chain and was found in one of the replicates of T1D019 and both replicates of T1D069. This aa replacement was also found in T1D001 antibody sample.

Amino acid replacements found in one replicate of each anti-IA-2A positive patient sample

The aa substitution of tyrosine (Y) to phenylalanine (F) at 58 position was found in 1st affinity purified antibody sample of T1D019 and 1st affinity purified antibody sample of T1D069. This aa substitution was also found in one negative control (T1D014). The aa substitution from Lysine (K) to Arginine (R) at aa position 64 was found in the 1st affinity purified antibody sample of T1D019 and 2nd affinity purified antibody sample of T1D069. This substitution was also found in one healthy control (CTR063).

5.3.5.3. The common amino acid replacements in IGKV 3-20 light chain peptide maps across patient and control samples

Amino acid replacements found in all anti-IA-2A positive samples

The analysis of the IGKV 3-20 light chain map revealed the common aa substitution replacements across samples. The most common aa replacement found was the substitution from Isoleucine (I) to Valine (V) at position 2, which was found in all anti-IA-2 positive antibody samples, one negative control sample (T1D001) and one healthy control sample (CTR063).

Amino acid replacements found three anti-IA-2A positive samples

The next most common aa replacements were Glutamic acid (E) to Aspartic acid (D) at position 1, which was found in both antibody samples of T1D019, and the 2nd affinity purified antibody sample of T1D069. This aa replacement was not found in the control antibody samples. The aa replacement from Y to F was found in both T1D019 antibody samples, 1st affinity purified antibody sample of T1D069 and one healthy control (CTR063) at position 50. At position 57 of IGKV 3-20 light chain peptide map, the amino acid replacement from T to Proline (P) was found and it appeared in the 2nd affinity purified antibody sample of T1D019, both antibody samples of T1D069, one negative control (T1D001) and one healthy control (CTR063).

Amino acid replacement from Serine (S) to Glycine (G) at position 66, was found in both antibody samples of T1D019, the 1st affinity purified antibody sample of T1D069 and one healthy control (CTR063). Substitution from T to Leucine (L) at position 73 was found in both antibody samples of T1D019, the 1st antibody sample of T1D069 and one negative control (T1D014). Amino acid replacement from T to K at position 75 was found in both antibody samples of T1D019, 1st affinity purified antibody sample of T1D069 and one negative control (T1D001).

Amino acid replacements found in one antibody sample from each anti-IA-2A positive patient

The amino acid replacement from I to T at position 2 was found in the 2nd affinity purified antibody sample of T1D019, the 1st antibody sample of T1D069, one negative control (T1D001) and one healthy control (CTR063). Substitution from aa Glutamine (Q) to K at position 6 was found in the 1st affinity purified antibody sample of T1D019 and T1D069. However, the mass of aa Q is 146.15 and aa K is 146.19. Therefore, it is likely that this is a misassignment. The amino acid replacement from L to Valine (V) at position 11 was found in the 2nd affinity purified antibody sample of T1D019, 1st affinity purified antibody sample of T1D069 and one healthy control sample (CTR063). The aa replacement from G to Tryptophan (W) at position 16 and aa substitution from E to R at position 17 were found in the 2nd affinity purified antibody sample from T1D019 and T1D069. Both aa replacements were found in one negative control (T1D001). Amino acid substitution from Tyrosine (Y) to Leucine (L) at position 33 was found in the 2nd affinity purified antibody sample of T1D019 and 1st antibody sample of T1D069. The aa replacement from Alanine (A) to Valine (V) at position 52 was found in the 2nd antibody sample of T1D019 and 1st antibody sample of T1D069. The aa substitution at position 54 from Serine (S) to Asparagine (N) was found in 1st antibody sample of T1D019 and T1D069. This aa replacement was found in one negative control (T1D001) and one healthy control (CTR063). The aa replacement from R to K at position 55 was found in the 1st antibody sample from T1D019 and T1D069. Amino acid substitution from (T) to (L) at position 57 was found in the 2nd affinity purified antibody sample of T1D019 and 1st antibody sample of T1D069 and one

healthy control (CTR063). The amino acid replacement from D to V at Position 61 was found in the 1st antibody sample of T1D019 and T1D069 as well as in one healthy control (CTR063). Amino acid substitution from G to A at aa 69 was found in the 2nd antibody sample of T1D019 and 1st antibody sample from T1D069.

5.3.5.4. Shared amino acid replacements in IGKV 1-9 light chain peptide map across patient samples

Amino acid replacements present in all four anti-IA-2A positive antibody samples

Heat map analysis of IGKV 1-9 variable region revealed the presence of 11 common aa replacements across all four anti-IA-2A positive antibody samples. The aa substitution from D to E was found at aa position 1. Amino acid substitution from L to M was present at aa position 4. Aa substitution from S to R was found at aa position 7. Aa replacement from F to S was present at aa position 10. Aa substitution from V to L was found at aa position 19. Aa replacement from L to R was found at aa position 54. Aa replacement from R to K was found at aa position 61. At aa position 70 aa substitution from E to D was present in all 4 antibody samples. Aa replacement from T to K was present at aa position 74. Aa substitution from S to R was present at aa position 76.

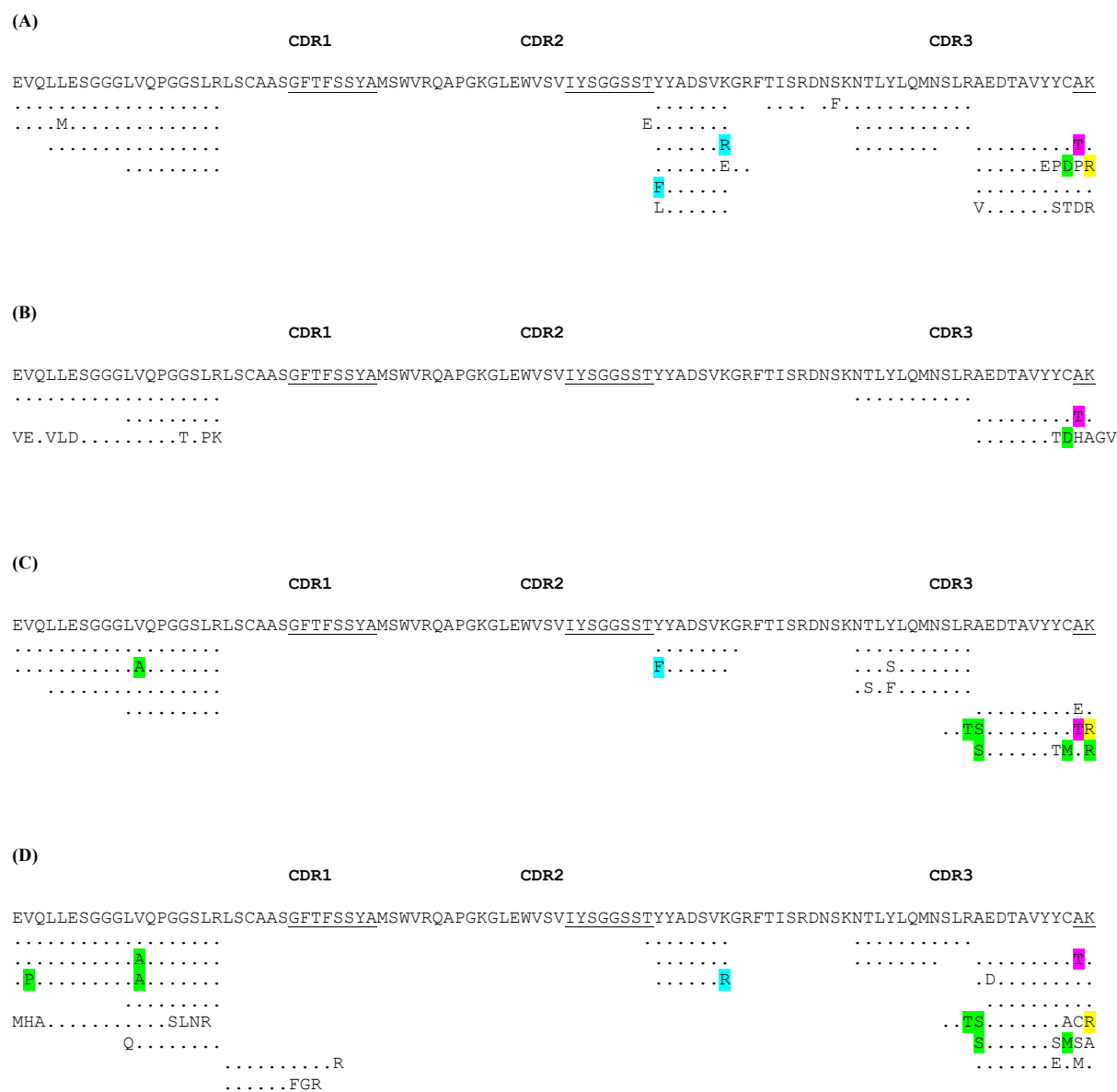
Amino acid replacements found in three anti-IA-2A positive samples

The analysis of the unique IGKV 1-9 light chain peptide maps revealed the presence of aa replacements that are present in one affinity purified antibody sample of IA-2A positive patient and in two affinity purified antibody samples of the other IA-2A positive patient. Amino acid substitution from Leucine (L) to Valine (V) at position 11 which was found in the 2nd affinity purified antibody sample of T1D019 and both antibody samples of T1D069. Aa replacement from Q to E was found in aa position 55 in both antibody samples of T1D019 and the 1st antibody sample of T1D069. At aa position 56, aa substitution from S to T was present in both antibody samples of T1D019 and the 1st antibody sample of T1D069. Aa replacement from S to D at aa position 60 was found in both antibody samples of T1D019 and the 1st antibody sample

of T1D069. At amino acid position 63, aa replacement from S to E was found in both antibody samples of T1D019 and the 1st antibody sample of T1D069. At amino acid position 67, aa replacement from S to A was found in both antibody samples from T1D019 and 2nd antibody sample of T1D069. Amino acid substitution from T to L was found at aa position 72 in the 2nd affinity purified antibody sample of T1D019 and both antibody samples of T1D069. At aa position 74, aa replacement from T to R was present in both antibody samples of T1D019 and 2nd antibody sample of T1D069. Amino acid replacement from S to K was found in aa position 77 in both antibody samples of T1D019 and 1st antibody sample of T1D069.

Amino acid replacements found in one antibody sample from each anti-IA-2A positive patient

The amino acid replacement from D to V was present at aa position 1 in the 2nd antibody sample of T1D019 and the 1st antibody sample of T1D069. At aa position 3, aa substitution from Q to P was present in the 1st antibody sample of T1D019 and the 2nd antibody sample of T1D069. Amino acid substitution from tyrosine (Y) to Leucine (L) at position 32 was present in the 2nd antibody sample of T1D019 and the 1st antibody sample of T1D069. At aa position 52, aa replacement from T to A was found in 1st antibody sample of T1D019 and 2nd antibody sample of T1D069. At aa position 56, aa substitution from S to G was found in the 1st antibody sample of T1D019 and T1D069. Amino acid substitution from G to C, at aa position 64 was found in 2nd antibody sample of T1D019 and the 1st antibody sample of T1D069. Amino acid substitution from Glycine (G) to Alanine (A) at position 68 was found in the 2nd affinity purified antibody sample of T1D019 and 1st affinity purified antibody sample of T1D069. At aa position 71, aa substitution from F to S was found in the 1st antibody sample of T1D019 and T1D069. Lastly, at aa position 76, aa substitution from S to N was present in the 2nd antibody sample of T1D019 and 1st antibody sample of T1D069.



Key

- aa replacements shared across all four samples
- aa replacements shared across three samples
- aa replacements shared across one sample from each anti-IA-2A positive sample
- aa replacements shared across samples from the same patient
- germline sequence
- underlined germline CDR regions

Figure 5.3. IGHV 3-23 heavy chain variable region heat map constructed from de novo sequencing data from affinity purified anti-IA-2 antibody samples generated from anti-IA-2 antibody positive sera displaying aa replacements compared to the germline sequence. **A.** IGHV 3-23 variable region sequence of the first affinity purified antibody sample of T1D019. **B.** IGHV 3-23 variable region sequence of the second affinity purified anti-IA-2 antibody

sample of T1D019. **C.** IGHV 3-23 variable region sequence of the first affinity purified antibody sample of T1D069 compared to the germline sequence. **D.** IGHV 3-23 variable region sequence of the second affinity purified antibody sample of T1D069. The germline CDR region sequence is underlined. Amino acid replacements are identified in text and highlighted in specific colour according to the incidence in the antibody samples. The germline sequence and CDR regions were defined by IMGT database.

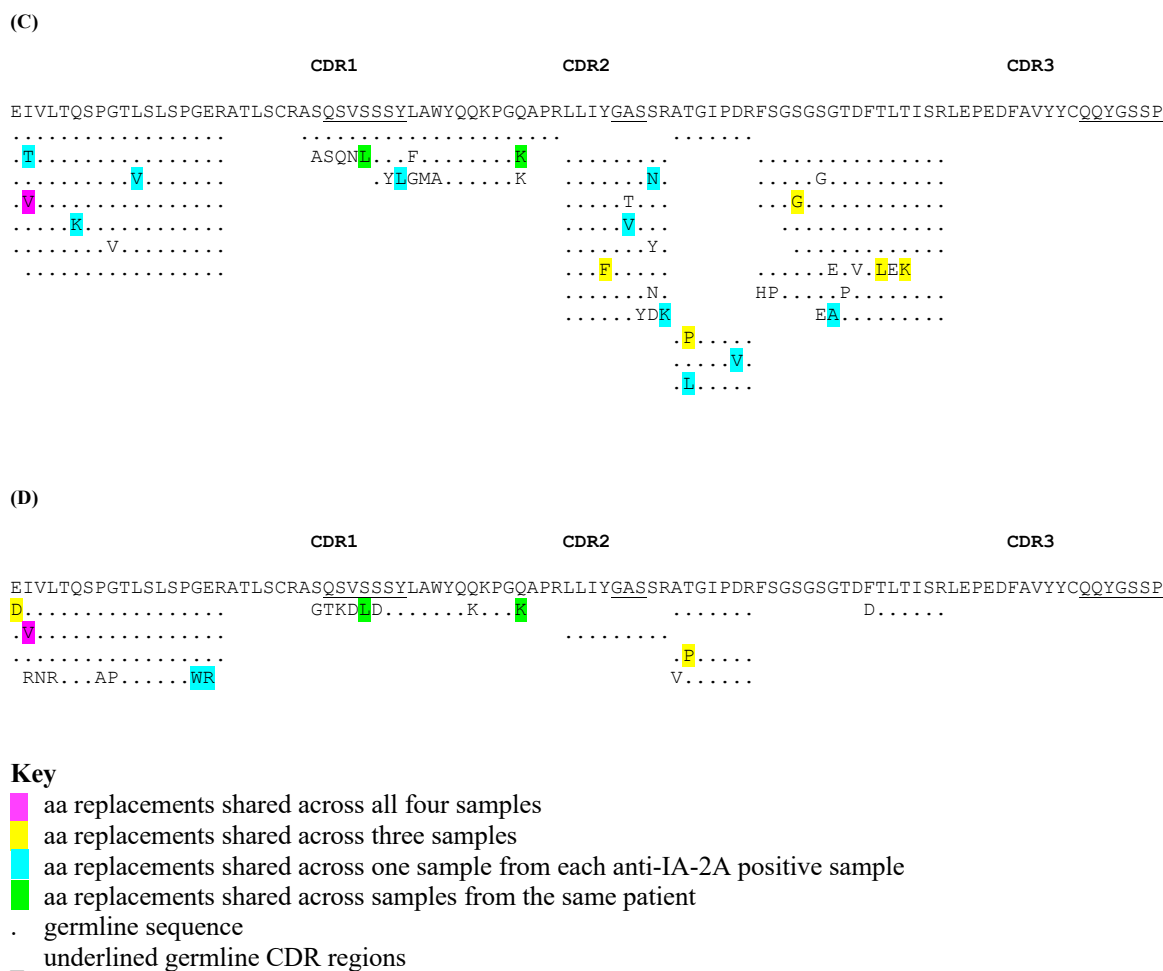


Figure 5.5. IGKV 3-20 light chain variable region heat map constructed from de novo sequencing data from affinity purified anti-IA-2 antibody samples. **A.** IGKV 3-20 variable region sequence of the first affinity purified antibody sample of T1D019. **B.** IGKV 3-20 variable region sequence of the second affinity purified anti-IA-2 antibody sample of T1D019. **C.** IGKV 3-20 variable region sequence of the first affinity purified antibody sample of T1D069 compared to the germline sequence. **D.** IGKV 3-20 variable region sequence of the second affinity purified antibody sample of T1D069 compared to the germline sequence. The germline CDR region sequence is underlined. Amino acid replacements are identified in text and highlighted in specific colour according to the incidence in the antibody samples. The germline sequence and CDR regions were defined by IMGT database.

Figure 5.6. IGKV 3-20 light chain variable region heat map constructed from de novo sequencing data from affinity purified anti-IA-2 antibody samples generated from anti-IA-2A negative sera and healthy controls. **A.** IGKV 3-20 variable region sequence of the first affinity purified antibody sample of T1D001. **B.** IGKV 3-20 variable region sequence of the second affinity purified anti-IA-2 antibody sample of T1D014. **C.** IGKV 3-20 variable region sequence of the affinity purified antibody sample of CTR063 compared to the germline sequence. The germline CDR region sequence is underlined. Amino acid replacements are identified in text and highlighted in specific colour according to the incidence in the antibody samples. The germline sequence and CDR regions were defined by IMGT database.

germline sequence. **D.** IGKV 1-9 variable region sequence of the second affinity purified antibody sample of T1D069 compared to the germline sequence. The germline CDR region sequence is underlined. Amino acid replacements are identified in text and highlighted in specific colour according to the incidence in the antibody samples. The germline sequence and CDR regions were defined by IMGT database.

(A)	(B)	(C)	(D)
YTFGQGTKLEIKELSR L.....E.RAELKTV.L.	YTFGQGTKLEIKL... L.....R	YTFGQGTKLEIKTVEVR CLGKSCC..LQR SE...QLELQR	YTFGQGTKLEIK
(E)	(F)	(G)	
YTFGQGTKLEIK	YTFGQGTKLEIK	YTFGQGTKLEIK VP.....T.D.. .S.....	

Figure 5.8. IGKJ2 light chain joining region heat map generated from de novo sequencing data from affinity purified anti-IA-2 antibody samples generated from anti-IA-2A positive patients, negative patients and healthy controls compared to the germline sequence. **A.** IGKJ2 joining region sequence of the first affinity purified antibody sample of T1D019. **B.** IGKJ2 joining region sequence of the second affinity purified anti-IA-2 antibody sample of T1D019. **C.** IGKJ2 joining region sequence of the first affinity purified antibody sample of T1D069. **D.** IGKJ2 joining region sequence of the second affinity purified antibody sample of T1D069. **E.** IGKJ2 joining region sequence of the affinity purified antibody sample of T1D001. **F.** IGKJ2 joining region sequence of the affinity purified antibody sample of CTR062. **G.** IGKJ2 joining region sequence of the affinity purified antibody sample of CTR063. Amino acid replacements are identified in text. The germline sequence was defined by IMGT database.

(A)	(B)	(C)	(D)
LTFGGGTKVEIK	LTFGGGTKVEIK	LTFGGGTKVEIK	LTFGGGTKVEIK
.....	S.....T.....
.L.....	.S.....	.S.....T..L.RSA.
V.....	V.....	VV.....	.S.....T..L.
TP....LRKT	.S.....T..L.	.P.....
F.....LR	VL.....TG.	
		.P.....	

(E)

LTFGGGTKVEIK
 ...NGTK
N.....

Figure 5.9. IGKJ4 light chain joining region map constructed from de novo sequencing data from affinity purified anti-IA-2 antibody samples generated from anti-IA-2A positive and negative patients and healthy controls aligned with the germline sequence. **A.** IGKJ4 joining region sequence of the first affinity purified antibody sample of T1D019. **B.** IGKJ4 joining region sequence of the second affinity purified anti-IA-2 antibody sample of T1D019. **C.** IGKJ4 joining region sequence of the first affinity purified antibody sample of T1D069. **D.** IGKJ4 joining region sequence of the second affinity purified antibody sample of T1D069. **E.** IGKJ4 joining region sequence of the affinity purified antibody sample of CTR063. Amino acid replacements are identified in text. The germline sequence was defined by IMGT database.



Figure 5.10. IGHJ6 heavy chain joining region map generated from de novo sequencing data from affinity purified anti-IA-2 antibody samples generated from anti-IA-2A positive patients, negative patients and healthy controls aligned with the germline sequence. **A.** IGHJ6 joining region sequence of the first affinity purified

antibody sample of T1D019. **B.** IGHJ6 joining region sequence of the second affinity purified anti-IA-2 antibody sample of T1D019. **C.** IGHJ6 joining region sequence of the first affinity purified antibody sample of T1D069. **D.** IGHJ6 joining region sequence of the second affinity purified antibody sample of T1D069. **E.** IGHJ6 joining region sequence of the affinity purified antibody sample of T1D001. **F.** IGHJ6 joining region sequence of the affinity purified antibody sample of CTR062. **G.** IGHJ6 joining region sequence of the affinity purified antibody sample of CTR063. Amino acid replacements are identified in text. The germline sequence was defined by IMGT database.

Heavy Chain	Light chain
V _H 3-23	V _K 1-9

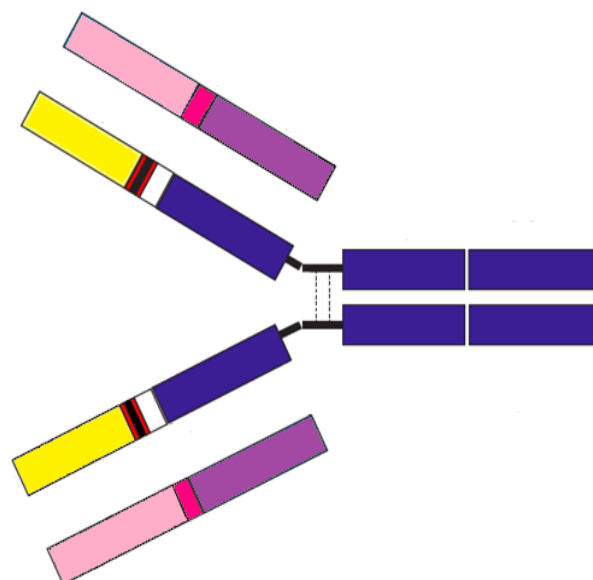


Figure 5.11. Schematic diagram of the putative anti-IA-2ic antibody identified in the affinity purified anti-IA-2ic antibody samples. The anti-IA-2ic antibody targeting a unique epitope within the intracellular domain of IA-2 expressed as a MBP fusion protein was found to be encoded by IGHV 3-23 heavy chain and IGKV 1-9 light chain.

5.4. Discussion

This chapter describes the proteomic analysis of affinity purified anti-IA-2 antibodies from T1D sera by mass spectrometry. Mass spectrometry (MS) enables heavy and light chain sequencing at the level of amino acids, in contrast to basic immunochemical methods that determines clonality based on anti-light chain antibodies. In this project, high-end performance liquid chromatography quadrupole time of flight (HPLC Q-TOF) mass spectrometer was used to analyse anti-IA-2 antibodies with high MS/MS accuracy and high resolution.

One of the major advantages of this method over hybridoma and single cell recombinant antibody cloning from plasmablasts, and B cells is that it investigates the secreted autoantibody proteome which is the final product of humoral response. Other advantages are ease of serum collection, easy and stable storage of antibodies and small serum volume requirements.

A key finding of this study is that the circulating anti-IA-2 antibody proteome in unrelated T1D patients are potentially governed by a kappa restricted IgG with a distinct light chain, IGKV 1-9. This supports the kappa skewing observed in the light chain usage of anti-IA-2 autoantibodies by the immunochemical methods described in chapter 4.1.

Interestingly, this chain has not been reported in autoimmunity thus far. However, it has been described in anti-viral responses. For instance, IGKV 1-9 usage has been reported in antibodies that target receptor binding domain of SARS CoV-2 Spike domain which have been specified by a clonotype with IGHV 3-66.DH3-10.JH3, VK1-9.JK4 heavy and light chain pairing. Another group has shown the use of IGKV 1-9 paired with IGHV 1-2 in the B cell repertoire of N123-VRC34 and VRC01- class HIV-1 broadly neutralizing antibodies (bnAbs) (Wu and Kong, 2016, Havenar-Daughton et al., 2018).

Reports of IGKV 1-9 light chain use in anti-viral responses is intriguing as several previous studies have postulated an association between viral infections such as Coxsackievirus B (CVB), rotavirus, mumps, rubella and CMV and the development of autoimmune diabetes. Coxsackievirus B particularly is of interest as studies have shown that a vast majority of the T1D patients have persistent enterovirus infections presenting inflammation in the gut mucosa. Moreover, CVB viruses have been detected in the islets and intestinal biopsies of T1D patients. Another study has shown that CVB4 strain isolated from the pancreas of a deceased diabetic patient can cause diabetes in murine beta cells (Filippi and von Herrath, 2008).

There are several mechanisms through which CVB4 infection is postulated to elicit an autoimmune response. It has been shown that CVB4 infection of the pancreatic cells upregulates the cell surface expression of beta cell antigens such as GAD. This implies that CVB4 infection of the islet cells could play a role in inducing immune responses against islet antigens via over expression of the cell surface proteins (Bason et al., 2013). By stander activation of T cells is likely to be another mechanism through which CVB4 could be inducing T1D, where viral infection cause inflammation and destruction of the target tissue releasing autoantigens that can activate autoreactive T cells. In addition, inflammation in the target tissue could cause stress in the endoplasmic reticulum leading to the generation of misfolded protein. These can be recognized as autoantigens by the T cells causing beta cell lysis and release of other existing beta cell autoantigens which further enhances the inflammation causing autoimmune diabetes (Ghazarian et al., 2013).

Despite the general proinflammatory nature of viral infections, molecular mimicry could be another mechanism through which autoimmune diabetes is induced. Studies have also shown that CVB4 infection may be inducing beta cell destruction due to molecular mimicry where a viral peptide shares homology with a self-peptide causing the host immune responses to target the self-proteins. One intriguing example is reported by Bason and the colleagues, where they showed that VP1 protein of Coxsackie B virus shares homology with autoantigens IA-2 β and voltage dependent L-type calcium channel alpha-1D subunit protein (Bason et al., 2013). The putative cross reactivity was further supported by the immunoprecipitation of the two self-proteins

using the antibodies purified against a peptide called T1DM peptide (SNLQHRRDVRP) that was targeted by 76% of the T1D patients. The same autoantigens were immunoprecipitated by antibodies purified against a Coxsackie B viral peptide called COXSA peptide (FKPKHVKAYVRP) to which 71% of the T1D patients had antibodies against (Bason et al., 2013). These findings strongly indicate that an immune response against CVB4 infection could elicit autoimmune responses that could lead to islet cell destruction. Therefore, CVB4 infection is a possible contributor to T1D onset.

Interestingly, IA-2 antigen shares homology in molecular moieties with IA-2 β phorgrin (Kolm-Litty et al., 2000). It has been shown that IA-2 and phorgrin JM domains share 50% homology while PTP domains share 88% homology. This is of significance as anti-IA-2 antibodies from T1D sera are known to target the intracellular region of IA-2 which includes JM and PTP domains. Furthermore, there are two known epitopes (aa 611-620, 621-630) within the JM region and aa 889-979 within the PTP domain have been demonstrated to play a crucial role in epitope formation for antibody binding by an amino acid substitution study (Kolm-Litty et al., 2000, Lampasona et al., 1996). Moreover, the T1DM peptide and COXSA peptide utilized by Bason and the colleagues share amino acid homology within the intracytoplasmic regions of IA-2 antigen (Bason et al., 2013). This implicates that CVB4 infection could also elicit autoimmune responses against the IA-2 antigen via molecular mimicry, which would lead to the activation of autoreactive B cells with the help of T helper cells that would in turn target epitopes within the IA-2 antigen as a result of epitope spreading. However, a direct causal link between viral infections and anti-IA-2 responses that could lead to the development of autoimmune diabetes have not been reported thus far and requires further investigation. This is beyond the scope of the current study.

In the current study, one unique IGKV 1-9 light chain was found in the Anti-IA-2A positive IgG samples indicating the presence of a distinct class switched B cell clone. While what drives the generation of these distinct autoreactive B cell clones is unknown, this implies that the anti-IA-2A response is potentially an epitope driven immune response rather than an arbitrary inflammatory response.

In addition to the IGKV 1-9 light chain, as described in chapter 5.2.4.1, IGKV 3-20 light chain was also present in the anti-IA-2A positive samples. However, IGKV 3-20 was found in the negative and healthy control samples with no significant difference in enrichment. Previous studies have shown the presence of IGKV 3-20 in a wide array of diseases. For instance, V_K 3-20 has been reported in the antibody proteome of cryoglobulinemia, SLE, Influenza, acute myeloid leukemia, Sjogren's syndrome and healthy repertoire (De Re et al., 2006, Wang et al., 2018, Wang et al., 2015). Therefore, the presence of IGKV 3-20 in all samples and controls in this study is likely from the general antibody population which are not specific to the anti-IA-2A response.

A single IGHV3-23 heavy chain use was also found to be common across the anti-IA-2A positive samples. Previously, V_H 3-23 has been reported to be widely used in the B cell proteome of other human autoantibodies such as in MALT lymphomas, primary SS, SLE, Clostridioides difficile toxin B, Chronic Lymphocytic Leukemia and anti-HIV bnAbs (Adam et al., 2008, Bomben et al., 2010, Dorner and Lipsky, 2005). Although, IGHV 3-23 was also found in the control samples, mass spectrometry analysis revealed the presence of a greater number of high-quality germline matched peptides with large spectral counts and high abundance resulting in greater coverage for IGHV 3-23 heavy chain in the anti-IA-2A positive samples compared to the control samples. This indicated an enrichment in the use of this chain in the anti-IA-2A positive samples in comparison to the controls suggesting that IGHV 3-23 is associated with the anti-IA-2A response. In addition, given that the positive antibody samples in the current study were specifically affinity purified against the IA-2ic target and that only one IGHV 3-23 heavy chain family was present and shared across the antibody samples, it is likely that IGHV 3-23 contributes to the anti-IA-2 response and is likely paired with IGKV 1-9.

Following variable region analysis, joining region usage of the heavy and light chains of the anti-IA-2 antibody samples were also examined. This revealed the presence of IGKJ2 and IGKJ4 joining regions for the light chain samples. IGKJ2 was found in all positive samples and 3 out of 4 control samples. While IGKJ4 samples were found in all positive samples and one control sample. Given that the Q-TOF mass spectrometry analysis method used in the current study was unable to detect peptides that matched to

CDR3 regions, the variable regions could not be matched to the joining regions. Similarly, a single IGJ6 joining region was found for the heavy chain samples. IGJ6 was found in all positive and control samples. Potentially, IGKV 1-9 is paired with either IGKJ2 or IGKJ4 while IGHV 3-23 is paired with IGJ6. Further analysis is required to confirm the variable region and joining region pairing.

Previously studies have investigated V region mutational signatures of serum antibodies in attempts to understand the clonality and the properties of the secreted antibody proteome. The presence of aa replacement mutations in a unique heavy and light chain pairing have been described to be indicative of long lived, class switched public B cell clonotypes that share a common autoimmune pathway (Lindop et al., 2011). A proteomic study that investigated the humoral responses in primary SS patients reported the presence of common aa replacements in the proteome of anti-Ro60 antibody response which was specified by a clonal pairing of IGHV3-23/IGKV 3-20 (Lindop et al., 2011, Wang et al., 2016). Amino acid replacements have also been described in the antibody repertoire that targets *Clostridioides difficile* toxin A and B. These studies suggested that the high frequency of aa replacements is indicative of memory recall of B cells that have undergone antigen driven somatic hypermutation and affinity maturation (Lindop et al., 2011, Adamson et al., 2020).

Heat map analysis of IGKV 1-9 from the T1D019 affinity purified antibody samples revealed the presence of 76 amino acid replacements spanning across the CDR1 to CDR3 regions of the variable region. Interestingly, both germline and mutated peptides were matched to the CDR1 and CDR2 regions while only mutated peptides were detected for the V region between CDR2-CDR3. Two mutations within the CDR2-CDR3 regions were found in multiple peptides suggesting that this aa replacement is potentially important for antibody binding.

However, given that peptides without these specific mutations and peptides with other mutations were also recognized for the same V region, these mutations are unlikely to be crucial for autoreactivity. The presence of multiple versions of peptides suggests the presence of a pool of B cell clones that are autoreactive to the IA-2 antigen incorporated in the fusion protein ELISA.

Similarly, as with T1D019, T1D069 antibody sample also had multiple germline peptides spanning the V region with germline and mutated peptides clustering near the CDR1 and CDR2 region while only mutated peptides were found to be clustering near CDR3. This repeated pattern supports the two observations that aa replacements around the CDR2 to CDR3 region might be important for autoreactivity and that there are multiple autoreactive B cell clones specified by one IGKV 1-9 light chain present in the affinity purified anti-IA-2 antibody samples.

Interestingly, Lindop and colleagues demonstrated the presence of shared public arginine aa residues within the light chain CDR3 region of the anti-Ro60 peg antibody proteome in SS patients. This study suggested, given that all anti-Ro60 peg reactive B cell clones appeared to contain these aa replacements, they may be important for antibody binding (Lindop et al., 2011). In the current study, 9 public aa replacements were found across the 2 anti-IA-2A patient samples, the majority of which clustered in the CDR2-CDR3 region. Of particular interest are two of these aa replacements that concentrated around aa 74 which involved a substitution from Threonine to either Arginine or Lysine. These aa replacements were found in all peptides that matched to this specific region of the IGKV 1-9 germline sequence. Therefore, it appears that the CDR2-CDR3 region is a hotspot for common (public) mutations, and as with anti-Ro60 peg antibodies, the lack of germline peptides suggests these aa replacements may also be potentially important for antibody binding, specificity, or affinity.

The observed distribution of V region aa replacements amongst the patient-derived affinity purified antibody samples raises several possibilities regarding the origins of the anti-IA-2 autoreactive B cell clonotype: i) One possibility is that a constant regeneration of autoreactive B cell clonotypes with the unique combination of the heavy and light chain occurs with antigen dependant aa replacements following germinal centre reactions that are crucial for high antibody binding affinity; ii) these autoantibodies arise from a periodic recall of a long-lived memory B cell pool that has previously undergone somatic mutation and affinity maturation; iii) long-lived circulating autoreactive plasma cells could be generating these anti-IA-2 autoantibodies over the span of the disease; iv) the possibility that genetic variations in the light chain

germline sequence results in inherited predisposition to generating autoreactive B cell clonotypes that lead to T1D onset.

In order to investigate the various possible origins of the autoreactive B cell clonotypes leading to IA-2 responses, further approaches outside of the scope of the current study are required. For example, the Lindop study attempted to address the kinetics of anti-Ro60peg antibody production by performing sequential serum collection from patients over a period of time, where they determined clonal turnover occurred every six months to new clonal variants containing common core mutations and a unique subset of mutations. This suggested that the anti-Ro60 peg antibody repertoire is generated by a periodic recall from a pool of autoreactive memory B cells. While a similar approach to the Lindop study would provide a broader understanding of the anti-IA-2 antibody proteome, it is important to recognize the evident difference in autoantigen abundance between Sjogren's syndrome, where the Ro60peg autoantigen is found in all nucleated cells, in contrast to T1D where the targeted autoantigen is mostly confined to the beta cells of the pancreas. This availability is further reduced as the disease progresses due to the removal of beta cells (Lebastchi et al., 2013).

Interestingly, it has been reported that humoral responses to IA-2 also diminish over the course of the disease (Kong et al., 2013, Pihoker et al., 2005). While the cause of the reduction of islet autoantibody titres in T1D is not well described, previous studies have reported that the clearance of the antigen leads to a decrease in antibody titres (Bahar et al., 2020). Therefore, it is possible that the decline in islet autoantigen availability during the progression of the T1D disease process may lead to the diminished production of autoantibodies due to reduced memory recall or reduced regeneration of new autoreactive B cell clones. Another possibility is the presence of previously established autoreactive plasma cells, which were generated during the early phases of anti-IA-2 autoimmunity that eventually depreciate over the span of the disease. Interestingly in the current study, only ~15% of the patients were detected as IA-2A positives by RSR ELISA, all of whom were younger patients. This observation supports the possibilities discussed above, where, as the availability of the autoantigen reduces during the progression of the disease, the autoantibody generation also deteriorates. However, further studies similar to the Lindop study involving sequential

collection of serum from a larger cohort of T1D patients that are selected for age onset, disease duration and span of the disease are required to gain a better understanding of the origin of anti-IA-2 humoral response.

An alternate to antigen driven generation of mutated clonotypes is genetic polymorphic inheritance leading to the generation of the autoreactive B cell clonotypes. In order to explore whether inherited genetic variations lead to the onset of the disease, further work involving genome sequencing studies must be carried out. Although this is a speculative possibility, the clinically relevant anti-ZnT8 antibodies have been reported to be generated against an inherited single nucleotide polymorphism at aa 325 of the ZnT8 transmembrane protein (Skärstrand et al., 2013). In addition, it has been well established that polymorphic HLA inheritance is associated with the risk of T1D onset. So far, a study that looked at the IA-2 islet antigen gene polymorphisms in the Japanese population has reported that IA-2 antigen gene polymorphisms are not associated with T1D onset (Nishino et al., 2001). However, to our knowledge, no studies have been done to investigate polymorphisms in the autoreactive anti-IA-2 lymphocyte genome. While the concept of inheriting lymphocyte variants that leads to autoimmune responses against IA-2 is very speculative, Mikocziva and colleagues revealed that heavy chain germline variations in the immunoglobulin genes can affect the B cell receptor and antibody repertoire which in turn may influence the susceptibility to diseases (Mikocziova et al., 2020). Another study discussed that a potent anti-HIV antibody is associated with two IGHG3 alleles that carry polymorphisms (E419 and K392) that are known to improve receptor binding and enhance antibody-dependent cell-mediated actions (Warrender and Kelton, 2020). Therefore, the possibility that anti-IA-2 antibodies are generated as a result of lymphocyte polymorphic variants in individuals is not without precedent.

However, the reduction of the anti-IA-2 antibody titres over the span of the disease implies that the IA-2 humoral response is antigen dependent, and the antibody levels decrease due to the clearance of the islet antigen. Therefore, in the case of generation of B cell clonotypes with inherited SNPs, it is likely that these B cell clones require antigen encounter to be activated to become antibody producing plasma cells which eventually drift off as the antigen become less available. Similarly, the memory B cell

pool will also deteriorate as antigen availability reduces. In contrast, the presence of antigen independent autoreactive B cell clonotype with inherited polymorphic variants is less likely, as these B cells are likely to produce autoantibodies consistently over the span of the disease.

While identification of a distinct light chain unique to anti-IA-2 antibodies allowed a detailed investigation of the relevance of the shared mutations, extending similar investigation to the heavy chains was problematic, given that IGHV 3-23 was heavily overrepresented in the control samples. During heat map analysis, both germline and mutated peptides were matched across the entire V region of the heavy chain in both patient samples. Furthermore, although aa replacements were more prominent in the patient samples, none were exclusive to the patients. Therefore, as previously discussed, screening a larger cohort of T1D patients may provide a better understanding of the heavy chain usage in the anti-IA-2 antibody repertoire.

In discussing the inherent limitations of the current approach, two major aspects are prominent, first is that little is known of the epitopes that are presented for antibody binding in the fusion protein ELISA. Secondly, the proteomics methodology utilized in this study is unable to recognize heavily mutated peptides. As described previously in chapter 3.3.3.1., it appeared that fusion protein ELISA was only able to detect sera with high anti-IA-2A titres out of the pool of anti-IA-2A positive patients by RSR ELISA, suggesting the fusion protein ELISA lacks sensitivity compared to the RSR ELISA. While the RSR ELISA has been commercially optimized and uses liquid phase IA-2 conjugated with biotin to detect monovalently bound anti-IA-2 antibodies and amplify the signal, little is known of the antigen-antibody reaction in the fusion protein ELISA. Furthermore, the lower frequency of anti-IA-2A positive patients detected by the fusion protein ELISA compared to the commercial RSR ELISA could also be due to the availability of a reduced number of epitopes. Thus far, IA-2 antigen has been reported to contain two known epitopes within the JM domain (aa 611-620, 621-630), while epitopes within the PTP domain are less well defined (Kolm-Litty et al., 2000). Although the IA-2ic domain incorporated in the fusion protein ELISA contains the JM and PTP domains, little is known about the tertiary structure of the recombinant protein, and which epitopes are available for antibody binding. Further work incorporating

amino acid substitutions may help in understanding which epitopes are presented in the fusion protein ELISA for antibody binding. Furthermore, the fusion protein ELISA utilises a recombinant fusion protein that contains a relatively large MBP fusion tag that may affect the presentation of the epitopes, while the final composition of the recombinant protein used by RSR ELISA is unknown. In terms of proteomics analysis limitations, the QTOF mass spectrometry in combination with peaks analysis used in this study only detected peptides with more than two aa substitutions with five or more consecutive amino acids making up >50% of the peptide that match the germline sequence. Therefore, it is possible that highly mutated peptides that match the CDR3 region are not detected by the Peaks software. Thus, incorporating new proteomics methods such as MRM methodology involving trypsin and chemotrypsin peptide digestion steps may allow detection of peptides that span across CDR regions.

In summary, these findings suggest that a unique high affinity, class switched, and affinity matured B cell clonotype specified by a distinct heavy and light chain pairing of IGHV 3-23.IGHJ6/IGKV 1-9.IGKJ2/IGKJ4 with unique aa replacements governs the immune response against a specific epitope within the intracellular domain of the IA-2 antigen in T1D patients. This suggests that an identical pathophysiological mechanism potentially drives the anti-IA-2 humoral response in T1D.

Chapter 6: Concluding remarks

6.1. Summary and Conclusions

This thesis discusses a novel proteomics approach to investigate clonality and variable region gene usage of B cells giving rise to anti-IA-2 antibodies in T1D patients, based on the development of IA-2 fusion protein ELISA coupled with de novo and database driven sequencing of variable region molecular signatures by Q-TOF mass spectrometry. As described previously, this method provides an approach to characterize the secreted autoantibody repertoire specific to a classic islet autoantigen, IA-2, in complex T1D patient sera. Importantly, the findings presented in this thesis provide novel insights into the origins of autoreactive B cells driving autoantibody responses in this disease. The approach therefore advances the field by helping to understand the pathophysiological underpinnings of autoimmune responses in T1D.

To date, studies focused on investigating the humoral response in T1D disease have often concentrated on identifying the primordial targets and antigenic regions of islet autoantigens. For instance, research over the last 50 years has identified four major islet antigens, IAA, IA-2, GAD, and ZnT8. These findings originally provided insights into the primary focus of the autoimmune responses in T1D disease process allowing the development of prognostic and diagnostic platforms. More recently, studies have then focused on fine specifying and mapping the antigenic regions within these islet antigens, which further improved the sensitivity and specificity of the diagnostic tools allowing accurate confirmation of autoimmunity in individuals. Recent studies have revealed clinical differences in what epitopes are targeted within an antigen by the humoral response which has led to better clinical treatment interventions. For example, while anti-GAD responses are found in both Latent Autoimmune Diabetes (LADA) and early onset T1D patients, studies have revealed that antibody responses to the NH₂ terminal epitopes of GAD are associated with progression to insulin dependency in patients with LADA while autoantibodies against the COOH terminus of GAD is associated with need for insulin therapy in early onset T1D (Tiberti et al., 2008, Falorni et al., 2000). Similarly, autoantibodies against COOH terminus of IA-2 have been reported to be associated with childhood-onset diabetes, whereas reduced autoreactivity

against the COOH terminus of IA-2 appears to be a feature in adult-onset T1D patients (Tiberti et al., 2008).

The findings discussed above where specific epitope recognition varies between early versus adult onset of T1D suggest that the pathophysiological pathways driving the humoral response differ. While the variance in age of onset between the two groups, disparities in autoepitope targeting could simply be due to factors including differences in maturity of the immune system, such speculation awaits a better understanding of the fundamental pathophysiological pathways leading to the generation of autoantibodies in T1D. As such, this thesis aimed to address key questions regarding the molecular pathways underpinning the humoral responses in T1D. The approach taken by this thesis was to investigate the origins of the autoreactive B cell clonotypes by examining the variable region gene usage of the circulating autoreactive B cell clonotypes that targets IA-2 in T1D patients.

Recent proteomic studies in systemic autoimmune diseases have demonstrated restriction and public sharing of variable region gene usage of B cells that generate autoantibodies. The presence of these epitope specific shared and restricted B cell clonotypes suggest that the pathophysiological pathway from genetic selection of B cell receptor variable region genes, subsequent escape from central and peripheral tolerance checkpoints, successful migration to lymph nodes, and antigen driven activation is identical in all patients. For instance, mass spectrometric sequencing of anti-Ro52 antibodies isolated from multiple unrelated primary SS patients have revealed that they are encoded by a specific B cell clonotype with IGHV 3-23/IGKV 3-20 heavy and light chain pairing (Wang et al., 2016). Interestingly this phenomenon of public sharing and clonal restriction in B cell clonotypes has also been reported in antibodies associated with infectious diseases. For example, a proteomic profiling study of antibodies against *C. difficile* toxoid A and B has reported the presence of unique B cell clonotypes specified by IGHV 3-23 heavy chain and IGKV3-11, 3-15, 3-20 and 4-1 light chains (Adamson et al., 2020). This suggests that while the capacity to generate diverse epitope recognition and immune responses is high, functional immune mechanisms appears to be restricted with similar features of clonal selection.

The new emerging understanding of restricted and public B cell clonotypes indicating the presence of common pathophysiological pathways in unrelated patients may provide insights into the development of novel therapeutic interventions by selective targeting of B cell clonotypes with potential pathogenic roles in the disease process. Over the last 50 years an understanding of the pathogenic role of autoantibodies has emerged along with the epitope selective nature of these responses. For instance, anti-Rib-P antibodies associated with lupus nephritis, hepatitis, and the active phase of the disease in patients with SLE are primarily directed to a main epitope within the carboxy terminus of the antigen (Mahler and Fritzler, 2010). In addition, a proteomic study carried out by Al kindi and colleagues reported that anti-Rib P antibodies targeting the carboxy terminal may be encoded by two distinct B cell clonotypes specified by IGHV 3.7-JH6/IGKV3.20-JK2 and IGHV1.3-JH4/IGKV1.39-JK4 pairing (Al Kindi et al., 2016). Similarly, anti-Sm antibodies also associated with Lupus nephritis, neuropsychiatric disease and SLE clinical onset is primarily directed towards the carboxy terminal of SmD1 and D3 proteins within the antigen (Mahler and Fritzler, 2010). A recent proteomic study has also reported that the anti-SmD autoantibody proteome is encoded by IgG1 kappa clonotypes specified by IGHV3-7 and IGHV 1-69 heavy chains and IGKV 3-20 and IGKV 2-28 light chains (Al Kindi et al., 2015). Therefore, identifying the specific B cell clonotypes that produce pathogenic antibodies could allow the development of novel therapeutic processes by facilitating selective removal or silencing of the pathogenic B cell clonotype.

To date a direct pathogenic role for islet autoantibodies is yet to be identified. Investigating the role and origin of the islet autoantibodies in T1D has been challenging given the low serum titres and the lack of persistence of the autoantibodies, unlike in systemic autoimmune diseases where antibodies are found in high titres throughout the disease process. Although understanding the role of islet autoantibodies is outside the scope of this thesis, the development of a novel ELISA based affinity purification method for IA-2 as described in this thesis should facilitate the use of affinity purified antibodies for addressing questions of pathogenicity for this autoantibody. Investigation of the role of epitope-specific anti-IA-2 autoantibodies in the disease process coupled with the emerging understanding of clonality may lead to the

development of new experimental approaches to identify potential pathogenic B cell clones that may be driving the T1D disease.

Establishment of an ELISA based detection method using MBP fusion protein.

In order to investigate the B cell origins of anti-IA-2 antibodies, we first developed a MBP fusion protein ELISA method to detect anti-IA-2 antibodies in T1D sera. The MBP fusion protein utilized in the ELISA to detect anti-IA-2 antibodies contained the immunodominant IA-2ic domain. As discussed previously, the use of recombinant fusion protein with the MBP tag has been reported to facilitate solubility, proper folding, better expression in the E.coli system and stability of recombinant fusion proteins in solid phase. Furthermore, incorporation of MBP fusion tag facilitate the use of proteins of interest in immunological methods such as ELISA and column chromatography. In addition, MBP fusion protein is easily reproducible and cost effective compared to commercially available ELISA assays. As described in chapter 3, a subset of the RSR ELISA positives (3/10) demonstrated OD values above the established assay cut-off of the MBP fusion protein ELISA. Interestingly, the positive patients detected by the fusion protein ELISA were high titre patients suggesting that fusion protein ELISA sensitivity is lower compared to commercial RSR ELISA. In addition, given the MBP fusion protein and IA-2ic protein is relatively of the same size, target protein available for antibody binding is potentially lower compared to RSR ELISA. Additionally, little is known of the tertiary structure of the recombinant protein, it is likely that the presentation of epitopes within the IA-2ic domain is hindered due to faulty folding. Furthermore, RSR ELISA uses biotin conjugates and has been commercially optimized for greater detection sensitivity. However, while MBP fusion protein ELISA is unable to detect all low titre anti-IA-2A positive patients, this method provided a platform to explore the generation of affinity purified antibody samples from high titre sera that can be subjected to proteomic analysis. While this ELISA plate affinity purification method successfully generated enriched anti-IA-2 antibody samples, alternate methods that could be utilized for affinity purification are column chromatography or incorporation of recombinant protein without fusion tags which are beyond the scope of this study.

Development of an affinity purification method based on the MBP fusion protein ELISA

As previously discussed, in attempts to investigate the B cell origin of the anti-IA-2 antibodies, we first successfully developed an anti-IA-2 antibody detection method. Subsequently, the validated MBP fusion protein ELISA was then utilized to form the basis of a four-plate affinity purification method described by Al Kindi et al to affinity purify anti-IA-2 antibodies from T1D sera (Al Kindi et al., 2015). Affinity-purified antibody samples were generated from two anti-IA-2 antibody-positive sera, two anti-IA-2 antibody-negative sera and two healthy controls. The affinity-purified antibody samples were then tested for purity and yield by SDS gel electrophoresis. This revealed that the ELISA plate affinity purification method generates high yield, undenatured, pure IgG antibody samples with low impurity from a small volume of complex T1D sera. Given that both the ELISA plate detection method and affinity purification method incorporate identical recombinant proteins, the same epitopes are potentially presented for antibody binding in both processes. This uniformity ensures that the same population of autoantibodies are both detected, and affinity purified. Hence, the consistency of epitope presentation applied in the workflow described in this thesis facilitates accurate investigation of the B cell origins of the IA-2 antibodies. Consequently, as demonstrated, this simple ELISA plate affinity purification method appears to be a helpful tool that can be utilized to affinity purify and subsequently facilitate proteomic analysis of specific anti-IA-2 antibodies and potentially other islet autoantibodies.

Confirmation of enrichment and specificity of the affinity purified antibody samples

The major challenge of affinity purification of antibodies is generating enriched antibody samples specific to the target. To assess this in our sample, we investigated the enrichment of IA-2ic specific antibodies by testing the affinity purified antibody samples by reactivity ELISA and comparing the affinity purified antibody sample binding to the target with the binding of the corresponding adjusted serum sample which was diluted to match the total IgG in affinity purified antibody sample. The affinity purified antibody sample binding revealed OD values above the assay cut off

for positivity revealing that antibodies specific to the IA-2ic target were affinity purified by the four-plate affinity purification method. The successful binding of the affinity-purified antibody to the IA-2 antigen also demonstrated that the ELISA plate affinity purification method effectively retains the functional activity of the antibodies. Another critical finding was that the binding of adjusted serum that was diluted to contain approximately the same amount of total IgG as the affinity purified antibody sample was below the assay cut off. This removal of IA-2A positivity from the serum further confirmed the enrichment of IA-2A antibodies in the affinity purified antibody sample.

To further verify the enrichment of specific antibodies by the affinity purification method, the affinity purified antibody sample generated from T1D069 serum validated to be positive for both IA-2A and ZnT8RA by both RSR ELISA and fusion protein ELISA was tested by reactivity ELISA. Interestingly, the reactivity ELISA revealed that the affinity purified antibody sample retained IA-2A positivity while ZnT8RA positivity was removed.

These findings confirmed that the established IA-2 fusion protein ELISA can be utilized as the basis of the ELISA plate affinity purification method described by Al kindi et al to successfully affinity purify relatively low titre autoantibodies from T1D patient serum. While the ELISA plate affinity purification method has previously been used to successfully affinity purify high titre antibodies such as anti-ribosomal P and anti-SmD autoantibodies in SLE patients, this study demonstrates for the first time that the ELISA plate affinity purification has the capacity to detect, and affinity purify low titre autoantibodies from patients with organ specific autoimmune diseases such as T1D.

These findings also indicated that the ELISA plate affinity purification method is able to generate enriched affinity purified antibody samples specific to the IA-2 target which are suitable for mass spectrometry analysis. This also suggests that the ELISA plate affinity purification method can be utilized to affinity purify other low titre autoantibodies for studies beyond proteomic analysis such as functional and molecular modelling studies.

Proteomic profiling of the affinity purified anti-IA-2 antibody samples

As discussed previously, variable region gene analysis of autoantibodies in systemic autoimmune diseases has revealed that the humoral response is clonally restricted in unrelated patients. For instance, as mentioned previously, Lindop et al reported that the anti-Ro60 peg antibody proteome in primary SS patients is driven by a B cell clonotype specified by IGHV 3-23 and IGKV 3-20 pairing (Lindop et al., 2011). In order to investigate whether this is a phenomenon occurring in organ specific autoimmune diseases such as diabetes, we attempted to examine the B cell origin of the humoral response against one of the major islet autoantigens, that being IA-2. Following successful validation of the affinity purification method, additional affinity purified antibody samples were generated from two IA-2A positive patients, two IA-2A negative patients and healthy controls. Firstly, the antibody samples were separated into heavy and light chain populations by SDS gel electrophoresis, with these samples then transferred to the mass spectrometer and the generated proteomic data were then analysed using Peaks software.

As discussed previously in chapter 5.2.3, in order to reliably examine the variable region gene usage of the heavy and light chains, we first analysed the antibody samples to select high quality peptides with high spectral counts, correct ion match, coverage and intensity that can be assigned to gene families. These peptides were then matched to gene families using IMGT database by Peaks software and confirmed manually. As per the selection criteria, gene families were assigned when one or more unique peptides were present along with multiple supporting peptides. Heat maps were then generated for each assigned gene family, which were examined for aa replacements.

The peptide analysis of the heavy and light chain joining, and variable region gene usage revealed the presence of a kappa restricted IgG1 potentially specified by IGHV 3-23 heavy chain aligned with IGHJ6, and IGKV 1-9 light chain aligned with either IGKJ2 or IGKJ4.

Remarkably this presentation was found in affinity purified antibody samples from both anti-IA-2A positive patients. These findings indicate that anti-IA-2 antibodies specific to the IA-2ic domain in unrelated patients with T1D are clonally restricted. The presence of this restricted autoreactive B cell clonotype that targets IA-2ic domain in unrelated T1D patients suggests that this unique combination of variable region gene usage leads to the generation of autoreactive anti-IA-2 antibodies in T1D. This extraordinary finding suggests that the humoral response against IA-2ic is likely to be driven by a unique, public, class switched, and affinity matured plasmablast with a distinct heavy and light chain gene pairing. Interestingly these findings suggests that the humoral responses driving the T1D disease process is potentially analogous to the autoimmune process described in systemic autoimmune diseases.

However, the mechanisms through which these autoreactive clonotypes may be arising in all autoimmune diseases are yet unknown. Previous studies in systemic autoimmune diseases have discussed several potential pathways that maybe resulting in the generation of autoreactive B cell clonotypes. For instance, Lindop et al discussed that the humoral response against Ro60 peg in SS patients is generated by a public B cell clonotype that escape central and peripheral tolerance checkpoints to be positively selected in the germinal centre (Lindop et al., 2011). They then demonstrated that the humoral response against Ro60 undergo periodic clonal turnover specified by unique aa mutations within the V region. Lindop et al proposed two pathways through which these short lived clonotypic antibodies may be generated due to antigen driven activation. One pathway where short lived plasmablasts are regenerated by continuous antigen driven activation of autoreactive B cells. Alternatively, new clonotypes are generated due to the repeated antigen driven expansion of a memory B cell pool (Lindop et al., 2013). Furthermore, Harley discussed that this anti-Ro60 peg humoral response is most likely generated by repeated activation of same or closely related memory cells in a manner that inhibits further somatic hypermutation (Smith et al., 2013).

As discussed previously in chapter 5.3, the humoral response against IA-2 in T1D patients is also likely to arise due to continuous antigen driven stimulation of plasma cells. This notion aligns with the deterioration of autoantibody titres observed over the

duration of the disease process, most likely due to the clearance of islet antigens. However, in order to investigate the nature of the autoreactive B cell clonotype, a similar approach to Lindop study where further work involving serial collection of antibodies across the span of the disease is required.

Nevertheless, the presence of this unique B cell clonotype suggests that patients with T1D who express this specific clonotype share a common pathway of autoimmunity against IA-2ic. A corollary that can be derived from this is that a common pathophysiological pathway drives the development of autoimmune responses in T1D patients. This finding along with recent findings in systemic autoimmune diseases, challenges the conventional understanding that the autoimmune responses are heterogenous, diversified and polyclonal while supporting the more recent findings where shared public clonotypes were reported potentially to be driving the immune responses in systemic autoimmune diseases such as SS and RA.

As discussed in chapter 5, heat map analysis of the IGKV 1-9 light chain revealed the presence of 9 common aa mutations clustering between CDR2 and CDR3 region that is shared across the IA-2A positive patient samples. This finding further supports the theory that the unique B cell clonotype specified by IGHV 3-23 and IGKV 1-9 has putatively undergone IA-2 antigen driven affinity maturation. The aa mutations resulting from somatic hypermutation events that are shared across the patient samples are potentially productive and permissive for antibody binding or improve antibody affinity. In addition to the shared mutations, the idiopathic aa replacements were present in individual antibody samples, however the role of these are unknown. As previously discussed, further studies involving serial collection of antibodies across disease progression aimed at examining appearance and roles of these mutations may help in distinguishing whether these amino acid replacements arise from antigen driven somatic hypermutation or inherited genetic recombination events.

Nonetheless, the presence of these circulating autoantibodies in T1D patients specified by IGHV 3-23 and IGKV 1-9 chains indicates that B cell clonotypes expressing this unique heavy and light chain combination survives central tolerance. As previously discussed, IGHV 3-23 heavy chain has also been described in the antibody repertoire

of other autoimmune diseases and responses against common pathogens. IGKV 1-9 light chain has also been described in the antibody repertoire of some infectious diseases (Chapter 5.3). Therefore, it appears that these two individual germline heavy and light chains are widely used and readily escape central tolerance. In addition, this study demonstrates the presence of a clonotype specified by IGHV 3-23 paired with IGKV 1-9 in patients with T1D indicating that the combined use of this chain also escapes central tolerance. While it is unknown whether this unique B cell clonotype that escape the central tolerance is in germline form, there is a possibility that the expression of this heavy and light chain is important for the effective generation of beneficial humoral responses. However, the expression of this unique combination of heavy and light chain has not been described previously. One possibility maybe because this unique B cell clone is generated but remains quiescent to only be activated at a disease setting, for instance during the inflammation of the pancreas. In contrast, as discussed previously, this B cell clonotype may potentially be uniquely generated in patients with T1D.

More importantly, the findings arising from this thesis suggest that these B cell clonotypes potentially acquire autoreactivity through aa modifications during antigen driven affinity maturation process in germinal centres. This process presumably involves escape from peripheral tolerance, and results in the development of autoantibody producing plasma cells. However, the mechanisms through which this occurs are as yet unknown. Nonetheless the emergence of these B cell clonotypes and their escape of peripheral tolerance checkpoints in an individual is likely to be multifactorial and complex. Studies over the years have attempted to investigate the potential mechanisms that may contribute to the generation of autoreactive B cells in systemic autoimmune diseases. Several pathways have been proposed as the potential mechanisms through which these autoreactive B cell clonotypes escape peripheral tolerance check points. Some contributing factors include raised BAFF cytokine levels allowing the differentiation and proliferation of autoreactive B cell clonotypes (Groom et al. 2002). Given the established role of T cells in T1D, it is likely that dysregulated T cell compartments contribute to the generation of autoimmune responses. This may include defective T regulatory cell suppression of the emergence of the self-reactive B cells resulting in anti-IA-2 autoantibody responses (Meffre 2008). In contrast elevated

ICOS expression and subsequent increased development of IA-2 epitope recognizing T helper cells resulting in enhanced IL-21 production may lead to robust IA-2 specific class switched antibody responses (Diplacido 2010). Studies have also discussed that specific HLA class inheritance engender the generation of these autoantigen specific autoimmune responses (Rishmueller et al 1998). Moreover, it has been proposed that viral infections resulting in enhanced inflammation can induce autoimmune responses. Previous studies in T1D have discussed that enterovirus infection of the islet cells can promote apoptosis of the beta cells leading to the over presentation of islet autoantigens by APC during an elevated immune response which can ultimately result in the targeting of self-antigens (Filipi 2008). Interestingly, another study discussed that immune responses may be directed to the IA-2 antigen due to molecular mimicry between IA-2 and CVB antigen further supporting the notion that viral infections can lead to the development of autoimmune responses in the pancreas (Bason et al. 2013).

While the mechanisms that results in the generation of these humoral responses are yet unknown, this study reveals the presence of a distinct B cell clonotype specified by IGHV 3-23 paired with IGKV 1-9 that governs a subset of the autoimmune response against the intracellular domain of IA-2 in T1D patients. The identification of this unique B cell clonotype may facilitate the development of novel therapeutic interventions to address the development of autoimmune responses in T1D. For instance, novel therapies involving peptide mimics or anti-idiotypic antibodies that target this unique B cell clonotype may be utilised to remove or silence this pathogenic B cell clone prior to activation hindering the development of the autoimmune response. In addition, these novel methods may be utilised to isolate this unique B cell clonotype which may assist us in understanding the mechanisms that underpins the generation of autoimmune responses from the generation of the pathogenic clonotype to the escape in tolerance checkpoints and ultimate targeting of the self-antigens in T1D disease process.

6.2 Future directions

This thesis reveals the presence of a unique B cell clonotype specified by IGHV 3-23, IGHJ6 and IGKV 1-9.IGKJ2/IGKJ4 that governs a subset of the humoral response against the IA-2ic domain in patients with T1D (Chapter 5.3). This finding suggests that the autoimmune responses against IA-2 in T1D are highly clonally restricted. The current study also revealed the presence of common public aa replacements within the variable region of the heavy and light chain indicating that this unique B cell successfully bypass central tolerance checkpoints and migrate to the germinal centres where they undergo affinity maturation. Herein the B cell clone obtain aa replacements through which they potentially acquire autoreactivity. However, further study involving serial collection of antibodies from a larger cohort of T1D patients is required to confirm these findings.

One of the limitations of the current study was that the QTOF mass spectrometry de novo sequencing method was unable to provide full sequence of the heavy and light variable regions. Therefore, incorporating more advanced proteomics methods such as MRM mass spectrometry that is able to supersede the method utilized in the current study may provide a better understanding of the aa mutation distribution and their contribution to the antibody binding or affinity.

Furthermore, a larger cohort of T1D patients selected for age onset and disease duration must be investigated in order to gain a broader understanding of the autoimmune response in T1D. In addition, identifying the nature of the antigen and the number of epitopes available for antibody binding in the detection platform utilized in the current study may help us determine the clonality of the autoimmune response against each epitope. This may reveal a panel of B cell clonotypes that is representative of the autoimmune response against IA-2. Moreover, this thesis reveals an approach that may be utilized to examine the responses against other clinically relevant islet antigens which may provide broader understanding of the clonal nature of the entire humoral response in T1D.

These discoveries have potential therapeutic and diagnostic implications. The finding of a clonotypic anti-IA-2 autoantibody specified by unique heavy and light chains with distinct variable region mutations may be utilised as MS based disease specific biomarker for clinical diagnosis. For instance, Arentz et al described a MS based V regional analysis method as a diagnostic tool for the detection of pathogenic anti-Ro-52 antibodies in patients with primary SS (Arentz 2012). The identification of these unique B cell clonotypes that targets IA-2 and other islet antigens may potentially facilitate the development of methods that allow the identification and removal of pathogenic B cells prior to the development of the disease or dampen the generation of pathogenic autoantibodies. Furthermore, the identification of these clonotypes may allow isolation of the B cell clone and investigation of the development of the B cell clone, mechanisms through which they escape tolerance check points, stages at which they acquire autoreactivity and the disease pathway which may help to develop more specific and sustained therapies.

Appendices

Appendix 1: Variable region peptides identified in the light chain samples from anti IA-2 antibody samples.

Appendix 2: Variable region peptides identified in the heavy chain samples from the anti-IA-2 antibody samples.

Appendix 3: Joining region peptides identified in the light and heavy chain samples from the affinity purified anti-IA-2 antibody samples.

Appendix 4: IA-2ic MBP fusion protein ELISA OD values.

Reference List

- Abbas, A. K., Lichtman, A. H. & Pillai, S. 2014. *Cellular and molecular immunology e-book*, Elsevier Health Sciences.
- Acevedo-Calado, M. J., Pietropaolo, S. L., Morran, M. P., Schnell, S., Vonberg, A. D., Verge, C. F., Gianani, R., Becker, D. J., Huang, S., Greenbaum, C. J., Yu, L., Davidson, H. W., Michels, A. W., Rich, S. S., Pietropaolo, M. & Group, F. T. T. D. T. S. 2019. Autoantibodies directed toward a novel ia-2 variant protein enhance prediction of type 1 diabetes. *Diabetes*, 68, 1819-1829.
- Adam, P., Haralambieva, E., Hartmann, M., Mao, Z., Ott, G. & Rosenwald, A. 2008. Rare occurrence of igvh gene translocations and restricted igvh gene repertoire in ocular malt-type lymphoma. *Haematologica*, 93, 319-20.
- Adamson, P. J., Wang, J. J., Anosova, N. G., Colella, A. D., Chataway, T. K., Kleantous, H., Gordon, T. P. & Gordon, D. L. 2020. Proteomic profiling of precipitated clostridioides difficile toxin a and b antibodies. *Vaccine*, 38, 2077-2087.
- Al Kindi, M. A., Chataway, T. K., Gilada, G. A., Jackson, M. W., Goldblatt, F. M., Walker, J. G., Colella, A. D. & Gordon, T. P. 2015. Serum smd autoantibody proteomes are clonally restricted and share variable-region peptides. *Journal of Autoimmunity*, 57, 77-81.
- Al Kindi, M. A., Colella, A. D., Beroukas, D., Chataway, T. K. & Gordon, T. P. 2016. Lupus anti-ribosomal p autoantibody proteomes express convergent biclonal signatures. *Clin Exp Immunol*, 184, 29-35.
- Andersson, C., Vaziri-Sani, F., Delli, A., Lindblad, B., Carlsson, A., Forsander, G., Ludvigsson, J., Marcus, C., Samuelsson, U., Ivarsson, S., Lernmark, A., Larsson, H. E. & Group, B. D. D. S. 2013. Triple specificity of znt8 autoantibodies in relation to hla and other islet autoantibodies in childhood and adolescent type 1 diabetes. *Pediatr Diabetes*, 14, 97-105.
- Atkinson, M. A. & Eisenbarth, G. S. 2001. Type 1 diabetes: New perspectives on disease pathogenesis and treatment. *Lancet*, 358, 221-9.
- Atkinson, M. A., Eisenbarth, G. S. & Michels, A. W. 2014. Type 1 diabetes. *Lancet*, 383, 69-82.
- Bahar, B., Jacquot, C., Mo, Y. D., Debiasi, R. L., Campos, J. & Delaney, M. 2020. Kinetics of viral clearance and antibody production across age groups in

- children with severe acute respiratory syndrome coronavirus 2 infection. *J Pediatr*, 227, 31-37 e1.
- Baizabal-Carvalho, J. F. & Jankovic, J. 2015. Stiff-person syndrome: Insights into a complex autoimmune disorder. *J Neurol Neurosurg Psychiatry*, 86, 840-8.
- Baneyx, F. 1999. Recombinant protein expression in escherichia coli. *Curr Opin Biotechnol*, 10, 411-21.
- Bason, C., Lorini, R., Lunardi, C., Dolcino, M., Giannattasio, A., D'annunzio, G., Rigo, A., Pedemonte, N., Corrocher, R. & Puccetti, A. 2013. In type 1 diabetes a subset of anti-coxsackievirus b4 antibodies recognize autoantigens and induce apoptosis of pancreatic beta cells. *PLoS One*, 8, e57729.
- Basten, A. & Silveira, P. A. 2010. B-cell tolerance: Mechanisms and implications. *Curr Opin Immunol*, 22, 566-74.
- Batista, F. D. & Harwood, N. E. 2009. The who, how and where of antigen presentation to b cells. *Nat Rev Immunol*, 9, 15-27.
- Bean, A. G., Baker, M. L., Stewart, C. R., Cowled, C., Deffrasnes, C., Wang, L. F. & Lowenthal, J. W. 2013. Studying immunity to zoonotic diseases in the natural host - keeping it real. *Nat Rev Immunol*, 13, 851-61.
- Bearzatto, M., Naserke, H., Piquer, S., Koczwar, K., Lampasona, V., Williams, A., Christie, M. R., Bingley, P. J., Ziegler, A. G. & Bonifacio, E. 2002. Two distinctly hla-associated contiguous linear epitopes uniquely expressed within the islet antigen 2 molecule are major autoantibody epitopes of the diabetes-specific tyrosine phosphatase-like protein autoantigens. *J Immunol*, 168, 4202-8.
- Boesgaard, T. W., Zilinskaite, J., Vanttinen, M., Laakso, M., Jansson, P. A., Hammarstedt, A., Smith, U., Stefan, N., Fritsche, A., Haring, H., Hribal, M., Sesti, G., Zobel, D. P., Pedersen, O., Hansen, T. & Consortium, E. 2008. The common slc30a8 arg325trp variant is associated with reduced first-phase insulin release in 846 non-diabetic offspring of type 2 diabetes patients--the eugene2 study. *Diabetologia*, 51, 816-20.
- Bomben, R., Dal-Bo, M., Benedetti, D., Capello, D., Forconi, F., Marconi, D., Bertoni, F., Maffei, R., Laurenti, L., Rossi, D., Del Principe, M. I., Luciano, F., Sozzi, E., Cattarossi, I., Zucchetto, A., Rossi, F. M., Bulian, P., Zucca, E., Nicoloso, M. S., Degan, M., Marasca, R., Efremov, D. G., Del Poeta, G., Gaidano, G. & Gattei, V. 2010. Expression of mutated ighv3-23 genes in chronic lymphocytic leukemia identifies a disease subset with peculiar clinical and biological features. *Clin Cancer Res*, 16, 620-8.

- Bonifacio, E. 2015. Predicting type 1 diabetes using biomarkers. *Diabetes Care*, 38, 989-96.
- Bonifacio, E., Genovese, S., Braghi, S., Bazzigaluppi, E., Lampasona, V., Bingley, P. J., Rogge, L., Pastore, M. R., Boggetti, E., Bottazzo, G. F. & Et Al. 1995. Islet autoantibody markers in iddm: Risk assessment strategies yielding high sensitivity. *Diabetologia*, 38, 816-22.
- Bonifacio, E., Lampasona, V. & Bingley, P. J. 1998. Ia-2 (islet cell antigen 512) is the primary target of humoral autoimmunity against type 1 diabetes-associated tyrosine phosphatase autoantigens. *The Journal of Immunology*, 161, 2648-2654.
- Brady, B. L., Steinel, N. C. & Bassing, C. H. 2010. Antigen receptor allelic exclusion: An update and reappraisal. *J Immunol*, 185, 3801-8.
- Bulek, A. M., Cole, D. K., Skowera, A., Dolton, G., Gras, S., Madura, F., Fuller, A., Miles, J. J., Gostick, E., Price, D. A., Drijfhout, J. W., Knight, R. R., Huang, G. C., Lissin, N., Molloy, P. E., Wooldridge, L., Jakobsen, B. K., Rossjohn, J., Peakman, M., Rizkallah, P. J. & Sewell, A. K. 2012. Structural basis for the killing of human beta cells by cd8(+) t cells in type 1 diabetes. *Nat Immunol*, 13, 283-9.
- Buzzetti, R., Spoletini, M., Zampetti, S., Campagna, G., Marandola, L., Panimolle, F., Dotta, F. & Tiberti, C. 2015. Tyrosine phosphatase-related islet antigen 2(256–760) autoantibodies, the only marker of islet autoimmunity that increases by increasing the degree of bmi in obese subjects with type 2 diabetes. *Diabetes Care*, 38, 513-520.
- Capra, J. D. & Kehoe, J. M. 1974. Variable region sequences of five human immunoglobulin heavy chains of the vh3 subgroup: Definitive identification of four heavy chain hypervariable regions. *Proc Natl Acad Sci U S A*, 71, 845-8.
- Chao, C., Huang, G., Li, X., Yang, L., Lin, J., Jin, P., Luo, S. M., Zhang, Y. Y., Pan, L. L. & Zhou, Z. G. 2013. Change of glutamic acid decarboxylase antibody and protein tyrosine phosphatase antibody in chinese patients with acute-onset type 1 diabetes mellitus. *Chin Med J (Engl)*, 126, 4006-12.
- Chimienti, F., Devergnas, S., Favier, A. & Seve, M. 2004. Identification and cloning of a beta-cell-specific zinc transporter, znt-8, localized into insulin secretory granules. *Diabetes*, 53, 2330-7.
- Chimienti, F., Devergnas, S., Pattou, F., Schuit, F., Garcia-Cuenca, R., Vandewalle, B., Kerr-Conte, J., Van Lommel, L., Grunwald, D., Favier, A. & Seve, M. 2006. In vivo expression and functional characterization of the zinc transporter

- znt8 in glucose-induced insulin secretion. *Journal of Cell Science*, 119, 4199-4206.
- Christgau, S., Aanstoot, H. J., Schierbeck, H., Begley, K., Tullin, S., Hejnaes, K. & Bækkeskov, S. 1992. Membrane anchoring of the autoantigen gad65 to microvesicles in pancreatic beta-cells by palmitoylation in the nh2-terminal domain. *J Cell Biol*, 118, 309-20.
- Christie, M. R., Genovese, S., Cassidy, D., Bosi, E., Brown, T. J., Lai, M., Bonifacio, E. & Bottazzo, G. F. 1994. Antibodies to islet 37k antigen, but not to glutamate decarboxylase, discriminate rapid progression to iddm in endocrine autoimmunity. *Diabetes*, 43, 1254-9.
- Clark, M., Kroger, C. J. & Tisch, R. M. 2017. Type 1 diabetes: A chronic anti-self-inflammatory response. *Frontiers in Immunology*, 8.
- Clement, C. C. & Santambrogio, L. 2013. The lymph self-antigen repertoire. *Front Immunol*, 4, 424.
- Culina, S., Brezar, V. & Mallone, R. 2013a. Insulin and type 1 diabetes: Immune connections. *Eur J Endocrinol*, 168, R19-31.
- Culina, S., Brezar, V. & Mallone, R. 2013b. Mechanisms in endocrinology: Insulin and type 1 diabetes: Immune connections. *European Journal of Endocrinology*, 168, R19-R31.
- Cyster, J. G. & Allen, C. D. C. 2019. B cell responses: Cell interaction dynamics and decisions. *Cell*, 177, 524-540.
- De Re, V., De Vita, S., Sansonno, D., Gasparotto, D., Simula, M. P., Tucci, F. A., Marzotto, A., Fabris, M., Gloghini, A., Carbone, A., Dammacco, F. & Boiocchi, M. 2006. Type ii mixed cryoglobulinaemia as an oligo rather than a mono b-cell disorder: Evidence from genescan and maldi-tof analyses. *Rheumatology (Oxford)*, 45, 685-93.
- Decochez, K., Tits, J., Coolens, J. L., Van Gaal, L., Krzentowski, G., Winnock, F., Anckaert, E., Weets, I., Pipeleers, D. G. & Gorus, F. K. 2000. High frequency of persisting or increasing islet-specific autoantibody levels after diagnosis of type 1 diabetes presenting before 40 years of age. The belgian diabetes registry. *Diabetes Care*, 23, 838-44.
- Delli, A. J., Vaziri-Sani, F., Lindblad, B., Elding-Larsson, H., Carlsson, A., Forsander, G., Ivarsson, S. A., Ludvigsson, J., Kockum, I., Marcus, C., Samuelsson, U., Ortqvist, E., Groop, L., Bondinas, G. P., Papadopoulos, G. K., Lernmark, A. & Better Diabetes Diagnosis Study, G. 2012. Zinc transporter 8 autoantibodies and their association with slc30a8 and hla-dq

- genes differ between immigrant and swedish patients with newly diagnosed type 1 diabetes in the better diabetes diagnosis study. *Diabetes*, 61, 2556-64.
- Delves, P. J. & Roitt, I. M. 2000. The immune system. *New England Journal of Medicine*, 343, 37-49.
- Dimeglio, L. A., Evans-Molina, C. & Oram, R. A. 2018. Type 1 diabetes. *Lancet*, 391, 2449-2462.
- Dorner, T. & Lipsky, P. E. 2005. Molecular basis of immunoglobulin variable region gene usage in systemic autoimmunity. *Clin Exp Med*, 4, 159-69.
- Dunn, M. F. 2005. Zinc-ligand interactions modulate assembly and stability of the insulin hexamer -- a review. *Biometals*, 18, 295-303.
- Edwards, A. M., Arrowsmith, C. H., Christendat, D., Dharamsi, A., Friesen, J. D., Greenblatt, J. F. & Vedadi, M. 2000. Protein production: Feeding the crystallographers and nmr spectroscopists. *Nat Struct Biol*, 7 Suppl, 970-2.
- Eide, D. J. 2006. Zinc transporters and the cellular trafficking of zinc. *Biochim Biophys Acta*, 1763, 711-22.
- Fagarasan, S. & Honjo, T. 2000. T-independent immune response: New aspects of b cell biology. *Science*, 290, 89-92.
- Falorni, A., Gambelungho, G., Forini, F., Kassi, G., Cosentino, A., Candeloro, P., Bolli, G. B., Brunetti, P. & Calcinaro, F. 2000. Autoantibody recognition of cooh-terminal epitopes of gad65 marks the risk for insulin requirement in adult-onset diabetes mellitus. *J Clin Endocrinol Metab*, 85, 309-16.
- Filippi, C. M. & Von Herrath, M. G. 2008. Viral trigger for type 1 diabetes: Pros and cons. *Diabetes*, 57, 2863-71.
- Gallegos, A. M. & Bevan, M. J. 2004. Central tolerance to tissue-specific antigens mediated by direct and indirect antigen presentation. *J Exp Med*, 200, 1039-49.
- Ganguly, D., Haak, S., Sisirak, V. & Reizis, B. 2013. The role of dendritic cells in autoimmunity. *Nat Rev Immunol*, 13, 566-77.
- Georgiou, G., Ippolito, G. C., Beausang, J., Busse, C. E., Wardemann, H. & Quake, S. R. 2014. The promise and challenge of high-throughput sequencing of the antibody repertoire. *Nat Biotechnol*, 32, 158-68.

- Ghazarian, L., Diana, J., Simoni, Y., Beaudoin, L. & Lehuen, A. 2013. Prevention or acceleration of type 1 diabetes by viruses. *Cell Mol Life Sci*, 70, 239-55.
- Gohlke, H., Ferrari, U., Koczwara, K., Bonifacio, E., Illig, T. & Ziegler, A. G. 2008. Slc30a8 (znt8) polymorphism is associated with young age at type 1 diabetes onset. *Rev Diabet Stud*, 5, 25-7.
- Gu, Y., Merriman, C., Guo, Z., Jia, X., Wenzlau, J., Li, H., Li, H., Rewers, M., Yu, L. & Fu, D. 2021. Novel autoantibodies to the β -cell surface epitopes of znt8 in patients progressing to type-1 diabetes. *Journal of Autoimmunity*, 122, 102677.
- Hagopian, W. A., Sanjeevi, C. B., Kockum, I., Landin-Olsson, M., Karlsen, A. E., Sundkvist, G., Dahlquist, G., Palmer, J. & Lernmark, A. 1995. Glutamate decarboxylase-, insulin-, and islet cell-antibodies and hla typing to detect diabetes in a general population-based study of swedish children. *J Clin Invest*, 95, 1505-11.
- Halverson, R., Torres, R. M. & Pelanda, R. 2004. Receptor editing is the main mechanism of b cell tolerance toward membrane antigens. *Nat Immunol*, 5, 645-50.
- Hampe, C. S., Hammerle, L. P., Bekris, L., Ortqvist, E., Kockum, I., Rolandsson, O., Landin-Olsson, M., Torn, C., Persson, B. & Lernmark, A. 2000. Recognition of glutamic acid decarboxylase (gad) by autoantibodies from different gad antibody-positive phenotypes. *J Clin Endocrinol Metab*, 85, 4671-9.
- Hansson, I., Lynch, K. F., Hallmans, G., Lernmark, A. & Rolandsson, O. 2011. High-titer gad65 autoantibodies detected in adult diabetes patients using a high efficiency expression vector and cold gad65 displacement. *Autoimmunity*, 44, 129-36.
- Havenar-Daughton, C., Sarkar, A., Kulp, D. W., Toy, L., Hu, X., Deresa, I., Kalyuzhniy, O., Kaushik, K., Upadhyay, A. A., Menis, S., Landais, E., Cao, L., Diedrich, J. K., Kumar, S., Schiffner, T., Reiss, S. M., Seumois, G., Yates, J. R., Paulson, J. C., Bosinger, S. E., Wilson, I. A., Schief, W. R. & Crotty, S. 2018. The human naive b cell repertoire contains distinct subclasses for a germline-targeting hiv-1 vaccine immunogen. *Sci Transl Med*, 10.
- Hawa, M. I., Fava, D., Medici, F., Deng, Y. J., Notkins, A. L., De Mattia, G. & Leslie, R. D. 2000. Antibodies to ia-2 and gad65 in type 1 and type 2 diabetes: Isotype restriction and polyclonality. *Diabetes Care*, 23, 228-33.
- Health, A. I. O. & Welfare 2020. Diabetes. Canberra: AIHW.

- Hibi, T. & Dosch, H. M. 1986. Limiting dilution analysis of the b cell compartment in human bone marrow. *Eur J Immunol*, 16, 139-45.
- Hirai, H., Miura, J., Hu, Y., Larsson, H., Larsson, K., Lernmark, A., Ivarsson, S. A., Wu, T., Kingman, A., Tzioufas, A. G. & Notkins, A. L. 2008. Selective screening of secretory vesicle-associated proteins for autoantigens in type 1 diabetes: Vamp2 and npy are new minor autoantigens. *Clin Immunol*, 127, 366-74.
- Huang, L. 2014. Zinc and its transporters, pancreatic beta-cells, and insulin metabolism. *Vitam Horm*, 95, 365-90.
- Huang, Q., Du, J., Merriman, C. & Gong, Z. 2019. Genetic, functional, and immunological study of znt8 in diabetes. *International Journal of Endocrinology*, 2019, 1524905.
- Huang, Q., Yin, J. Y., Dai, X. P., Wu, J., Chen, X., Deng, C. S., Yu, M., Gong, Z. C., Zhou, H. H. & Liu, Z. Q. 2010. Association analysis of slc30a8 rs13266634 and rs16889462 polymorphisms with type 2 diabetes mellitus and repaglinide response in chinese patients. *Eur J Clin Pharmacol*, 66, 1207-15.
- Ilonen, J., Hammais, A., Laine, A. P., Lempainen, J., Vaarala, O., Veijola, R., Simell, O. & Knip, M. 2013. Patterns of beta-cell autoantibody appearance and genetic associations during the first years of life. *Diabetes*, 62, 3636-40.
- Jansen, J., Rosenkranz, E., Overbeck, S., Warmuth, S., Mocchegiani, E., Giacconi, R., Weiskirchen, R., Karges, W. & Rink, L. 2012. Disturbed zinc homeostasis in diabetic patients by in vitro and in vivo analysis of insulinomimetic activity of zinc. *J Nutr Biochem*, 23, 1458-66.
- Kanatsuna, N., Papadopoulos, G. K., Moustakas, A. K. & Lenmark, A. 2012. Etiopathogenesis of insulin autoimmunity. *Anat Res Int*, 2012, 457546.
- Kappler, J. W., Roehm, N. & Marrack, P. 1987. T cell tolerance by clonal elimination in the thymus. *Cell*, 49, 273-80.
- Kasimiotis, H., Fida, S., Rowley, M. J., Mackay, I. R., Zimmet, P. Z., Gleason, S., Rabin, D. U. & Myers, M. A. 2001. Antibodies to sox13 (ica12) are associated with type 1 diabetes. *Autoimmunity*, 33, 95-101.
- Kawasaki, E., Nakamura, K., Kuriya, G., Satoh, T., Kobayashi, M., Kuwahara, H., Abiru, N., Yamasaki, H., Matsuura, N., Miura, J., Uchigata, Y. & Eguchi, K. 2011. Zinc transporter 8 autoantibodies in fulminant, acute-onset, and slow-onset patients with type 1 diabetes. *Diabetes Metab Res Rev*, 27, 895-8.

- Kelleher, S. L., McCormick, N. H., Velasquez, V. & Lopez, V. 2011. Zinc in specialized secretory tissues: Roles in the pancreas, prostate, and mammary gland. *Adv Nutr*, 2, 101-11.
- Ki, M.-R. & Pack, S. P. 2020. Fusion tags to enhance heterologous protein expression. *Applied Microbiology and Biotechnology*, 104, 2411-2425.
- Kirchhoff, K., Machicao, F., Haupt, A., Schafer, S. A., Tschritter, O., Staiger, H., Stefan, N., Haring, H. U. & Fritsche, A. 2008. Polymorphisms in the *tcf7l2*, *cdk11* and *slc30a8* genes are associated with impaired proinsulin conversion. *Diabetologia*, 51, 597-601.
- Knip, M., Korhonen, S., Kulmala, P., Veijola, R., Reunanen, A., Raitakari, O. T., Viikari, J. & Akerblom, H. K. 2010. Prediction of type 1 diabetes in the general population. *Diabetes Care*, 33, 1206-12.
- Kockum, I., Sanjeevi, C. B., Eastman, S., Landin-Olsson, M., Dahlquist, G. & Lernmark, A. 1999. Complex interaction between hla dr and dq in conferring risk for childhood type 1 diabetes. *Eur J Immunogenet*, 26, 361-72.
- Kolm-Litty, V., Berlo, S., Bonifacio, E., Bearzatto, M., Engel, A. M., Christie, M., Ziegler, A. G., Wild, T. & Endl, J. 2000. Human monoclonal antibodies isolated from type 1 diabetes patients define multiple epitopes in the protein tyrosine phosphatase-like ia-2 antigen. *J Immunol*, 165, 4676-84.
- Kong, Y. H., Kim, M. S. & Lee, D. Y. 2013. Comparison of the prevalence of islet autoantibodies according to age and disease duration in patients with type 1 diabetes mellitus. *Ann Pediatr Endocrinol Metab*, 18, 65-70.
- Kulmala, P., Savola, K., Petersen, J. S., Vahasalo, P., Karjalainen, J., Lopponen, T., Dyrberg, T., Akerblom, H. K. & Knip, M. 1998. Prediction of insulin-dependent diabetes mellitus in siblings of children with diabetes. A population-based study. The childhood diabetes in finland study group. *J Clin Invest*, 101, 327-36.
- Kumar, B. V., Connors, T. J. & Farber, D. L. 2018. Human t cell development, localization, and function throughout life. *Immunity*, 48, 202-213.
- Lampasona, V., Bearzatto, M., Genovese, S., Bosi, E., Ferrari, M. & Bonifacio, E. 1996. Autoantibodies in insulin-dependent diabetes recognize distinct cytoplasmic domains of the protein tyrosine phosphatase-like ia-2 autoantigen. *J Immunol*, 157, 2707-11.
- Lampasona, V. & Liberati, D. 2016. Islet autoantibodies. *Current Diabetes Reports*, 16, 53.

- Lanzavecchia, A. 1985. Antigen-specific interaction between t and b cells. *Nature*, 314, 537-9.
- Lanzavecchia, A. & Sallusto, F. 2000. Dynamics of t lymphocyte responses: Intermediates, effectors, and memory cells. *Science*, 290, 92-7.
- Lebastchi, J., Deng, S., Lebastchi, A. H., Beshar, I., Gitelman, S., Willi, S., Gottlieb, P., Akirav, E. M., Bluestone, J. A. & Herold, K. C. 2013. Immune therapy and beta-cell death in type 1 diabetes. *Diabetes*, 62, 1676-80.
- Lindop, R., Arentz, G., Bastian, I., Whyte, A. F., Thurgood, L. A., Chataway, T. K., Jackson, M. W. & Gordon, T. P. 2013. Long-term ro60 humoral autoimmunity in primary sjogren's syndrome is maintained by rapid clonal turnover. *Clin Immunol*, 148, 27-34.
- Lindop, R., Arentz, G., Chataway, T. K., Thurgood, L. A., Jackson, M. W., Reed, J. H., Mccluskey, J. & Gordon, T. P. 2011. Molecular signature of a public clonotypic autoantibody in primary sjogren's syndrome: A "forbidden" clone in systemic autoimmunity. *Arthritis Rheum*, 63, 3477-86.
- Lu, J., Li, Q., Xie, H., Chen, Z. J., Borovitskaya, A. E., Maclaren, N. K., Notkins, A. L. & Lan, M. S. 1996. Identification of a second transmembrane protein tyrosine phosphatase, ia-2beta, as an autoantigen in insulin-dependent diabetes mellitus: Precursor of the 37-kda tryptic fragment. *Proceedings of the National Academy of Sciences of the United States of America*, 93, 2307-2311.
- Mahler, M. & Fritzler, M. J. 2010. Epitope specificity and significance in systemic autoimmune diseases. *Ann N Y Acad Sci*, 1183, 267-87.
- Mathis, D., Vence, L. & Benoist, C. 2001. Beta-cell death during progression to diabetes. *Nature*, 414, 792-8.
- Mayr, A., Schlosser, M., Grober, N., Kenk, H., Ziegler, A. G., Bonifacio, E. & Achenbach, P. 2007. Gad autoantibody affinity and epitope specificity identify distinct immunization profiles in children at risk for type 1 diabetes. *Diabetes*, 56, 1527-33.
- Mcheyzer-Williams, M., Okitsu, S., Wang, N. & Mcheyzer-Williams, L. 2012. Molecular programming of b cell memory. *Nature Reviews Immunology*, 12, 24-34.
- Mckee, A. & Tracy, J. A. 2017. Gad65 neurological autoimmunity. *Muscle & Nerve*, 56, 15-27.
- Miao, D., Yu, L., Tiberti, C., Cuthbertson, D. D., Rewers, M., Di Mario, U., Eisenbarth, G. S. & Dotta, F. 2002. Ica512(ia-2) epitope specific assays

- distinguish transient from diabetes associated autoantibodies. *J Autoimmun*, 18, 191-6.
- Mikocziova, I., Gidoni, M., Lindeman, I., Peres, A., Snir, O., Yaari, G. & Sollid, L. M. 2020. Polymorphisms in human immunoglobulin heavy chain variable genes and their upstream regions. *Nucleic Acids Res*, 48, 5499-5510.
- Mobasserri, M., Shirmohammadi, M., Amiri, T., Vahed, N., Hosseini Fard, H. & Ghojzadeh, M. 2020. Prevalence and incidence of type 1 diabetes in the world: A systematic review and meta-analysis. *Health Promot Perspect*, 10, 98-115.
- Naserke, H. E., Ziegler, A. G., Lampasona, V. & Bonifacio, E. 1998. Early development and spreading of autoantibodies to epitopes of ia-2 and their association with progression to type 1 diabetes. *J Immunol*, 161, 6963-9.
- Neuberger, M. S., Ehrenstein, M. R., Rada, C., Sale, J., Batista, F. D., Williams, G. & Milstein, C. 2000. Memory in the b-cell compartment: Antibody affinity maturation. *Philos Trans R Soc Lond B Biol Sci*, 355, 357-60.
- Nguyen, A. V. & Soulika, A. M. 2019. The dynamics of the skin's immune system. *International Journal of Molecular Sciences*, 20, 1811.
- Nishino, M., Ikegami, H., Kawaguchi, Y., Fujisawa, T., Kawabata, Y., Shintani, M., Ono, M., Horiki, M., Kawasaki, E. & Ogiwara, T. 2001. Polymorphism in gene for islet autoantigen, ia-2, and type 1 diabetes in japanese subjects. *Hum Immunol*, 62, 518-22.
- Notkins, A. L. & Lernmark, A. 2001. Autoimmune type 1 diabetes: Resolved and unresolved issues. *J Clin Invest*, 108, 1247-52.
- Palmer, J. P., Asplin, C. M., Clemons, P., Lyen, K., Tatpati, O., Raghu, P. K. & Paquette, T. L. 1983. Insulin antibodies in insulin-dependent diabetics before insulin treatment. *Science*, 222, 1337-9.
- Palmiter, R. D. & Huang, L. 2004. Efflux and compartmentalization of zinc by members of the slc30 family of solute carriers. *Pflugers Arch*, 447, 744-51.
- Patterson, C. C., Karuranga, S., Salpea, P., Saeedi, P., Dahlquist, G., Soltesz, G. & Ogle, G. D. 2019. Worldwide estimates of incidence, prevalence and mortality of type 1 diabetes in children and adolescents: Results from the international diabetes federation diabetes atlas, 9th edition. *Diabetes Research and Clinical Practice*, 157, 107842.
- Pihoker, C., Gilliam, L. K., Hampe, C. S. & Lernmark, A. 2005. Autoantibodies in diabetes. *Diabetes*, 54 Suppl 2, S52-61.

- Pober, J. S., Merola, J., Liu, R. & Manes, T. D. 2017. Antigen presentation by vascular cells. *Frontiers in Immunology*, 8.
- Pociot, F. & Lernmark, Å. 2016. Genetic risk factors for type 1 diabetes. *The Lancet*, 387, 2331-2339.
- Pozzilli, P. & Pieralice, S. 2018. Latent autoimmune diabetes in adults: Current status and new horizons. *Endocrinol Metab (Seoul)*, 33, 147-159.
- Pryor, K. D. & Leiting, B. 1997. High-level expression of soluble protein in escherichia coli using a his6-tag and maltose-binding-protein double-affinity fusion system. *Protein Expr Purif*, 10, 309-19.
- Regazzi, R., Wollheim, C. B., Lang, J., Theler, J. M., Rossetto, O., Montecucco, C., Sadoul, K., Weller, U., Palmer, M. & Thorens, B. 1995. Vamp-2 and cellubrevin are expressed in pancreatic beta-cells and are essential for ca(2+)-but not for gtp gamma s-induced insulin secretion. *EMBO J*, 14, 2723-30.
- Rondard, P., Bregegere, F., Lecroisey, A., Delepierre, M. & Bedouelle, H. 1997. Conformational and functional properties of an undecapeptide epitope fused with the c-terminal end of the maltose binding protein. *Biochemistry*, 36, 8954-61.
- Routzahn, K. M. & Waugh, D. S. 2002. Differential effects of supplementary affinity tags on the solubility of mbp fusion proteins. *J Struct Funct Genomics*, 2, 83-92.
- Rungby, J. 2010. Zinc, zinc transporters and diabetes. *Diabetologia*, 53, 1549-51.
- Sabbah, E., Savola, K., Kulmala, P., Reijonen, H., Veijola, R., Vahasalo, P., Karjalainen, J., Ilonen, J., Akerblom, H. K. & Knip, M. 1999. Disease-associated autoantibodies and hla-dqb1 genotypes in children with newly diagnosed insulin-dependent diabetes mellitus (iddm). The childhood diabetes in finland study group. *Clin Exp Immunol*, 116, 78-83.
- Sadighi Akha, A. A. 2018. Aging and the immune system: An overview. *Journal of Immunological Methods*, 463, 21-26.
- Salonen, K. M., Ryhanen, S., Harkonen, T., Ilonen, J., Knip, M. & Finnish Pediatric Diabetes, R. 2013. Autoantibodies against zinc transporter 8 are related to age, metabolic state and hla dr genotype in children with newly diagnosed type 1 diabetes. *Diabetes Metab Res Rev*, 29, 646-54.
- Schroeder, H. W., Jr. 2006. Similarity and divergence in the development and expression of the mouse and human antibody repertoires. *Dev Comp Immunol*, 30, 119-35.

- Shahaf, G., Zisman-Rozen, S., Benhamou, D., Melamed, D. & Mehr, R. 2016. B cell development in the bone marrow is regulated by homeostatic feedback exerted by mature b cells. *Frontiers in Immunology*, 7.
- Shen, Y., Prinyawiwatkul, W. & Xu, Z. 2019. Insulin: A review of analytical methods. *Analyst*, 144, 4139-4148.
- Skärstrand, H., Lernmark, A. & Vaziri-Sani, F. 2013. Antigenicity and epitope specificity of znt8 autoantibodies in type 1 diabetes. *Scand J Immunol*, 77, 21-9.
- Sladek, R., Rocheleau, G., Rung, J., Dina, C., Shen, L., Serre, D., Boutin, P., Vincent, D., Belisle, A., Hadjadj, S., Balkau, B., Heude, B., Charpentier, G., Hudson, T. J., Montpetit, A., Pshezhetsky, A. V., Prentki, M., Posner, B. I., Balding, D. J., Meyre, D., Polychronakos, C. & Froguel, P. 2007. A genome-wide association study identifies novel risk loci for type 2 diabetes. *Nature*, 445, 881-5.
- Smith, K., James, J. A. & Harley, J. B. 2013. Editorial for lindop et al. "Long-term ro60 humoral autoimmunity in primary sjogren's syndrome is maintained by rapid clonal turnover". *Clin Immunol*, 148, 110-2.
- Solimena, M., Dirx, R., Jr., Hermel, J. M., Pleasic-Williams, S., Shapiro, J. A., Caron, L. & Rabin, D. U. 1996. Ica 512, an autoantigen of type i diabetes, is an intrinsic membrane protein of neurosecretory granules. *EMBO J*, 15, 2102-14.
- Sorensen, J. S., Vaziri-Sani, F., Maziarz, M., Kristensen, K., Ellerman, A., Breslow, N., Lernmark, A., Pociot, F., Brorsson, C., Birkebaek, N. H. & Danish Study Group for Childhood, D. 2012. Islet autoantibodies and residual beta cell function in type 1 diabetes children followed for 3-6 years. *Diabetes Res Clin Pract*, 96, 204-10.
- Staiger, H., Machicao, F., Stefan, N., Tschritter, O., Thamer, C., Kantartzis, K., Schafer, S. A., Kirchhoff, K., Fritsche, A. & Haring, H. U. 2007. Polymorphisms within novel risk loci for type 2 diabetes determine beta-cell function. *PLoS One*, 2, e832.
- Steck, A. K., Johnson, K., Barriga, K. J., Miao, D., Yu, L., Hutton, J. C., Eisenbarth, G. S. & Rewers, M. J. 2011. Age of islet autoantibody appearance and mean levels of insulin, but not gad or ia-2 autoantibodies, predict age of diagnosis of type 1 diabetes: Diabetes autoimmunity study in the young. *Diabetes Care*, 34, 1397-9.
- Steinman, R. M. 2012. Decisions about dendritic cells: Past, present, and future. *Annu Rev Immunol*, 30, 1-22.

- Sticht, J., Alvaro-Benito, M. & Konigorski, S. 2021. Type 1 diabetes and the hla region: Genetic association besides classical hla class ii genes. *Front Genet*, 12, 683946.
- Thurgood, L. A., Arentz, G., Lindop, R., Jackson, M. W., Whyte, A. F., Colella, A. D., Chataway, T. K. & Gordon, T. P. 2013. An immunodominant la/ssb autoantibody proteome derives from public clonotypes. *Clin Exp Immunol*, 174, 237-44.
- Tiberti, C., Giordano, C., Locatelli, M., Bosi, E., Bottazzo, G. F., Buzzetti, R., Cucinotta, D., Galluzzo, A., Falorni, A. & Dotta, F. 2008. Identification of tyrosine phosphatase 2(256-760) construct as a new, sensitive marker for the detection of islet autoimmunity in type 2 diabetic patients: The non-insulin requiring autoimmune diabetes (nirad) study 2. *Diabetes*, 57, 1276-83.
- Vaziri-Sani, F., Oak, S., Radtke, J., Lernmark, K., Lynch, K., Agardh, C. D., Cilio, C. M., Lethagen, A. L., Ortqvist, E., Landin-Olsson, M., Torn, C. & Hampe, C. S. 2010. Znt8 autoantibody titers in type 1 diabetes patients decline rapidly after clinical onset. *Autoimmunity*, 43, 598-606.
- Von Scholten, B. J., Kreiner, F. F., Gough, S. C. L. & Von Herrath, M. 2021. Current and future therapies for type 1 diabetes. *Diabetologia*, 64, 1037-1048.
- Wang, C., Xia, M., Sun, X., He, Z., Hu, F., Chen, L., Bueso-Ramos, C. E., Qiu, X. & Yin, C. C. 2015. Igk with conserved igkappav/igkappaj repertoire is expressed in acute myeloid leukemia and promotes leukemic cell migration. *Oncotarget*, 6, 39062-72.
- Wang, J. J., Al Kindi, M. A., Colella, A. D., Dykes, L., Jackson, M. W., Chataway, T. K., Reed, J. H. & Gordon, T. P. 2016. Igv peptide mapping of native ro60 autoantibody proteomes in primary sjogren's syndrome reveals molecular markers of ro/la diversification. *Clin Immunol*, 173, 57-63.
- Wang, J. J., Colella, A. D., Beroukas, D., Chataway, T. K. & Gordon, T. P. 2018. Precipitating anti-dsna peptide repertoires in lupus. *Clin Exp Immunol*, 194, 273-282.
- Warrender, A. K. & Kelton, W. 2020. Beyond allotypes: The influence of allelic diversity in antibody constant domains. *Front Immunol*, 11, 2016.
- Warshauer, J. T., Bluestone, J. A. & Anderson, M. S. 2020. New frontiers in the treatment of type 1 diabetes. *Cell Metabolism*, 31, 46-61.
- Wenzlau, J. M., Frisch, L. M., Hutton, J. C. & Davidson, H. W. 2011. Mapping of conformational autoantibody epitopes in znt8. *Diabetes Metab Res Rev*, 27, 883-6.

- Wenzlau, J. M., Liu, Y., Yu, L., Moua, O., Fowler, K. T., Rangasamy, S., Walters, J., Eisenbarth, G. S., Davidson, H. W. & Hutton, J. C. 2008a. A common nonsynonymous single nucleotide polymorphism in the *slc30a8* gene determines *znt8* autoantibody specificity in type 1 diabetes. *Diabetes*, 57, 2693-7.
- Wenzlau, J. M., Moua, O., Liu, Y., Eisenbarth, G. S., Hutton, J. C. & Davidson, H. W. 2008b. Identification of a major humoral epitope in *slc30a8* (*znt8*). *Ann N Y Acad Sci*, 1150, 252-5.
- Wing, K., Larsson, P., Sandstrom, K., Lundin, S. B., Suri-Payer, E. & Rudin, A. 2005a. Cd4+ cd25+ foxp3+ regulatory t cells from human thymus and cord blood suppress antigen-specific t cell responses. *Immunology*, 115, 516-25.
- Wing, K., Suri-Payer, E. & Rudin, A. 2005b. Cd4+cd25+-regulatory t cells from mouse to man. *Scand J Immunol*, 62, 1-15.
- Wong, F. S. & Wen, L. 2005. B cells in autoimmune diabetes. *Rev Diabet Stud*, 2, 121-35.
- Wu, X. & Kong, X. P. 2016. Antigenic landscape of the hiv-1 envelope and new immunological concepts defined by hiv-1 broadly neutralizing antibodies. *Curr Opin Immunol*, 42, 56-64.
- Yu, L., Rewers, M., Gianani, R., Kawasaki, E., Zhang, Y., Verge, C., Chase, P., Klingensmith, G., Erlich, H., Norris, J. & Eisenbarth, G. S. 1996. Antiislet autoantibodies usually develop sequentially rather than simultaneously. *J Clin Endocrinol Metab*, 81, 4264-7.
- Ziegler, A. G., Hummel, M., Schenker, M. & Bonifacio, E. 1999. Autoantibody appearance and risk for development of childhood diabetes in offspring of parents with type 1 diabetes: The 2-year analysis of the german babydiab study. *Diabetes*, 48, 460-8.
- Ziegler, A. G., Rewers, M., Simell, O., Simell, T., Lempainen, J., Steck, A., Winkler, C., Ilonen, J., Veijola, R., Knip, M., Bonifacio, E. & Eisenbarth, G. S. 2013. Seroconversion to multiple islet autoantibodies and risk of progression to diabetes in children. *JAMA*, 309, 2473-9.